A Systems Science View on Cell Death Signalling

Eine systemwissenschaftliche Betrachtung der Zelltod-Signaltransduktion

Von der Fakultät Maschinenbau der Universität Stuttgart
zur Erlangung der Würde eines Doktoringenieurs (Dr.-Ing.)
genehmigte Abhandlung

vorgelegt von

Thomas Eißing
aus Dorsten-Wulfen

Hauptberichter:	Prof. Dr.-Ing. Frank Allgöwer
Mitberichter:	Dr. sc. techn. Eric Bullinger
Mitberichter:	Prof. John Lygeros, Ph.D.
Mitberichter:	Prof. Dr. rer. nat. Peter Scheurich

Eingereicht am: 18. Juni 2007
Tag der mündlichen Prüfung: 25. Oktober 2007

Institut für Systemtheorie und Regelungstechnik
Universität Stuttgart
2007

Preface and Acknowledgements

The results described in this thesis were developed during my time as a research assistant at the Institute for Systems Theory and Automatic Control (IST) in Stuttgart. The work describes an interdisciplinary approach to address and solve biological questions. Especially because of this interdisciplinary character, it was very helpful to receive help and advise from experts in the respective fields. Therefore, I would like to express my sincere thanks to the many colleagues who contributed in various ways to this thesis, highlighting the following:

First of all, I would like to thank my teachers in the doctoral exam committee, not only for the involved work as such. Frank Allgöwer, professor at and head of the IST, for giving me the opportunity to work at his institute and explore scientific fields that were unfamiliar to me at the beginning of my thesis. His blend of support, guidance and freedom were crucial for the development of the thesis. Eric Bullinger, Habilitant at the IST and later on also lecturer at the Hamilton Institute at the National University of Ireland and then Strathclyde University in Scotland, for advising and helping me in many aspects, especially related to mathematical and computational issues. Further, my time with him at the Hamilton Institute was very helpful in finishing the thesis. John Lygeros, professor at the Institute of Automatic Control at ETH Zürich, for his interest in and excellent input on my thesis. Peter Scheurich, professor at the Institute of Cell Biology and Immunology in Stuttgart, for his full support and guidance throughout the years. Not only his advice on biological aspects are much appreciated, and without him I would likely not have entered systems biology.

Several additional people were very helpful in the development of this thesis. These are graduate students whom I (co-)supervised and colleagues from Stuttgart, which I would like to thank a lot. Birgit Schöberl, and her supervisor Prof. Ernst-Dieter Gilles, were crucial in the initialization of the project that also gave rise to my thesis. The contributions of Holger Conzelmann were significant, especially in the early phase of my thesis. The joint work with Steffen Waldherr and Madalena Chavez towards the end of my doctoral studies were pleasant and fruitful, opening up new roads especially on the methodological side. The work of Monica Schliemann is providing a great perspective for the project. Carla Cimatoribus, Christian Ebenbauer, Cedric Gondro, Kai Heussen, Philipp Rumschinski, and Thomas Sauter contributed on interesting side aspects of this thesis.

Further, I would like to thank all my colleagues and friends at the IST, for creating an excellent and very enjoyable atmosphere to work (and partly live) in, and for all the “little” help on my way. This thanks extends to the people from the SysBio group in Stuttgart.

I also would like to acknowledge the financial help of the funding agencies supporting the project framework this thesis is part of, especially the Deutsche Forschungsgemeinschaft (DFG).

Abschließend möchte ich meiner Familie und meinen Freunden danken. Im Besonderen meiner Freundin Britta für ihr Verständnis für ein doch leicht eingeschränktes Privatleben während der Promotionszeit und ihren Beistand, sowie die ausgleichende und erfüllende Mitgestaltung der verbliebenen Zeit. Meinen Eltern für ihr Vertrauen und ihre Unterstützung, die erst ein Studium ermöglicht haben. Und meinen Schwestern, ohne deren Vorbildfunktion ich eventuell erst gar nicht auf die Idee gekommen wäre zu studieren.

Stuttgart, January 2008 Thomas Eißing

"What is life?"

We must therefore not be discouraged by the difficulty of interpreting life by the ordinary laws of physics. For that is what is to be expected from the knowledge we have gained of the structure of living matter. We must be prepared to find a new type of physical law prevailing in it. Or are we to term it a non-physical, not to say a super-physical law?

– Erwin Schrödinger (1944)

Contents

Abstract

This thesis provides new insight into cellular signal transduction by integrating biological knowledge into mathematical models, which are subsequently analysed using systems theoretic methods. Signal transduction has been dissected using molecular and genomic approaches providing exciting insight into the biochemistry of life. However, a detailed understanding of its dynamic properties remains elusive. The application of systems science ideas to biology is promising to put the pieces of molecular information back together, as important properties of life arise at the system level only. For example, certain signalling pathways convert graded input signals into all-or-none output signals constituting biological switches. These are implicated in cellular memory and decisions. One such decision is whether or not to undergo programmed cell death (apoptosis). Apoptosis is an important physiological process crucially involved in the development and homoeostasis of multicellular organisms. Switches, such as in apoptosis, can be represented by ordinary differential equation models showing bistable behaviour. Different biochemical mechanisms generating bistability in reaction schemes as encountered in apoptosis are presented and compared in this thesis. Bifurcation studies reveal structural and parametric requirements for bistability. In combination with reported kinetic information, inconsistencies in the literature view of apoptosis signalling in humans are revealed. An additional regulatory mechanism is proposed, which is now supported by experimental evidence. Extended robustness analyses indicate that the cell has achieved a favourable robustness-performance trade-off, imposed by network structure and evolutionary constraints. On the one hand, inhibitors of apoptosis function as noise filters and reduce variability caused by the stochastic nature of reactions. Further, qualitative properties such as bistability are comparably robust to parameter changes supporting proper decisions. On the other hand, quantitative aspects are comparably sensitive. This allows for variability in a population, as observed in experiments, and which is likely important for physiological function as recently indicated in immunological studies. The analyses further indicate that the trade-off leads to fragilities. For example, an up-regulation of inhibitors of apoptosis, as observed in certain cancers, can not only desensitise cells to apoptotic stimuli, as also suggested by experimental studies, but can contribute to cancer aggressiveness and progression through additional mechanisms. Thereby, the analyses provide insight of pharmaceutical relevance. Several results presented in this thesis are not restricted to apoptosis signalling only, but are conceptually relevant to various other signal transduction pathways.

Deutsche Kurzfassung

Die vorliegende Niederschrift befasst sich mit Fragestellungen aus dem Bereich der Systembiologie. Einem systembiologischen Ansatz folgend gewährt die Dissertation neue Einblicke in die zelluläre Signaltransduktion, indem biologisches Wissen in mathematische Modelle integriert wird, welche im Weiteren mit systemtheoretischen Methoden analysiert werden. Im Folgenden wird zunächst die mathematische Modellierung und Analyse biologischer Systeme motiviert und eingeführt, sowie der mit diesen Methoden untersuchte biologische Vorgang des programmierten Zelltods erläutert. Anschließend wird die Struktur der Arbeit aufgezeigt und die Ergebnisse werden zusammengefasst. Hierbei sind die Hauptbeiträge dieser Arbeit Differentialgleichungsmodelle zu Schlüsselvorgängen des programmierten Zelltods, deren Analyse mit Hinblick auf Anzahl und Stabilität von Ruhelagen, Sensitivitäts- und Robustheitsuntersuchungen sowie Betrachtungen stochastischer Einflüsse.

Einführung

In seinem bekannten Werk „Was ist Leben?“ hat Erwin Schrödinger 1944 die Frage gestellt, ob die bekannten physikalischen Gesetze auf die Biologie anwendbar sind. Physikalische Gesetze werden im Allgemeinen durch mathematische Formeln beschrieben. Obwohl mittlerweile klar ist, dass die bekannten physikalischen Gesetze auch für die Biochemie des Lebens gelten, bleibt eine mathematische Beschreibung aufgrund dieser Gesetze schwierig. Und obwohl die Idee im Prinzip nicht neu ist, gibt es neuerlich einen verstärkten Bedarf und ein erneuertes Interesse in dem aufstrebenden Gebiet der Systembiologie, solche Ansätze zu verfolgen, wie im Folgenden dargelegt wird.

Systemwissenschaften und Biologie. Systembiologie ist ein ganzheitlicher Ansatz zum Verständnis der Biologie. Er zielt darauf ab, biologische Systeme als solche zu verstehen. Dies bedeutet eine Untersuchung der Struktur und Dynamik zellulärer und physiologischer Vorgänge, und nicht primär die Charakterisierung der einzelnen Bestandteile von Zellen und Organismen. Viele Eigenschaften des Lebens entstehen erst auf der Ebene des Systems, weswegen das Verhalten des Systems nicht durch seine Bestandteile alleine verstanden werden kann. Erst die dynamische Interaktion dieser Bestandteile formt das Verhalten des Ganzen. Zum Beispiel können viele Funktionen nicht einzelnen Molekülen oder Reaktionen zugeordnet werden, sondern erwachsen erst auf der Ebene des Reaktionsnetzwerkes.
Systembiologie ist ein multidisziplinäres Forschungsgebiet, welches in dem zurückliegenden Jahrzehnt ein stark wachsendes Interesse erfahren hat und entsprechend Ideen aus sehr vielen Diszi-

plinen anzieht. Als Schwerpunkt ist es im Grenzbereich der Lebens-, Informations- und Systemwissenschaften anzusiedeln (vergleiche Abbildung 1.1, Seite 2). Auch wenn schon seit Mitte des letzten Jahrhunderts zellbiologische Prozesse durch mathematische Modelle beschrieben und untersucht werden und Visionen eines Verständnisses auf Systemebene beschrieben sind, lässt sich das neuerliche Interesse an diesen Ansätzen durch die bahnbrechenden Fortschritte in der Molekularbiologie begründen, welche der Wissenschaft neue Daten, aber auch neue Herausforderungen beschert haben.

Molekularbiologie und Genetik haben viele spannende Fragen beantworten können, zumeist ohne die Hilfe mathematischer Modelle zu benötigen. Ein qualitatives Verständnis vieler biochemischer Vorgänge des Lebens ist daraus hervorgegangen. DNS wurde als Erbsubstanz identifiziert und es ist verstanden, wie die enthaltene Information in Proteine übersetzt wird, welche die eigentliche 'Arbeit' innerhalb der Zelle erledigen (vergleiche Abbildung 1.2, Seite 3). Proteine fungieren unter anderem als Enzyme, welche grundlegend für den Stoffwechsel und die Energiegewinnung der Zelle sind. Sie geben der Zelle Form und Struktur und ermöglichen Mobilität. Des Weiteren übertragen und verarbeiten sie Signale, welche essentiell für die Koordinierung der unterschiedlichen Vorgänge innerhalb einer Zelle, aber auch zwischen den Zellen innerhalb eines Organismus, sind.

Auch wenn viele prinzipielle Funktionsweisen des Lebens auf biochemischer Ebene mittlerweile gut verstanden sind, bleibt ein detailliertes Verständnis des dynamischen Zusammenspiels vieler Prozesse verborgen. Das humane Genomprojekt markiert somit nicht das Ende, sondern den Anfang zu einer neuen Ebene des Verständnisses. Obwohl man die 'Buchstaben' entziffert hat, bleibt ihre Bedeutung unklar – für viele der ungefähr 30.000 identifizierten Gene beziehungsweise Genprodukte ist die molekulare Funktion noch ungeklärt und für die meisten sind keine detaillierten Eigenschaften bekannt. Das dynamische Zusammenspiel ist noch kaum untersucht. Mathematische und systemwissenschaftliche Ansätze zur Beschreibung dieser Vorgänge, lange Zeit vernachlässigt, rücken in der postgenomischen Ära ins Rampenlicht. Während molekulare und genomische Ansätze viele Daten liefern, kann die Systembiologie die Bausteine an molekularer Information wieder zusammenfügen. Quantitative und dynamische Modellierung werden essentiell, um biologisches Wissen zu organisieren und in seiner Komplexität zu verstehen. Modellanalysen werden schneller Einblicke liefern können als klassische Experimente, und insbesondere auch Einblicke in Vorgänge, die sich nicht leicht mit klassischen Experimenten erschließen lassen. Somit verspricht die Systembiologie nachhaltige Beiträge für die Medizin und Biotechnologie zu liefern. In den Worten von Cornish-Bowden (2006) wird dies nötig sein, um die Natur des Lebens zu verstehen, denn so lange Organismen nur als eine Ansammlung von Einzelteilen betrachtet werden, kann man nicht die richtigen Fragen stellen und diese sicherlich nicht beantworten.

Während die Systembiologie das System als Ganzes im Blick hat, lässt die Komplexität in der Biologie keine detaillierten und dynamischen Beschreibungen z. B. 'des Menschen' zu (und vermutlich wird sie das nie). Jedoch lassen sich Untersysteme und funktionelle Einheiten, welche mathematisch untersucht werden können, isolieren. Hierbei entsprechen Modelle nie 'exakt' der 'Wirklichkeit', und es ist wichtig, sinnvolle Ebenen der Abstraktion zu finden und sinnvolle Annahmen zu treffen, so dass Modellierung als eine Kunst angesehen werden kann. Aber, wie schon Pablo Picasso es formulierte, ist Kunst eine Lüge, die uns den Blick auf die Wahrheit eröffnet. Anders ausgedrückt, ein biologisches Modell mag nicht jedes bekannte Detail wiedergeben und dennoch neue Einblicke in Prozesse liefern, für die es konzipiert wurde.

Mathematische Modellierung hat eine lange Tradition und ist Standard in der Physik, Chemie und vor allem in vielen technischen Disziplinen. Wie beschrieben, ist sie noch nicht Standard in der Biologie. Diverse mathematische Modellbeschreibungen dynamischer Vorgänge sind bekannt und beinhalten Automaten, Boolesche Ansätze und diverse Typen von Differentialgleichungen. Viele grundlegende Ideen wurden in den Bereichen der mathematischen Biologie, Enzymkinetik und (bio-)chemischen Verfahrenstechnik entwickelt. In dieser Arbeit werden vor allem gewöhnliche Differentialgleichungen benutzt werden, die dynamische Änderungen von Proteinkonzentrationen beschreiben. Die Differentialgleichungen ergeben sich aus den betrachteten Reaktionen unter Annahmen bestimmter Kinetiken, wie dem Massenwirkungsgesetz oder der Michaelis-Menten-Kinetik.

Zusammenfassend lässt sich sagen, dass molekulare und genomische Ansätze viele Einblicke in die grundsätzliche Biochemie von Zellen liefern, während systemwissenschaftliche Ansätze tiefer gehende Erkenntnisse über das dynamische Zusammenspiel mehrerer Komponenten beitragen. Ein interessantes Verhalten, welches üblicherweise erst durch die dynamische Interaktion von mehreren Komponenten ermöglicht wird, ist, dass bestimmte zelluläre Signalwege kontinuierliche Eingänge in Alles-oder-Nichts Ausgänge umwandeln, obwohl die einzelnen beteiligten Komponenten kein solches Schaltverhalten zeigen. Dies ist im Allgemeinen für zelluläre Gedächtnis- und Entscheidungsprozesse wichtig. Ein für die Zelle wichtiger Entscheidungsprozess ist, ob sie einen programmierten Zelltod (Apoptose) ausführt oder nicht.

Programmierter Zelltod – Apoptose. Apoptose ist ein wichtiger physiologischer Prozess, durch den einzelne Zellen zum Wohl des Organismus als Ganzen abgetötet werden. Während dies oft als altruistischer Tod bezeichnet wird, könnte man auch von Todesstrafe oder Mord sprechen. Apoptose ist essentiell, um Zellen zu eliminieren, die alt, infiziert oder potentiell gefährlich sind oder einfach nicht länger benötigt werden.

Im menschlichen Körper sterben jeden Tag durchschnittlich 10 Milliarden Zellen, um ein Gleichgewicht mit neu hergestellten Zellen zu gewährleisten. Störungen oder Fehlregulationen dieser Homöostase sind an der Entstehung zahlreicher Krankheiten wie Krebs, Diabetes oder Alzheimer beteiligt. Dementsprechend wird der Apoptoseforschung weltweit viel Aufmerksamkeit gewidmet und mehr als 100.000 Publikationen zu dem Thema sind in wissenschaftlichen Datenbanken zu finden.

Apoptose kann extrinsisch durch Zytokine, oder intrinsisch als Antwort auf DNS- oder anderweitige intrazelluläre Schäden initiiert werden. Die unterschiedlich initiierten Wege konvergieren, und Caspasen können als Kernkomponenten der apoptotischen Maschinerie angesehen werden. Caspasen gehören zur Enzymfamilie der Proteasen. Dies sind Proteine, die andere Proteine spalten können. Caspasen werden in einer inaktiven Form produziert (Pro-Form oder Zymogen) und selbst durch proteolytische Spaltung aktiviert. Aktivierung und Aktivität werden durch zahlreiche weitere Proteine reguliert. Initiator-Caspasen nehmen apoptotische Stimuli wahr und spalten darauf hin Effektor-Caspasen. Deren Aktivierung führt zur kontrollierten Selbstzerstörung der Zelle, und die Reste werden anschließend von benachbarten Phagozyten aufgenommen, ohne Entzündungsreaktionen hervorzurufen.

Während die Aktivierung von Effektor-Caspasen innerhalb einer Population von Zellen normalerweise als langsamer Vorgang beobachtet wird, zeigen neue experimentelle Ergebnisse auf Einzelzellebene, dass diese sehr schnell aktiviert werden. Zwischen apoptotischem Stimulus und schlagartiger Aktivierung vergehen dabei oft mehrere Stunden (Verzögerungsphase), und Zellen innerhalb einer Population sterben zu unterschiedlichen Zeitpunkten, obwohl alle dem gleichen Stimulus ausgesetzt sind. Während in seltenen Fällen eine partielle Aktivierung von Initiator-Caspasen von physiologischer Relevanz zu sein scheint, führt die Aktivierung von Effektor-Caspasen unweigerlich zum Zelltod. Somit ist zwischen dem Eingang in die Caspase-Kaskade und dem Ausgang ein irreversibler Schaltvorgang zu beobachten.

Systembiologie und Apoptose. Schaltvorgänge (in der Apoptose) können mathematisch durch gewöhnliche Differentialgleichungen beschrieben werden, die Bistabilität erlauben. Bistabilität in biochemischen Reaktionsnetzwerken benötigt in der Regel zwei Vorraussetzungen auf Reaktionsebene. Die erste ist Ultrasensitivität, die ein Ein-/ Ausgangsverhalten (Stimulus-/ Antwortverhalten) beschreibt, welches sensitiver bezüglich des Eingangs ist als eine hyperbolische Michaelis-Menten-Kinetik (z. B. Hill-Kinetik). Die zweite ist eine positive Rückwirkung des Ausgangs auf den Eingang. Während diese Bedingungen für bestimmte Systemklassen notwendig sind, sind sie nicht hinreichend und sagen im Allgemeinen nichts über die notwendigen Parameterkonstellationen aus. Diese können durch Phasenraum und Bifurkationsbetrachtungen erschlossen werden. Eine Illustration von Bifurkationsanalysen im Zusammenhang der Apoptose ist in Abbildung 2.4 (Seite 19) ersichtlich.
Das Schaltverhalten in der Apoptose entscheidet über Leben und Tod einzelner Zellen. Somit erwartet man, dass diese Entscheidung robust ist und kleine Schwankungen im physiologischen Zustand der Zelle keinen starken Einfluss auf die Entscheidung haben. Allgemeiner kann Robustheit als die Erhaltung von Funktion in Anbetracht von Störungen bezeichnet werden. Robustheit wird als weit verbreitetes Prinzip für viele biologische Vorgänge postuliert und als Funktionsprinzip durch theoretische und experimentelle Betrachtungen unterstützt. Die Struktur komplexer Netzwerke als solche, wie auch spezifische Leistungsanforderungen führen jedoch zu einem Kompromiss zwischen Robustheit und Funktionalität und dem Auftreten von Schwachstellen (Fragilitäten). In Differentialgleichungsmodellen kann die Abhängigkeit des Verhaltens von Parameteränderungen durch Sensitivitätsanalysen untersucht werden. Hierbei wird oft von Linearisierungen des Systems ausgegangen. Sensitivitäten, teilweise an verschiedenen Stellen im Parameterraum ausgewertet, werden häufig als Maß für die Robustheit gewertet – wenn (lokale) Parameteränderungen nur einen geringen Einfluss zeigen, ist dies ein Zeichen für Robustheit gegenüber Parameteränderungen. Vor allem Differentialgleichungssysteme, die nichtlineare Phänomene wie Bistabilität zeigen, werden hierdurch jedoch nur begrenzt charakterisiert (und damit auch die mit diesen Modellen beschriebene Biologie). Robustheit gegenüber Parameteränderungen kann auch mit Hilfe von Bifurkationsanalysen untersucht werden, und Robustheitsmaße auf dieser Basis wurden beschrieben. Außer Parameterabhängigkeiten wird im Zusammenhang mit Robustheit teilweise auch der Einfluss von stochastischen Effekten untersucht.
Prinzipiell sind biologische Vorgänge stochastische Vorgänge. Vor allem bei Betrachtung kleiner Molekülzahlen ist eine kontinuierliche und deterministische Sichtweise, wie sie bei Verwendung von gewöhnlichen Differentialgleichungen implizit angenommen wird, oft problematisch. Die Va-

riabilität aufgrund des stochastischen Charakters von Reaktionen wird in dieser Arbeit als ‘intrinsisches’ Rauschen bezeichnet. Im Gegensatz hierzu werden beim ‘extrinsischen’ Rauschen äußere Einflüsse auf die Reaktionen betrachtet. Diese resultieren zumeist aus dem intrinsischen Rauschen in Prozessen, die im untersuchtem Modell nicht näher spezifiziert werden, oder außerhalb der betrachteten Systemgrenzen liegen. Zum Beispiel führt intrinsisches Rauschen in Transkription und Translation zu unterschiedlichen Proteinkonzentrationen in verschiedenen Zellen innerhalb einer Population. Auch wenn diese Vorgänge nicht im Detail im Modell berücksichtigt werden, wirkt sich dies z. B. in den Anfangsbedingungen der Differentialgleichungen aus. Somit lässt sich extrinsisches Rauschen mit Parameteränderungen in Verbindung bringen. Diese Thematik ist relevant für die Apoptose, da wie oben beschrieben, stochastische Effekte beobachtet werden – während einzelne Zellen schnell und zu verschiedenen Zeitpunkten schalten, zeigt die Population kein Schaltverhalten mehr, sondern ein langsames Anwachsen der Effektor-Caspase Aktivität. Dies kann als Mittelungseffekt gedeutet werden (vergleiche Abbildung 2.5, Seite 21).

Zusammenfassend wurde Apoptose hier als ein robustes, bistabiles System eingeführt. Die Beschreibung als ein solches ist im Laufe der Arbeit entstanden und gereift und stellt somit bereits ein erstes Teilergebnis dar. Einige Annahmen, wie die Rechtfertigung der Untersuchung des Systems anhand von Differentialgleichungen, werden durch erzielte Ergebnisse nachhaltig gestärkt. Andere Annahmen, wie die der Robustheit, werden kritisch evaluiert und diskutiert. Die Ergebnisse werden im Folgenden zusammenfassend vorgestellt.

Gliederung und Forschungsbeiträge der Arbeit

Der folgende Überblick erläutert die Gliederung der Dissertation und fasst die darin vorgestellten Beiträge kurz zusammen. Kapitel 1 und 2 beschreiben in erster Linie Grundlagen und gedankliche Konzepte wie oben stehend zusammengefasst. Kapitel 3 und 4 haben einen Schwerpunkt auf der Modellierung, die von grundlegenden Analysen begleitet wird. Kapitel 5 und 6 beschreiben weitergehende Analysen mit einem Fokus auf Sensitivität und Robustheit bezüglich Parameteränderungen und stochastischen Einflüssen. Kapitel 7 fasst die Ergebnisse bewertend zusammen und zeigt mögliche zukünftige Arbeitsrichtungen auf.

Kapitel 3 – Modellierung und Bistabilität einfacher Protease-Reaktionsnetzwerke – beschreibt verschiedene einfache Modelle interagierender Proteasereaktionen, welche durch Phasenraum- und Bifurkationsanalysen auf Ruhelagen und Stabilität untersucht werden (Eissing et al., 2007c). Drei Modelle werden beschrieben, die alle zwei Proteasen beinhalten und sich im Reaktionsmechanismus zur Generierung von Ultrasensitivität unterscheiden. Die Ultrasensitivität wird erzeugt durch *a)* Sättigungseffekte (nullter Ordnung), *b)* Inhibitoren und *c)* Kooperativität. In Kombination mit positiver Rückkopplung zwischen den Proteasen erlauben alle Modelle Bistabilität. Während zur Generierung von Ultrasensitivität nullter Ordnung klassischerweise Sättigungseffekte in den Rückreaktionen reversibler Reaktionen betrachtet werden, kann eine Sättigung im Protein-Abbau in irreversiblen Proteasenetzwerken denselben Effekt erzielen. Der Einfluss von Zymogenität wird untersucht. Die Analysen zeigen, dass dieser Einfluss vor allem die Generierung von Bista-

bilität durch den kooperativen Mechanismus erschwert. Die Ergebnisse sind unmittelbar für die Caspase-Kaskade, aber auch für weitere Signalwege wie den der Blutgerinnung, relevant.

Kapitel 4 – Modellierung und Bistabilität des direkten Weges der Rezeptor-induzierten Apoptose – beschreibt zwei Modelle, die den direkten Weg der Rezeptor-induzierten Apoptose widerspiegeln und vergleicht diese durch Bifurkationsuntersuchungen und Simulationsstudien (Eissing et al., 2004, 2005b).

Bifurkationsanalysen zeigen notwendige strukturelle und parametrische Voraussetzungen für Bistabilität in einem grundlegenden Modell auf. Zusammen mit in der Literatur beschriebenen kinetischen Informationen können Inkonsistenzen in der Literatursicht der Apoptose-Signaltransduktion offen gelegt werden. Ein zusätzlicher Regulationsmechanismus wird postuliert, welcher nun durch aktuelle experimentelle Ergebnisse anderer Gruppen gestützt wird. Das Modell reproduziert wichtige Verhaltensweisen, wie Toleranz von unterschwelligen Eingängen (Bistabilität) und eine schnelle Caspaseaktivierung nach einer Verzögerungsphase, deren Länge invers proportional zur Größe des Stimulus ist. Simulationsstudien zeigen, wie ein Zusammenspiel von verketteten Rückkopplungen das charakteristische Zeitverhalten von langsamen und schnellen Vorgängen ermöglicht.

Kapitel 5 – Sensitivitäts- und Robustheitsaspekte – beschreibt weiterführende Sensitivitäts- und Robustheitsuntersuchungen der zuvor vorgestellten Modelle (Cimatoribus et al., 2005; Eissing et al., 2005a, 2006, 2007a,b).

Unterschiedliche Sensitivitätsuntersuchungen und Simulationsstudien des erweiterten Apoptosemodells zeigen, wie das beobachtete Verhalten von den Parametern abhängt. Die Analysen zeigen z. B., dass hoch regulierte Inhibitoren, wie sie in zahlreichen Krebserkrankungen beobachtet werden, Zellen nicht nur wie bisher angenommen gegen apoptotische Stimuli desensibilisieren, sondern ebenfalls zur Aggressivität und Progression der Tumore beitragen könnten. Da diese Inhibitoren als Ziele zur medikamentösen Intervention erkannt wurden, liefern die Analysen somit Erkenntnisse von medizinischer und pharmakologischer Relevanz. Globalere Betrachtungen des qualitativen Systemverhaltens werden als Indikatoren für Robustheit herangezogen. Ein Robustheitsmaß, basierend auf einem Monte Carlo Ansatz zur Bestimmung des Gebietes im höherdimensionalen Parameterraum, welcher Bistabilität erlaubt, wird beschrieben. In Kombination mit anderen in der Literatur beschriebenen Maßen wird die Robustheit der vorgestellten Modelle untersucht und verglichen. Die Analysen zeigen, dass alle drei in Kapitel 3 eingeführten Mechanismen grundsätzlich ein robustes bistabiles Verhalten erzeugen können und berichtigen damit anderweitige Literaturergebnisse. Der Vergleich der in Kapitel 4 beschriebenen Modelle zeigt, dass die Modellerweiterung auch die Robustheit verstärkt. Des Weiteren erlaubt die Modellerweiterung vor allem eine schnelle Caspaseaktivierung in Kombination mit langsameren Halbwertszeiten der beteiligten Proteine, was im Einklang mit biologischen Messungen ist.

Kapitel 6 – Stochastische Einflüsse – untersucht den Einfluss von stochastischen Effekten anhand von stochastischen Simulationen und deterministischen Simulationen mit Parametern mit stochastischen Verteilungen (Eissing et al., 2004, 2005a).

Stochastische Simulationen der Apoptosemodelle zeigen, wie Inhibitoren als Rauschfilter wirken und die Variabilität aufgrund der intrinsischen Stochastizität stark begrenzen. Demgegenüber können Parameter mit stochastischen Verteilungen, die biologisch motiviert werden, experimentell beobachtete stochastische Effekte erklären und erlauben ein besseres konzeptionelles Verständnis

von widersprüchlichen Ergebnissen in Experimenten an einzelnen Zellen gegenüber Zellpopulationen.

Kapitel 7 – Schlussfolgerungen – fasst die Ergebnisse zusammen und zeigt an aktuellen Arbeiten, die auf den Ergebnissen dieser Arbeit basieren, potentielle zukünftige Arbeitsrichtungen auf (Chaves et al., 2006, 2008; Schliemann et al., 2007; Waldherr et al., 2007). Ausgewählte Aspekte werden zusammenfassend diskutiert und bewertet.

Möglichkeiten zur experimentellen Verifikation bestimmter Modellaussagen werden dargelegt, welche teilweise derzeit bearbeitet werden (Institut für Zellbiologie und Immunologie, Universität Stuttgart). Potentielle Erweiterungsmöglichkeiten der vorgestellten Modelle und Analysemethoden werden beschrieben. Eine Erweiterung beinhaltet die Integration anti-apoptotischer Signalwege. Die in diesem Zusammenhang weitergehend diskutierte physiologische Bedeutung ermöglicht eine zusammenfassende Interpretation der in Kapitel 5 und 6 erzielten Ergebnisse. Zellen scheinen einen vorteilhaften Kompromiss zwischen Robustheit und Verhaltensanforderungen gefunden zu haben, welcher durch die Netzwerkstruktur und evolutionäre Selektionsbedingungen vorgegeben wird. Einerseits wird das intrinsische Rauschen gefiltert und das qualitative Modellverhalten ist vergleichsweise robust, um sorgfältige Entscheidungen zu gewährleisten. Andererseits erlaubt die Sensitivität von quantitativen Aspekten eine Beeinflussung des Verhaltens durch interagierende Signalwege und weiterhin eine Variabilität innerhalb einer Population von Zellen. Eine solche Variabilität wird in Experimenten beobachtet und ist, wie aktuelle Arbeiten aus dem Bereich der Immunologie zeigen, wahrscheinlich von wichtiger physiologischer Bedeutung zur Regulation von Immunantworten. Die Analysen zeigen ebenfalls, dass dieser Kompromiss zu Schwachstellen führt, die von klinischer Relevanz sind.

Zahlreiche Ergebnisse dieser Arbeit sind nicht auf die Apoptosesignaltransduktion beschränkt, sondern konzeptionell relevant für weitere Signalwege und deren systemwissenschaftliche Betrachtung. Auf die anfängliche Frage von Erwin Schrödinger zurückkommend lässt sich abschließend bemerken, dass die Komplexität biologischer Vorgänge momentan keine einfache mathematische Beschreibung erlaubt. Dennoch zeichnen sich Grundmuster und Gesetzmäßigkeiten ab, die zukünftige Modellierungsansätze erleichtern werden und schon jetzt zu einem besseren Verständnis der Biochemie des Lebens beitragen.

Chapter 1

Introduction

This chapter introduces how systems science ideas have been recently applied to biological processes. The demand for a systems approach to increase biological understanding is motivated. As described in Section 1.1, the field of systems biology emerged and has been growing enormously in recent years to be considered by now as an own scientific (inter-)discipline. Section 1.2 relates the general framework of systems biology to the more specific aspects of this thesis: apoptosis, bistability, and robustness. The structure of the thesis is outlined and main contributions are stated. Extended introductions to the special aspects directly relevant for the rest of the thesis are provided in Chapter 2.

1.1 Systems biology

In his famous book "What is life?" Erwin Schrödinger asked whether the known physical laws apply to biology (Schrödinger, 1944). Physical laws are typically captured in mathematical expressions. Although it has become clear by now that in principle the known physical laws do apply to the chemistry of life, a mathematical description based on these laws remains difficult. And although the basic ideas are anything but new, there is now a strong demand and a renewed interest in perusing such approaches in the emerging field of systems biology.

Systems biology is a wholistic approach to understanding biology (Chong and Ray, 2002). It aims at system-level understanding of biology, and to understand biological systems as a system. This means an examination of the structure and dynamics of cellular and organismal function, rather than the characterisation of isolated parts of a cell or organism (Kitano, 2002b). Many properties of life arise at the systems level only, as the behaviour of the system as a whole cannot be explained by its constituents alone. Only the dynamic interaction of different constituents shapes the behaviour of the whole. Prominent examples for biological systems are the immune system or the nervous system, which already have the word system included – but where system-level understanding is still far away.

Systems biology is an interdisciplinary field of research that has been witnessing a strongly growing interest in the last decade and is spanning a large area of science, attracting ideas from many different disciplines. Diverse definitions for systems biology have been proposed. Recently, the constituent 'systems' is sometimes interpreted as 'systematic' (in the sense of systematic and large

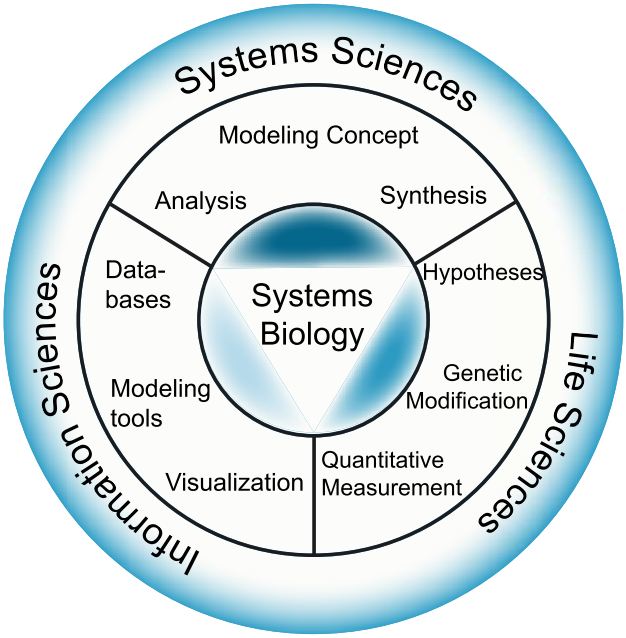

Figure 1.1: Systems biology overview (www.sysbio.de).

scale data generation). However, the origin and the interpretation used here is different. The particular aspect about systems biology distinguishing it from other areas such as bioinformatics is the contribution of the systems sciences (Mesarović, 1968; Rosen, 1968; Wolkenhauer and Mesarović, 2005; Cornish-Bowden, 2006). At the heart of systems sciences in this context are mathematical modelling based on available biological knowledge and model analysis using mathematical tools from systems theory (compare Figure 1.1). This approach then motivates further biological experiments to test model predictions. The new experimental data can either support the model or be used to refine the model formulation. A systems approach can indicate requirements on single molecular species, e.g. regarding their kinetic properties. Most notably, properties are highlighted that cannot be attributed to single molecules but only emerge at the network level.

The multi-disciplinary character as well as the recent and enormous interest in systems biology is evidenced by the fact that various journals from different scientific domains have dedicated special issues to this field of activity (e.g. Chaos 11:227 (2001), Nature Insight 420:6912 (2002) & Connections Series (2007), Science 295:5560 (2002) & 301:5641 (2003), IEEE Control Systems Magazine 24:4 (2004), Nature Biotechnology 22:10 (2004), Computers & Chemical Engineering 29:3 (2005), Nature Reviews Molecular Cell Biology 7:11 (2006)) and new dedicated journals have been established (e.g. BMC Systems Biology, IET Systems Biology, Molecular Systems Biology). The ideas of system-level understanding and mathematical modelling are not new to biology as evidenced by well-known older publications, e.g. Wiener (1948); Hodgkin and Huxley (1952); Mesarović (1968); Bertalanffy (1969). However, the recent popularity can be attributed to the breakthrough advances in molecular biology in the last decades providing new data and new challenges.

Biological basics, challenges in the post-genome era, and the need for systems biology. Biology is a thriving science where exciting new discoveries are made almost on a daily basis. Thereby, biology has always been in close touch to other scientific disciplines, which strongly contributed

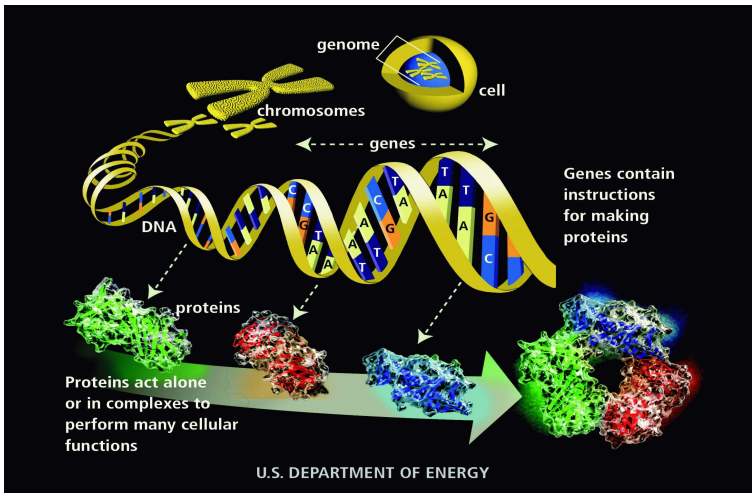

Figure 1.2: Central dogma of molecular biology – simplified view by U.S. Department of Energy Genome Programs (http://genomics.energy.gov).

to its development. Quantitative reasoning based on mathematical considerations had strong and driving influences on biology (Wingreen and Botstein, 2006). However, with the emergence of molecular biology and modern genetics, many exciting questions were raised and answered that did not require mathematical models. As a result, a qualitative understanding of many processes that make up life has emerged.

The principle unit of life is the cell. It is a chemical system where thousands of reactions and transformations are carried out to allow its own survival and reproduction. The human body consists of approximately 10^{14} cells, which can be grouped into tissues and organs. The cell itself can be sub-grouped into organelles, which reside in the cytoplasm and are separated by membranes. One of these is the nucleus where deoxyribonucleic acid (DNA), the molecule of inheritance, is the major constituent. The helical structure of the double strand was discovered by Watson and Crick (1953).

Importantly, DNA encodes for proteins, the work horses of the cell. Proteins are composed of amino acids. Decoding is accomplished by transcribing DNA information into messenger ribonucleic acid (mRNA), which is translated into protein. This flow of information is often referred to as the central dogma of molecular biology (Figure 1.2). Oversimplified, one gene codes for one protein, and a triplet of three bases determines the corresponding amino acid in a linear fashion. Twenty different amino acids offer a wide variety of physiochemical properties important for the intimately connected folding and function. Proteins can act as enzymes, catalysing chemical reactions, e.g. those involved in metabolism providing energy or those replicating or transcribing DNA, as scaffolding proteins giving the cell shape and structure, or as motor proteins enabling motility of the cell or within the cell.

Another important role of proteins is that of signalling. They are required to receive, integrate and distribute signals that regulate cellular function. Thereby, different levels of regulation can be distinguished. In principle, the amount of a certain protein can be regulated first by the amount of production and second by its stability (time of permanency). Further, the activity of the protein can be modified representing another level of regulation. This very short description of basic biological

principles is extended in many excellent textbooks, e.g. Alberts et al. (2002), Berg et al. (2007). A specific introduction to the biology immediately relevant to this thesis is provided in Section 2.1.

Although many principle aspects are understood, a detailed and dynamic understanding remains elusive and by now the wealth of information about molecular players and their interactions is becoming overwhelming and cannot be understood by merely drawing pictures and looking at them. The human genome project does not mark the completion but the beginning of the next level of understanding. Although the letters of the book of life have been deciphered, their meaning remains unclear – many of the about 30,000 identified genes have so far no ascribed molecular function and for the majority of them detailed properties remain elusive. The system properties emerging from their dynamic interactions have been hardly investigated. Mathematical biology and engineering approaches towards the cell or an organism, for a long time rather peripheral sciences, are emerging as the "post-(gen)omic" frontiers. Whereas the "-omic" technologies produce large amounts of data that are orchestrated by bioinformatics, systems biology is promising to integrate the wealth of information and put the molecular biology pieces back together.

Quantitative and dynamic modelling approaches describing cellular and physiological processes will become essential to organize and understand biological complexity. The analysis of these models will allow to more rapidly test biological hypotheses and provides insight not easily accessible by classical experimentation. Thereby, systems biology is promising to make a strong and lasting contribution to biotechnology and medicine. At a more abstract level, as for example Cornish-Bowden (2006) argues, it is necessary for the understanding of the nature of life, because as long as an organism is treated as no more than a collection of components, one cannot ask the right questions, and certainly cannot answer them.

While systems biology is aiming to understand the system as a whole, the complexity intrinsic to biology does currently not allow a detailed and dynamic description of systems as complex as a human organism (and probably never will). However, subsystems and functional modules can be identified and isolated (Hartwell et al., 1999; Kitano, 2002a; Kurata et al., 2006; Lauffenburger, 2000; Saez-Rodriguez et al., 2004, 2005; Yi et al., 2000). These are open to mathematical modelling but not even the most detailed model can exactly reproduce the 'real world'. Rather, it is important to find a useful level of abstraction, which requires reasonable assumptions, making modelling an art. But, as Pablo Picasso argued, art is a lie that makes us realize the truth (Wolkenhauer and Mesarović, 2005). In other words, a biological model might not reproduce every piece of knowledge but still reveal new insight into what it was conceived for.

Mathematical modelling of biological processes. Mathematical modelling approaches have a long tradition and are standard in physics, chemistry and many technical disciplines. As outlined in the previous paragraphs, they are not yet standard in biology, although having a rather long history there as well. Very diverse mathematical notations have been successfully employed and many basic ideas have been developed in the areas of mathematical biology, enzyme kinetics and chemical engineering. In particular the branch of systems biology focussing on high-throughput data to build static interaction maps relies on graph theoretical approaches (Mason and Verwoerd, 2007). Here we will focus on approaches to capture the dynamic aspects of biological systems. Popular modelling approaches include automata, Boolean descriptions and stochastic, partial, de-

lay or ordinary differential equations (De Jong, 2002; Fall et al., 2002; Klipp et al., 2005; Ventura et al., 2006).
In this thesis, we will mainly focus on ordinary differential equations (ODEs) based model descriptions, which is a common approach for biochemical networks based on chemical kinetics. ODEs do not capture spatial behaviour and state variables develop in a continuous and deterministic fashion. A process described by ODEs should therefore be well approximated by such a description. In an ODE, the concentrations of n biological compounds like proteins can be represented as state variables x_i, which can be grouped into a vector $x \in \mathbb{R}^n$. ODEs describe how x, i.e. the compound concentrations, changes over time. A common notation for biochemical ODEs is

$$\frac{dx_i}{dt} = \dot{x_i} = \sum_{j=1}^{m} T_{i,j} J_j(x,p) \qquad i = 1...n, \tag{1.1}$$

where $T \in \mathbb{R}^{n \times m}$ is the stoichiometric matrix and $J \in \mathbb{R}^m$ is the rate (or flux) vector, which depends on the current state x and the parameter vector $p \in \mathbb{R}^q$. The notation captures the common derivation of biochemical ODEs. Biochemical reactions are translated into rates, e.g. using mass action or Michaelis-Menten kinetics, and the stoichiometric matrix entry $T_{i,j}$ associates how the rate J_j influences the compound concentration x_i. In this thesis, we will both use expanded versions of the autonomous ODE system (1.1) and more compactly rewritten versions employing the vector notation for the states

$$\dot{x} = TJ(x,p) = f(x,p), \tag{1.2}$$

where $f : D \to \mathbb{R}^n$ is a vector field on domain $D \subset \mathbb{R}^n \times \mathbb{R}^q$.
Apart from efficient simulation, ODEs are accessible by a wide variety of additional analysis techniques. In fact, mathematical modelling is only the first step to understanding and has to be followed by model analysis. Only the analysis will unveil the true power of mathematical modelling to reveal characteristic properties of the models and the processes described thereby. Important characteristics include attraction phenomena such as steady state behaviour or limit cycles (oscillations) and transients. Despite the inherent nonlinearity of biological systems, chaotic attractors appear to be of less importance (Shmulevich et al., 2005). Biological processes rather operate in an ordered regime and are robust against perturbations as is also supported by the analysis of various mathematical models (Stelling et al., 2004b). The modelling and analysis concepts employed throughout this thesis will be illustrated and motivated in Section 2.2, and detailed at the relevant places. The basic ideas are also introduced in several good text books on nonlinear systems, e.g. Khalil (2002); Strogatz (2001), or books more directly aiming at biochemical systems, e.g. Fall et al. (2002); Keener and Sneyd (1998); Klipp et al. (2005).

1.2 About this thesis

The general framework of this thesis, i.e. applying systems science ideas to biological processes, implies interdisciplinarity. In addition, the integration of systems and biological sciences has only recently become more widespread. Therefore, this framework has been introduced and motivated

from a broader perspective. Of course, the contributions of this thesis are more focussed on selected aspects, which will be shortly outlined in the following.
From a biological point of view, the main motivation is a better understanding of apoptosis signalling. Apoptosis, also called programmed cell death, is a very important biological process that can eliminate selected cells for the benefit of the organism as a whole. It is crucial during development and for cellular homoeostasis balancing cellular reproduction. In the adult human approximately 10 billion cells die every day to balance those reproduced during mitosis (Heemels et al., 2000). Too little apoptosis and uncontrolled reproduction are hallmarks of cancer whereas too much apoptosis is implicated in neurodegenerative diseases such as Alzheimer (Danial and Korsmeyer, 2004; Hanahan and Weinberg, 2000).
From a systems science perspective, this thesis provides new mathematical models of apoptosis signalling. Moreover, an in-depth analysis is carried out focussing on the view of apoptosis as a robustly bistable system. The analysis provides new biological insight and hypotheses, which are currently under experimental investigation. Also, design principles and possibilities to achieve important characteristics in apoptosis signalling based on biochemical reaction networks are indicated. For example, it is shown that interlinked feedback loops in apoptosis signal transduction allow a fast and decisive switching from normal cell growth to cell death, after a decision or delay phase, which allows cells to integrate additional signals. During this signal transduction, inhibitors function as noise filters to reduce stochastic influences. Moreover, an interesting trade-off between robustness and performance, and further, fragilities of medical relevance are indicated.

Outline. Chapter 1 introduces and motivates a systems approach towards biology. The more specific topics of this thesis are motivated in Chapter 2 introducing the relevant (systems) biological ideas. The main results of the thesis are then structured into two chapters with a focus on modelling combined with basic analysis (Chapters 3 & 4) followed by two chapters with an extended analysis (Chapters 5 & 6) before conclusions are presented in Chapter 7. Parts of the chapters are based on publications as indicated in the “Contributions” paragraph (below).
Chapter 2 introduces the background on the main topics of the thesis: apoptosis, bistability, and robustness. It also introduces key ideas and observations relating those aspects to form the basis for the models and analyses presented in the following.
Chapter 3 presents simple models of the biochemical setup encountered during apoptosis signalling but also during blood clotting or other cellular processes. Principle ways for generating bistable behaviour in such simple biochemical networks are established using phase plane and bifurcation analysis. Chapter 4 more specifically addresses the direct pathway of receptor induced apoptosis. Mainly again employing bifurcation analysis, a model as outlined by literature knowledge is falsified before a model extension is presented to match experimental observations as illustrated by simulation studies. Further, it is discussed how the different components and reactions act in concert to achieve the desired characteristics.
Chapter 5 describes different sensitivity and robustness results for the presented models considering parameter perturbations. Sensitivity analyses indicate an important role for inhibitors of apoptosis. These results are relevant for possible future model extensions and also indicate how these molecules could contribute to cancer progression. While most known sensitivity and robustness measures mainly provide local information and require a reference parameter set, we devise a

Monte Carlo approach overcoming these restrictions. Mainly employing this approach, the robustness of the different models is analysed highlighting that different mechanisms are equally capable of producing a robust bistable behaviour and that the model extension in the direct pathway also increases the robustness. Chapter 6 evaluates the influence of noise as an additional perturbation. Stochastic simulations of the apoptosis models complement and support the deterministic framework applied in the other chapters indicating that the inhibitors filter out noise by functioning similarly to a chemical buffer. However, stochastically distributed parameters and inputs influence the deterministic single cell model behaviour. Such distributions conceptually enable a reconciliation of stochastic effects observed on the single cell level with average results observed on the population level within a deterministic framework.
Chapter 7 summarizes the thesis and discusses selected aspects, before a perspective on selected facets and possible future research directions concludes the thesis.

Contributions. The main contributions of the thesis can be summarized as follows:

- mathematical modelling of apoptosis signalling
  - interpretation, description and evaluation of apoptosis and caspase activation as a bistable process (Chapters 2 and 4; Eissing et al., 2004, 2005b)
  - requirements and design principles to generate ultrasensitivity and thereby bistability in proteolytic cascades such as encountered in apoptosis (Chapter 3; Eissing et al., 2007c)
- bifurcation analysis and simulation studies
  - revelation of inconsistencies in current literature view of receptor induced apoptosis and proposal of a new regulatory mechanisms now supported by experimental data (Chapter 4; Eissing et al., 2004)
  - revelation of system properties responsible for characteristic signalling behaviour (Section 4.3)
- sensitivity and robustness analysis
  - indication how IAPs can contribute to tumour progression outlining drug targeting strategies (Section 5.1; Eissing et al., 2006)
  - a new robustness measure based on higher dimensional bistability evaluation (Section 5.2; Eissing et al., 2005a, 2007a)
  - evidences that basic design principles are similarly robust (Section 5.3; Eissing et al., 2007b)
  - evidences that certain model extensions increase robustness (Section 5.4; Eissing et al., 2005a)
- evaluation of stochastic influences
  - revelation how inhibitors can function as noise filters (Section 6.1; Eissing et al., 2005a)

– a conceptual framework for reconciling single cell and population data (Section 6.2; Eissing et al., 2004)

Further, the models derived have stimulated further investigations by colleagues within the group (Bullinger, 2005; Chaves et al., 2006, 2008; Cimatoribus et al., 2005; Schliemann et al., 2007; Waldherr et al., 2007) and other groups (e.g. Carotenuto et al., 2007a,b; Choi et al., 2007; Nordling et al., 2007).

Chapter 2

Cell Death as a Robustly Bistable System

This chapter introduces the background and literature on the main topics of this thesis: apoptosis, bistability, and robustness. Further, key ideas and observations relating those topics are introduced and illustrated. These considerations motivate the models and analyses presented in the rest of the thesis. Section 2.1 provides an overview on the current knowledge of apoptosis relevant for this thesis. Section 2.2 introduces the systems biology aspects, which will be deepened in the following chapters. Mathematical modelling approaches to apoptosis signalling are summarized in Section 2.2.1. One developing research direction is based on the perception, introduced by our work, of viewing apoptosis as a bistable system. Bistability in cell signalling will be introduced in Section 2.2.2, and its interpretation explained in the context of apoptosis. The topic is deliberately introduced in a figurative way to also carry over the ideas to people less familiar with (nonlinear) dynamical systems. Thereafter, robustness aspects of biological systems are introduced in Section 2.2.3, and the relevance to apoptosis signalling is motivated. Finally, important differences between single cells and populations of apoptotic cells are illustrated in Section 2.2.4. The differences observed can be understood and reconciled within a stochastic framework and general stochastic influences in biological systems are discussed.

2.1 Apoptosis – programmed cell death

Apoptosis, also called programmed cell death, is a very important biological process to eliminate selected cells for the benefit of the organism as a whole. While it is often referred to as an 'altruistic' death, one might as well classify it as capital punishment or murder. The apoptotic program is essential to remove cells that are old, infected, potentially dangerous, or no longer needed. As discussed in the introduction, in the adult human approximately 10 billion cells die every day to balance those reproduced during mitosis (Heemels et al., 2000). Imbalances or misregulation are implicated in severe pathological alterations. Accordingly, apoptosis has attracted a lot of attention in the last decades resulting in more than 100,000 publications relating to the topic (PubMed[1] or ISI Web of Science[2] search for "apoptosis"). Therefore, a truly comprehensive overview is hardly possible and certainly beyond the scope of this thesis. In the following, we will overview the most

[1] http://www.ncbi.nlm.nih.gov/entrez/
[2] http://portal.isiknowledge.com/

important aspects, focussing on those relevant for this thesis. We will begin with an overview on apoptosis signalling pathways in human cells, although similar molecules and pathways can be found in many other organisms. The physiological role of death receptors, which are at the beginning of one important apoptotic route, will be introduced next. Finally, we will provide additional information on the reactions at the heart of apoptosis, which will be a focus in this study. Similar reactions occur in other important signalling pathways such as blood clotting. Although the names of the involved proteins differ, the mathematical interpretation and treatment can be considered analogous. Therefore, several results of this thesis focus on apoptosis signalling but are of relevance beyond this pathway.

Overview on apoptosis signalling. Two principle routes of apoptosis signalling can be distinguished, as outlined in Figure 2.1. Firstly, apoptosis can be triggered externally (extrinsic pathway), e.g. by certain cytokines binding to so-called death receptors. Secondly, apoptosis can be triggered internally (intrinsic pathway), e.g. in response to DNA or other intracellular damage (Danial and Korsmeyer, 2004; Hanahan and Weinberg, 2000; Hengartner, 2000). Both pathways converge and lead to the activation of caspases, which are central in apoptosis signal transduction. Caspases are enzymes that are able to cleave selected other proteins. The cleavage can result in the activation or deactivation of target proteins. Caspases are produced in an inactive pro-form (zymogen) and themselves become activated through proteolytic cleavage. Initiator caspases sense apoptotic stimuli and propagate the signal to executioner caspases. These cleave many targets within the cell leading to its destruction and removal. For example, an inhibitor of the Caspase Activated DNase (CAD) is cleaved, liberating the DNase to fragment nuclear DNA.
Internally triggered apoptosis proceeds via mitochondrial cytochrome c (cyt C) release leading to the activation of the initiator caspase 9 (C9; Jiang and Wang, 2004). Caspase 9 then activates executioner caspases, most prominently caspase 3 (C3). Externally triggered apoptosis is initiated by the activation of receptor associated initiator caspases, most prominently caspase 8 (C8) (Debatin and Krammer, 2004). It then proceeds either also via the activation of the mitochondrial pathway (type II) or by direct activation of caspase 3 (type I; Samraj et al., 2006; Scaffidi et al., 1998, 1999). Thus, caspases are at the heart of the apoptosis pathway, dismantling cells, which are then packaged into small membrane-bound fragments for engulfment and disposal by neighbouring phagocytes without invoking inflammation (Eckelman et al., 2006; Savill and Fadok, 2000).
The caspase activation steps are regulated at different levels, e.g. Bcl-2 family member proteins regulate the mitochondrial cytochrome c release, Inhibitor of Apoptosis Protein (IAP) family members inhibit activated caspases 3 and 9, and FLICE-inhibitory proteins (FLIPs) block the activation of receptor associated initiator caspases in the death inducing signalling complex (DISC). In addition, several feedback loops have been established yielding a complex reaction network (Sohn et al., 2005; Stennicke and Salvesen, 1999).
Importantly, recent experimental evidences show that key steps during apoptosis, including caspase activation, are generally very rapid processes. Experiments in which apoptosis is triggered by serine/threonine phosphatase inhibitors show a full caspase activation within only 3 minutes (Fladmark et al., 1999). Also upon extrinsic induction of apoptosis via caspase 8/10, the development of the whole apoptotic program can be very fast. When cells over-expressing TNF receptor/Fas chimera were stimulated with the respective agonists, most of the cells showed the phenotype of

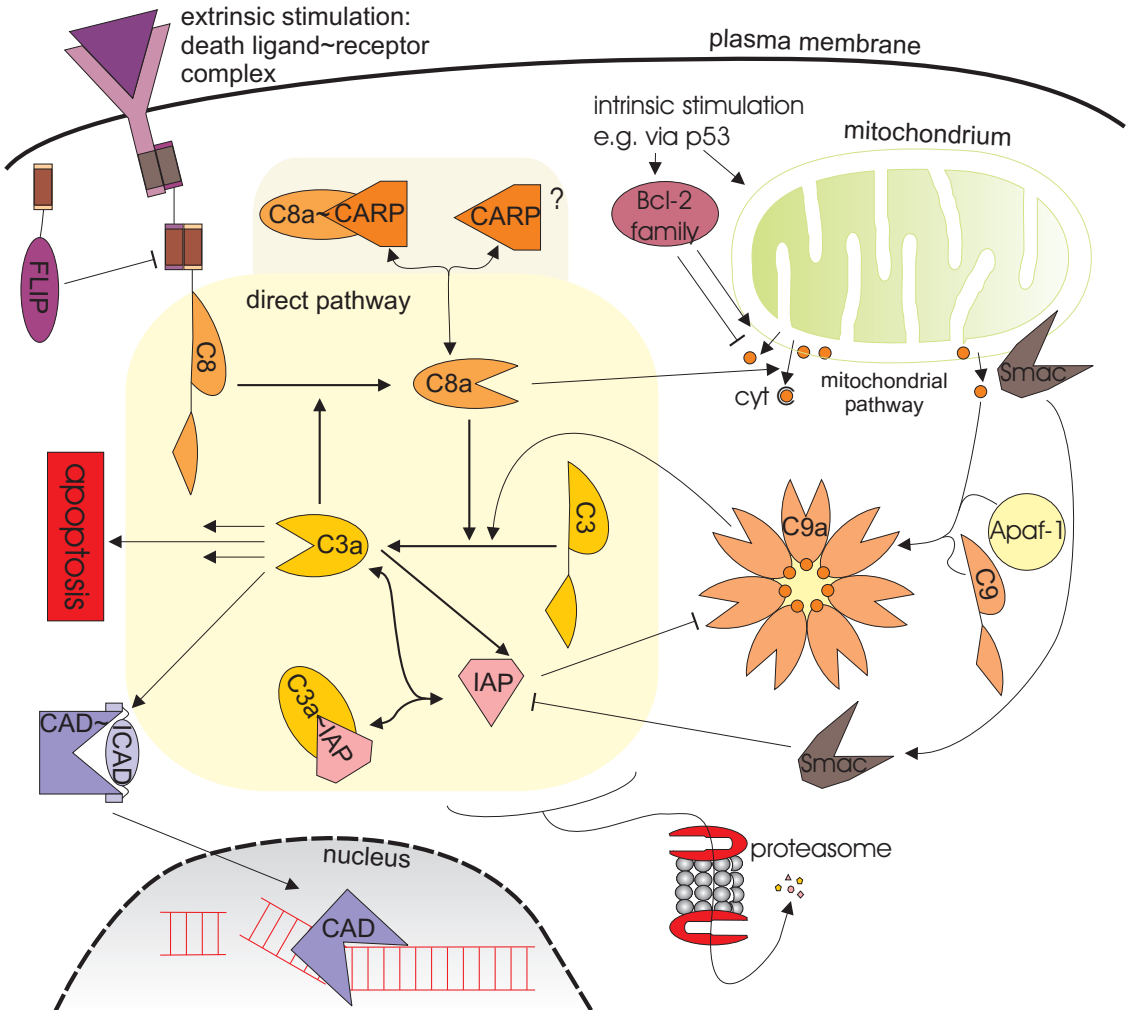

Figure 2.1: Apoptosis signalling pathways. Extrinsic and intrinsic pathway converge on caspase activation.

apoptosis within 40 minutes (Krippner-Heidenreich et al., 2002; and unpublished data, Institute of Cell Biology and Immunology, University of Stuttgart). Further experimental support for a rapid development of caspase 3 activation comes from studies performed at the single cell level (Goldstein et al., 2000; Luo et al., 2003; Rehm et al., 2002, 2006; Tyas et al., 2000). Interestingly, these single cell studies reveal a delay of up to several hours before the fast events can be measured (see Section 2.2.4).

The above overview shows that caspases are at the heart of apoptosis signal transduction and are generally rapidly activated within a single cell. Caspase activation and activity are regulated by different mechanisms, embedding them into a complex reaction network.

Death ligands and Tumor Necrosis Factor signalling. This thesis focuses mainly on the extrinsic pathway of apoptosis. Extracellular signals (death ligands) are sensed by the corresponding members of the death receptor family. These receptors are integrated throughout the plasma membrane and are crucial to transform extracellular signals into intracellular ones. After ligand binding, a death-inducing signalling complex (DISC) is formed, which leads to the activation of intracellular caspase 8 (Chen and Goeddel, 2002; Wajant, 2002). Death receptors are part of the Tumor

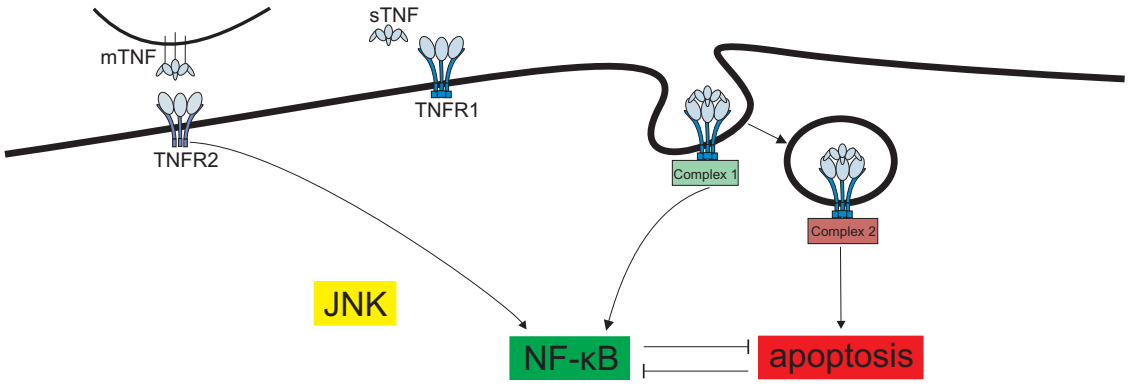

Figure 2.2: TNF signalling pathways overview. See Figure 7.1 for a more detailed illustration of TNFR1 signalling pathways.

Necrosis Factor Receptor (TNFR) superfamily of receptors. Other family members besides the name giving TNFR1 include Fas (also called Apo-1 or CD95) and TNF-related apoptosis inducing ligand (TRAIL) among others (Wajant et al., 2003b).

Interestingly, TNFR1, as well as other death receptors, induce proliferation and survival signals in parallel to the induction of apoptosis. Well defined signalling pathways initiated in this context include the Mitogen-Activated Protein (MAP) kinase cascade and the Nuclear Factor κB (NFκB) pathway (Hsu et al., 1995; Janes et al., 2005, 2006; Perkins, 2007; Wajant et al., 2003a). For example, soluble TNF (sTNF or simply TNF) initiates the NFκB and the apoptotic pathway in a sequential manner. First, a signalling complex 1 is formed to activate the NFκB pathway, then a signalling complex 2 is formed, which activates caspases (Figure 2.2). The signalling complexes are distinguished by the adapter proteins they contain, and it is these adaptors that determine the signalling events initiated (Micheau and Tschopp, 2003; Schneider-Brachert et al., 2004; Wajant et al., 1999, 2003b). In addition, the c-Jun N-terminal Kinase (JNK) is activated by TNF. Whether this pathway inhibits or facilitates apoptosis signalling is still a matter of debate. Matters are even more complicated when not soluble but membrane bound TNF (mTNF) is the primary stimulus. mTNF can in addition to TNFR1 also trigger TNFR2. TNFR2 can as well activate the NFκB pathway but not apoptosis (Grell et al., 1994, 1995, 1998, 1999). In addition, TNFR2 exerts indirect effects by competing with TNFR1 for adaptor proteins and by inducing autocrine TNF signalling on longer time-scales (Fotin-Mleczek et al., 2002; Grell et al., 1999; Weingärtner et al., 2002). Nevertheless, TNFR1 is thought to be the dominating TNF receptor in most physiological settings.

The short overview on TNF signalling indicates that a rather complex interplay of pro- and anti-apoptotic signalling pathways finally decides on the life and death of individual cells. This interplay will not be the focus of this study but will rather be discussed as an outlook (Section 7.2). Still, it is important to bear the physiological context in mind, when evaluating the apoptotic core reactions in the following chapters. Interestingly, the basic principles of the core reaction mechanisms are not restricted to apoptosis as will be shortly outlined next.

Caspases and wider relevance of proteases. As introduced, caspases are at the heart of the apoptotic program. Caspases belong to the family of proteases. From a signalling point of view, proteases are special enzymes distinguished by their ability to transmit signals by hydrolysing the

peptide bond between amino acids resulting in the cleavage of proteins (or polypeptides). They can either recognize specific amino acid sequences and cleave specific peptide bonds (limited proteolysis) or break down complete proteins (unlimited proteolysis). Proteases are divided into different classes based on the exact reaction mechanism they depend on (i.e. which amino acids are involved in the nucleophilic attack). Caspases, for example, depend on cysteine (C) in their active centre and specifically recognize and cleave the target protein at aspartic acids (asp, hence the name). Proteases are a wide-spread class of enzymes implicated in diverse metabolic and regulatory functions. This study focuses on protease cascades, i.e. inter-winded protease reactions. The role of specific protease inhibitors will be evaluated at several places.

Apart from apoptosis signalling, similar reaction schemes can be found in other areas of biology (Eckelman et al., 2006). The blood clotting system heavily relies on the proteolytic cleavage of key regulators and clotting substrates with several inhibitors and feedback loops being known (Beltrami and Jesty, 1995; Dahlbäck, 2000; Zarnitsina et al., 2001). Several proteins of the complement system are proteases and again specific inhibitors are known (Bureeva et al., 2005; Carroll, 2004; Janeway et al., 2004). Further, proteases such as cathepsin or metallo-proteases are implicated in many regulatory processes within and outside of the cell, also critically involved in diverse and severe diseases (Dash et al., 2003; Grabowskal et al., 2005; Overall and López-Otín, 2002; Sloane et al., 2005; Thurmond et al., 2005; Yamashima, 2004).

The above overview shows that reaction networks of interacting and mutually activating proteases are frequently used in cellular systems and that one important role is the finding or execution of cellular decisions. Decisions often involve molecular switches that convert continuous inputs into discrete outputs to safeguard transitions between different cellular states. When using ODEs to describe these processes, steady states of the ODE system correspond to these cellular states and a switch is commonly represented by a bistable system (Section 2.2.2).

In summary, apoptosis was introduced as an important physiological process. Caspases are at the heart of apoptosis signalling and execution. Caspase activity is controlled by different mechanisms involving feedback loops and the activation displays interesting dynamic features. Similar reaction schemes are found in other physiological processes. Therefore, apoptosis signalling is an interesting object for a systems biology approach to reveal additional features not easily understood by classical experimental approaches. The rapid development of apoptosis research as well as the need for systems biology approaches has been highlighted by Lazebnik (2002) from a very entertaining perspective.

2.2 Systems biology of apoptosis

Biological signal transduction allows the coordination of the different processes defining life. The transduction, integration and processing of these signals is a complex and dynamic process that cannot be deeply understood by only drawing pictures such as shown in Figure 2.1. The knowledge has to be organised into mathematical models to reveal reoccurring motifs and allow understanding of phenomena such as biological switches, rhythms, or adaptation (Bhalla and Iyengar, 1999; Bhalla et al., 2002; Ferrell, 1996, 1997, 2002; Ferrell and Xiong, 2001; Ingolia and Murray, 2002;

Mangan and Alon, 2003; Milo et al., 2002; Pomerening et al., 2003; Tyson et al., 2001, 2003; Wolf and Arkin, 2003; Xiong and Ferrell, 2003; Yeger-Lotem et al., 2004). Accordingly, one important contribution of systems biology is the elucidation of how interacting proteins in concert can give rise to a behaviour not seen when looking at those proteins in isolation. Due to its importance and complexity, apoptosis signalling is a challenging but exciting field for applying these ideas. Section 2.2.1 summarizes available mathematical models of apoptosis pathways. However, the modelling is only the first step to understanding. These models need to be analysed to reveal their specific properties and behaviour. In the following, we will present properties and analysing concepts relevant for this thesis. Specifically, we introduce bistability (Section 2.2.2), robustness (Section 2.2.3) and stochasticity (Section 2.2.4) in cell signalling and point to their relevance and relation to apoptosis.

2.2.1 Mathematical modelling of apoptosis pathways

As outlined in the last section, apoptosis is a complex but crucial phenomenon. Recently, several mathematical approaches to apoptosis signalling have been published. These range from large scale static models mainly used to organize and interpret large amounts of experimental data (Janes et al., 2005, 2006) to small scale dynamic models used to better understand selected aspects as shortly summarized in the following. Further details relevant to this study will be discussed in the context of the results presented in this work.

Models and challenges. One of the first dynamic models of apoptosis signalling covers large parts of the involved processes in a simplified manner and nicely describes several facets of both the externally and the internally triggered signalling pathways (Fussenegger et al., 2000). The hybrid model contains heuristic parts but is able to illustrate principle features and known regulatory mechanisms. A similar approach was taken by Schoeberl (Schoeberl, 2002; Schoeberl et al., 2001; Eissing, 2002) and Bentele (Bentele et al., 2004; Lavrik et al., 2007) focussing on death receptor induced apoptosis. There, also experimental time course data of relevant molecules on the population level are presented in order to identify the model parameters. However, the number of parameters is generally large compared to the available amount and quality of data, making the identification process difficult. Using apoptosis signalling as a model challenge, Gadkar et al. (2005a,b) have presented interesting progress on the problem of identification developing an iterative procedure including a state regulator algorithm.
Several theoretical studies focussed on the role of death receptor–ligand interactions as the signal initiating event and investigated the potential role of receptor clustering and the ligand trimer structure (Guo and Levine, 1999; Lai and Jackson, 2004). Several other studies have focussed on the mitochondrial pathway of apoptosis or selected parts thereof (Bagci et al., 2006; Chen et al., 2007a,b; Huber et al., 2007; Legewie et al., 2006; Rehm et al., 2006; Stucki and Simon, 2005). Rehm et al. (2006) were able to closely link their mathematical model to own experiments and thereby experimentally verify their model predictions at the single cell level. This example nicely indicates the great potential of mathematical models to guide experimentation.
One problem in apoptosis modelling and model identification is the different behaviour of cell populations compared to single cells. In a population of cells a slow gradual activation of cas-

pases is generally observed, whereas caspase activation is very rapid at the single cell level (see Sections 2.1 and 2.2.4). Naturally, the single cell level reflects the underlying mechanisms better, while hardly allowing quantitative experimental data needed for rigorous identification. Therefore, single cell models can usually only be considered qualitative or semi-quantitative. In fact, the fast activation itself poses a problem to the modelling and understanding of apoptosis signalling as introduced below (Figure 2.3) and addressed in several parts of this thesis.
As we argue in Section 2.2.2, apoptosis at the level of the single cell is a rapid and essentially all-or-none process – the cell dies or continues to live. Several evidences indicate that this all-or-none behaviour is determined at the level of executioner caspases. ODE models can reflect such a behaviour by exhibiting bistability, i.e. two stable steady states. Consequently, several studies examined the steady state and stability properties of apoptosis models to reveal important ingredients to achieve bistability, indicate possibilities to shift the delicate balance of death and survival, and illustrate how pathological states of the cell can arise (Bagci et al., 2006; Carotenuto et al., 2007b; Chen et al., 2007a,b; Eissing et al., 2004, 2006, 2007c; Legewie et al., 2006; Tyson, 2007). When neglecting certain processes, caspase activation can also be viewed as monostable and Aldridge et al. (2006) have used Lyapunov exponent analysis to reveal phase-space domains that delineate regions exhibiting qualitatively different transient activities corresponding to different outcomes. These domains are conceptually similar to manifolds separating areas of attraction that can be identified when modelling the process as bistable.

Caspase activation can be a rapid process – the true challenge? As outlined before, new experimental techniques at the single cell level have revealed that caspase activation can be a very rapid process. This can be supported theoretically by some simple calculations. The two most important parameters for caspase activation (at least in the direct pathway of receptor induced apoptosis) are presumably the mutual activation rates of caspases 8 and 3. We consider a very simple model including only these two reactions. The ODEs for the active and inactive caspases are given by

$$\begin{aligned} [\dot{C3a}] &= k_1 \cdot [C8a] \cdot [C3] \\ [\dot{C8a}] &= k_2 \cdot [C3a] \cdot [C8] \\ [\dot{C3}] &= -k_1 \cdot [C8a] \cdot [C3] \\ [\dot{C8}] &= -k_2 \cdot [C3a] \cdot [C8]. \end{aligned} \tag{2.1}$$

More detailed information on the reactions, assumptions and initial conditions will be introduced in Section 4.1. We use the *in vitro* literature value for pro-caspase 3 activation by active caspase 8 ($k_1 = 10^6\ M^{-1}s^{-1}$; Stennicke and Salvesen, 1999; Stennicke et al., 1998) and assume the positive feedback (k_2) to be a factor of 5 lower than this value, i.e. we choose conservative values compared to those determined for caspase 3 using fluorogenic substrates (Garcia-Calvo et al., 1999; Van de Craen et al., 1999). We consider an inflow of C8a, which is produced by upstream processes, as a model input. We assume a pulsed inflow, which allows the input to be represented as an initial concentration of C8a. C3a can be considered as an output. When the system is triggered by only 100 molecules of activated caspase 8, the obtained simulation results show a full caspase 3 activation after only 4 minutes (Figure 2.3). This simulation neglects the potential amplification step via caspase 6 in the feedback loop, but also the inhibitory effects of IAP proteins and protein

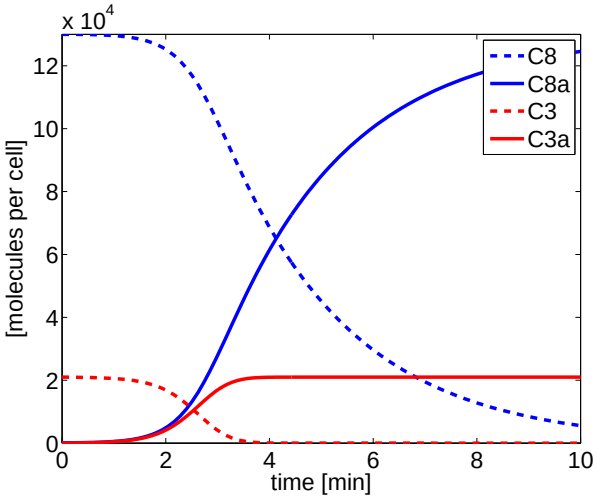

Figure 2.3: Apoptosis can be a rapid process. The figure shows simulation results for a simple model (2.1), where only 2 reactions are included (Figure 4.1, v_1 and v_2). On the time scale displayed, additional reactions lead to a slower rise of C8a and to C3a complexed to IAPs rather than free, but a complete C3 processing can still be observed within 10 minutes. In the simulation, 100 molecules per cell of C8a were used as an apoptotic trigger (initial concentration of C8a). For k_1 the literature value was chosen ($10^6\ M^{-1}s^{-1}$, see Table 4.2) and k_2 was chosen five-fold smaller ($2 \cdot 10^5\ M^{-1}s^{-1}$).

turnover. Even when reducing both mutual activation rates by a factor of 10, 90% of caspase 3 molecules still become activated within 30 minutes (data not shown). These data clearly indicate that an ideal caspase cascade is capable of acting very rapidly even for very low triggers.
Simple calculations highlight the problem posed by the above results. If we assume 100 molecules of active caspase 8 (< 0.1% of the total caspase 8 in a single HeLa cell, Section 4.1) as the initial trigger and use the literature value for the cleavage reaction of caspase 3, approximately 200 molecules of caspase 3 will be activated within the first minute. If we further consider these 200 molecules of activated caspase 3 to be quickly degraded (half-life time of 30 min, e.g. through IAP mediated ubiquitylation and subsequent proteasomal degradation), less than 5 molecules of the 200 molecules available are degraded within this first minute. Together, these results indicate that the caspase cascade can hardly be stopped once initiated. Thus, while experimental evidences indicate caspase activation to be a rapid process and this can easily be confirmed by a simple calculation, an important and not so easy to answer question is how cells prevent accidental apoptosis after minor amounts of caspases are activated (which is in fact constantly the case, see Section 2.2.2)? Thorough investigations of this aspect and a possible solution are presented in Chapter 4. The basic idea is to require the normal state of the cell (‘life’) to be stable, i.e. small pertubations should not lead to apoptosis but to recovery. Further, the apoptosis state (‘death’) can also be considered as a stable state in the set-up considered in this thesis, as will be further motivated in Section 2.2.2. Mathematically these requirements can then be translated into bistability.

2.2.2 Bistability in cell signalling and apoptosis

Bistability is a nonlinear phenomenon implicated in diverse biochemical processes and appears to be a reoccurring motif in biology (Cherry and Adler, 2000; Eissing et al., 2004; Ferrell, 1996; Ferrell and Xiong, 2001; Novick and Weiner, 1957; Oppenheim et al., 2005; Qu et al., 2003;

Thron, 1997; Tyson et al., 2003; Vanag et al., 2006; Vilar et al., 2003). It is implicated in cell decision processes and cellular memory, as a bistable system can convert continuous input signals into discrete (all-or-none) output signals and thereby switch reversibly or irreversibly between two cellular states. Motivated by mathematical model analysis, bistability has, for example, been experimentally demonstrated at the single cell level for the *lac* operon in *E. coli* and for the MAP kinase cascade in *Xenopus* oocytes (Ozbudak et al., 2004; Xiong and Ferrell, 2003). The best studied biological example with respect to bistability are kinase cascades as exemplified by the mitogen activated protein kinase (MAPK) cascade (Bhalla et al., 2002; Blüthgen and Herzel, 2001; Ferrell, 1996, 1997; Ferrell and Xiong, 2001; Huang and Ferrell, 1996; Markevich et al., 2004).

Requirements for bistability. In models of biochemical reaction networks, bistability generally requires two ingredients (Angeli et al., 2004; Cinquin and Demongeot, 2002; Ferrell and Xiong, 2001). The first is an ultrasensitive reaction mechanism. Ultrasensitivity refers to a system response that is more sensitive to changes in the component concentrations than is the normal hyperbolic response given by the Michaelis-Menten equation (Koshland, 1998; Koshland et al., 1982), e.g. a Hill type response (Weiss, 1997). The second is positive feedback, which can be implemented by only positive (activatory) feedback or an even number of negative (inhibitory) interactions along the loop (Angeli et al., 2004; Cinquin and Demongeot, 2002). However, both ingredients are only necessary but not sufficient to generate bistability. Whether the system is then bistable or not is strongly dependent on the parameter values (Ferrell and Machleder, 1998; Xiong and Ferrell, 2003; see also Section 3.2.1). Despite several case studies, the development of general approaches to determine bistability is rather difficult. Recently, promising approaches have been described (Angeli, 2006; Angeli et al., 2004; Craciun et al., 2006). However, these more general results are restricted to special system classes and provide conditions on structural requirements. Numerical analyses to reveal for which range of parameters a system is bistable and for which parameter values it is not remain important.

Methods for evaluating bistability. The number and stability properties of steady states in a model can change when varying the parameters. In this thesis we will use phase-plane and bifurcation analyses to enable an illustrative insight into the qualitative system behaviour (Khalil, 2002; Strogatz, 2001). These methods allow an efficient analysis of steady states with respect to number, location and stability. Classical phase-plane analysis is considering the phase-space of second order systems. It is able to illustrate the vector field governing the differential equations, or selected properties thereof, for a fixed parameter set. If larger systems can be reduced by the elimination of variables, they are also amenable to a phase-plane analysis, e.g. Tyson et al. (2003). For simple models, the steady states and their stability properties can be explicitly calculated in dependence of the parameters. Generally, they can be tracked in the parameter space employing continuation methods (Kuznetsov, 1995). Thus, bifurcation analyses explore how phase space properties like steady states and limit cycles depend on the parameters. Restrictions are only introduced by numerical accuracy, computational power and graphical illustration.

Bistability and apoptosis. Bistability is also an obvious and mandatory property of the apoptotic machinery, as the status ‘life’ must be stable and resistant towards minor, accidental trigger

signals (i.e. 'noise'; Tyson et al., 2003). Also, caspases are known to possess zymogenicity (Stennicke and Salvesen, 1999; see also Section 3.2.4) and partial activation of initiator caspases is observed in some physiological processes (Lamkanfi et al., 2007; Newton and Strasser, 2003). Contrarily, no partial activation of executioner caspases has been reported in a physiological setting, which is understandable as the wide spectrum of substrates that are cleaved by executioner caspases would probably lead to pathological effects (Fischer et al., 2003). However, if the apoptotic initiation signal is beyond a certain threshold, the cell must irreversibly enter the pathway to develop apoptosis.

These results, together with the rapid caspase activation observed at the single cell level, indicate that bistability in apoptosis is manifested at the caspase level. In the 'life' steady state there are no (or a few) activated caspase molecules, whereas in the 'death' steady state a strong activation of executioner caspases inevitably leads to apoptosis. However, even though conclusive experiments, such as those available for a very few other signalling systems (Ozbudak et al., 2004; Xiong and Ferrell, 2003), are in preparation (Institute of Cell Biology and Immunology, University of Stuttgart), definite results are missing to date. Also, when considering the caspase cascade as a bistable process, one has to bear in mind that apoptosis finally leads to the complete destruction of the cell including active caspases. Therefore, the activation level of caspase in the remainders of the cell will eventually fade again. However, this is only due to processes in the final stages of apoptosis occurring after the real decision of entering apoptosis or not has been made. These processes will not be further considered in this study, and, as they are not included in the model, a sustained caspase activity should be expected in the virtual apoptotic cell. Figure 2.4 illustrates the situation for apoptosis in the context of parameter dependencies and bifurcation analysis.

In the following, we use this information in a reverse engineering manner (Csete and Doyle, 2002) and take bistability as a 'conditio sine qua non' to evaluate possible models with respect to this expected behaviour. Accordingly, in Chapter 3 we will investigate how bistability can be realized in proteolytic cascades such as encountered during apoptosis. In Chapter 4, we will then analyse expanded models closely resembling the direct pathway of receptor induced apoptosis. The analyses reveal requirements and insight not easily accessible by classical experimentation. We further analyse these apoptosis model for how robust their behaviour is – a property introduced in the following.

2.2.3 Robustness in biology and apoptosis

Robustness refers to the resistance of a function to perturbations in operating conditions and appears to be an inherent common property of biological systems (Barkai and Leibler, 1997; Hartwell, 1997; Stelling et al., 2004b).

Clearly, many biological systems have to function reproducibly despite disturbances of internal and environmental conditions. This is especially important when considering processes deciding on the cell fate, as for example in programmed cell death. The 'relative' character of robustness always requires the specification of the perturbations and functions considered and it is difficult to define just how much robustness makes a biological system optimally fit to survive evolution. 'Total robustness' would imply that the system does not respond to any perturbation and thus be unable to communicate with its surrounding as a perturbation can also be a signal to the system. Vice versa,

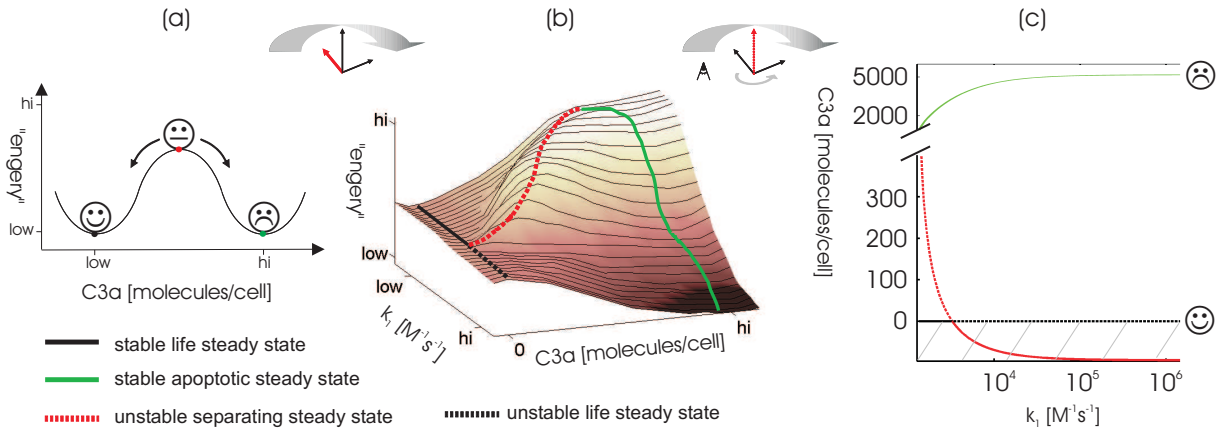

Figure 2.4: Illustration of bistability in apoptosis. (a) illustrates a bistable system with two stable and one unstable steady state. A steady state (other common synonyms are equilibrium point or fixed point) implies that the concentrations in the system do not change over time, similar to the position of a ball in a cavity. If we start at concentrations close to steady state, the system will move towards the steady state if it is stable, but move away if it is unstable. Nonlinear systems can allow for several steady states, having distinct stability properties as indicated in the figure. A similar situation can be expected for apoptosis where the stable steady states can be associated with 'life' and 'death', respectively. The unstable steady state can be seen as a 'decision' point. (b) illustrates how the number and stability properties may change in dependence on a parameter. Although the illustration is per se arbitrarily, it qualitatively resembles the situation we found in different mathematical models describing apoptosis signalling (see Sections 3.2.3 and 4.2). Solid lines represent stable steady states, dashed lines unstable ones. Black and green correspond to 'life' and 'death', respectively. For small k_1-values the system has a stable 'life', for large k_1-values a stable 'death' steady state. In-between the systems displays the desired bistable behaviour. (c) shows the typical representation in a bifurcation diagram, which will be further discussed in Section 4.2. The bifurcation diagram can be interpreted as a projection of (b). **Remarks:** In the context of stability theory, the ball in a cavity in (a) can be interpreted as a generalized energy function for a scalar system, which can be related to Lyapunov theory. Then, (b) can be interpreted as such a generalized energy function in dependence of one parameter. Steady states classified as stable in this thesis, more precisely correspond to asymptotically stable steady states.

a 'totally robust' system does not change its behaviour and thus cannot signal to the outside itself. Clearly, most biological systems do and need to communicate with their environment. Therefore, biological functionality requires a trade-off between robustness and performance (El-Samad et al., 2005; Kurata et al., 2006; Stelling et al., 2004b). Further, a more general consequence of the design of complex systems, such as biological systems, appears to be a 'robust yet fragile' character. This can also be viewed as a trade-off between robustness to certain (e.g. anticipated) perturbations but fragility to other (e.g. unanticipated) perturbations (Carlson and Doyle, 2000, 2002; Chaves et al., 2005; Stelling et al., 2004b).

To better understand this robustness balance and to discover common schemes that arose during evolution requires the analysis of different systems with adequate methods. Different levels of organisation of systems can be distinguished and have been investigated, e.g. by Barkai and Leibler (1997); Kollmann et al. (2005); Mangan and Alon (2003); Milo et al. (2002); Morohashi et al. (2002); Oltvai and Barabasi (2002); Stelling et al. (2002, 2004a,b). The classical approach to analyse robustness is sensitivity analysis (Heinrich and Rapoport, 1974; Kacser and Burns, 1973;

Savageau, 1971; Stelling et al., 2004a; see also Section 5.1). Recently, system theory and control engineering inspired different methods such as (structural) singular values or bifurcation analysis (Chen et al., 2005; Kim et al., 2006; Ma and Iglesias, 2002; Morohashi et al., 2002). These are better suited to evaluate models displaying nonlinear behaviour such as bistability. Robustness measures based on bifurcations were also used as a plausibility measure for models, and the authors could identify weaknesses for the investigated models (Morohashi et al., 2002; see also Sections 5.3 and 5.4).
We follow up on these ideas in Chapter 5, partly extending existing techniques to describe new robustness measures and evaluate robustness to parameter variations in apoptosis models. Parameter variations are commonly studied in the context of robustness as these generally reflect diverse perturbations well. In the following, we would like to more specifically also consider other perturbations that biological systems are constantly exposed to and which are of a stochastic nature.

2.2.4 Stochastic influences in biology and apoptosis

As introduced in Section 1.1, in major parts of this thesis we rely on an ODE based description of the involved precesses. For a given model with fixed parameters and initial conditions the time evolution is fixed, i.e. deterministic (if certain mild assumptions on the model are satisfied). This implies that the processes under investigation can be well approximated by a deterministic description, i.e. stochastic influences can be neglected. Then, ODEs represent the time evolution of the mean concentration values. However, due to the small volume of cells and low number of molecules often involved, biological systems sometimes belie a deterministic and continuous description as assumed when employing ODEs (Elowitz et al., 2002; Fall et al., 2002; Rao et al., 2002).
Also, stochastic effects are observed during apoptosis. For example, after applying an apoptotic stimulus to a population of identical cells, generally individual cells die at different time points. Further, there are strong experimental evidences that the activation of caspase 3, the major output considered in the apoptotic models, although proceeding gradually and slowly on the population level, in fact proceeds rapidly within minutes at the single cell level (see Section 2.1 and Figure 2.5). In experiments, the activation of effector caspases both in type I as well as type II cell populations occurs gradually within a few hours (Fotin-Mleczek et al., 2002; Hentze et al., 2002; Scaffidi et al., 1998), as schematically depicted in Figure 2.5 (black line). However, at the single cell level, rapid caspase 3 activation has been observed after a lag phase in the very same experimental setup (Figure 2.5, red lines; Goldstein et al., 2000; Luo et al., 2003; Rehm et al., 2002, 2006; Tyas et al., 2000). These observations indicate that the slow population response presents an average of single cells where caspases are activated quickly but at different time instances. Stochastic effects are likely to be the cause for this different timing in individual cells.
In this thesis we consider as ‘intrinsic noise’, stochastic fluctuations due to the inherently stochastic nature of the reactions immediately considered in the model under investigation (Elowitz et al., 2002; Gillespie, 1976). We refer to ‘extrinsic’ noise when considering other stochastic influences as explained next. Generally, extrinsic noise will arise from intrinsic noise in processes, which are not detailed in the model or outside of the system boundary considered. For example, fluctuations in the protein concentration can be considered ‘extrinsic’ because the source of stochasticity

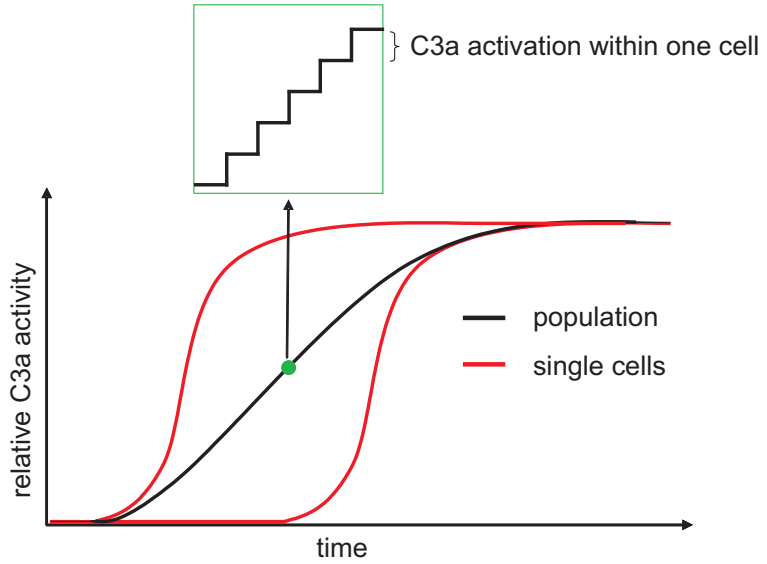

Figure 2.5: Single cell versus population behaviour illustration. Single cells activate the majority of caspase 3 within minutes after a certain delay or lag phase. The length of the delay differs among individual cells and is statistically distributed within a population. On the population level, the caspase 3 activity increases in small steps (due to individual cells activating their caspase pool). The high cell numbers and averaging effects lead to a gradual increase of caspase 3 activity.

is not further specified, although it can be easily imagined how fluctuations arise when considering the intrinsic noise inherent to the processes of protein production involving transcription and translation. Thereby, extrinsic noise affects the parameters of the models, relating this aspect to considerations on robustness to parameter changes (Section 2.2.3).

We will evaluate the influence of both intrinsic and extrinsic noise on apoptosis models in Chapter 6. A major finding, in support of a deterministic model description, is that intrinsic noise hardly influences the model behaviour for a relevant and large range of inputs because the inhibitors buffer the activated caspases and thereby filter out noise (Section 6.1). In contrast, extrinsic influences have a comparably large impact on the system behaviour allowing the reconciliation of single cell and population experiments both in terms of modelling and understanding (Section 6.2).

2.3 Summary and outline

In this chapter, we introduced the background and key ideas relevant for this thesis. We first provided an overview on apoptosis signalling and its relevance in physiology and medicine (Section 2.1). We then introduced systems science concepts relevant to apoptosis and this thesis: mathematical modelling (Section 2.2.1), bistability (Section 2.2.2) and robustness (Sections 2.2.3 and 2.2.4). Thereby, we motivated and illustrated the underlying ideas rather than providing mathematical formulas. However, all three aspects will be deepened and formalized in the following. Chapter 3 introduces simple models capturing principle properties of proteolytic cascades such as encountered in apoptosis. These models will be analysed for bistability, and robustness aspects will be touched. Similarly, Chapter 4 presents mathematical models and bistability analyses specifically targeted towards the direct pathway of receptor induced apoptosis. In Chapter 5 differ-

ent techniques for analysing the sensitivity and robustness of these models to parameter variations will be presented. Chapter 6 will evaluate stochastic influences on the model behaviour.

Chapter 3

Modelling and Bistability of Simple Proteolytic Networks

Proteolytic cascades are frequently encountered in biology with apoptosis signalling and the blood clotting cascade as prominent examples, as was introduced in Section 2.1. This chapter focusses on simple proteolytic cascades to evaluate principle mechanisms regarding their role in generating reversible or irreversible switches in such cascades. Further, methods for bistability evaluation are introduced and candidate assumptions for simplification evaluated. Thereby, insights gained are valuable for the modelling of the direct pathway of receptor induced apoptosis as presented in Chapter 4. Section 3.1 outlines the models, which are detailed and analysed for steady states and stability properties in Section 3.2. Three established mechanisms for generating ultrasensitivity and, in combination with positive feedback, bistability are compared: cooperative, inhibitor and zero-order ultrasensitivity. Using the example of the cooperative model the concept of phase plane analysis is explained in Section 3.2.1, which is subsequently applied to the two other models (Section 3.2.2). The analysis shows that the established mechanisms can be applied to proteolytic cascades, but the interpretation of the involved reactions differs in the case of zero-order ultrasensitivity: whereas 'classically' the back reaction has to be saturated, in irreversible proteolytic reactions a saturated degradation is required. Bifurcation analysis will be presented in Section 3.2.3 to complement the analysis and investigate differences between reversible and irreversible switches. Section 3.2.4 investigates the influence of zymogenicity. Especially the cooperative model is strongly influenced by this 'perturbation'. The results will be summarized and discussed in Section 3.3. Extended robustness analysis of the models will be presented in Sections 5.2 and 5.3. Major parts of this chapter are published in Eissing et al. (2007c).

3.1 Model overview and notation

We consider the models outlined in Figure 3.1. The simplest model considers two proteases X and Y (Figure 3.1, white background). The inactive protease X_i is activated by an input (or external stimulus) U yielding the activated form of the protease X_a (reaction rate r_0). X_a itself is then able to activate the inactive protease Y_i to give Y_a (r_2), which can feed-back on X (r_1). In general we use mass action kinetics. We also consider the effects of a cooperative mechanism in the

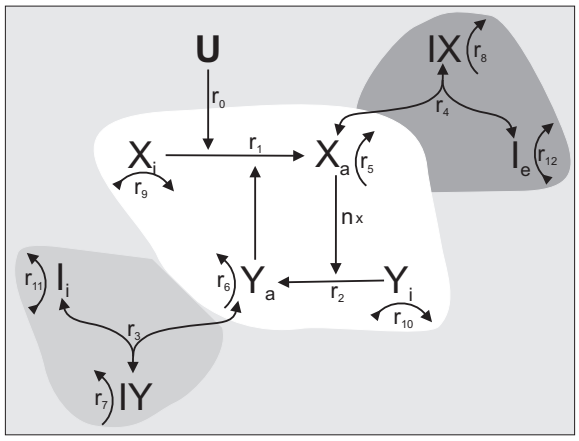

Figure 3.1: Model outline. Schematic sketch of the models detailed and analysed in this chapter. X and Y represent two proteases. The subscripts indicate the activated and inactivated form. Different inhibitors I are distinguished by their subscript letters and U describes an external input. Reaction rates r are numbered and n indicates a cooperative step.

activation of Y (r_2) and compare the results to effects conferred by inhibitors of activated proteases (I_i and I_e, r_3 and r_4) or a saturation in the degradation (see below). In apoptosis signalling, X, Y and I correspond to initiator and executioner caspases and inhibitor of apoptosis proteins (IAPs), respectively. Thereby initiator caspases represent the receptor associated initiator caspases 8 and 10 or the intrinsic pathway initiator caspase 9. We further study the influence of zymogen activity (r_{13} and r_{14} omitted in Figure 3.1 for clarity, see Section 3.2.4), i.e. the inactive proteases have a residual activity and can thus catalyse the same reactions as the activated protease, but with a lower efficiency.

We consider a turnover of all involved components ($r_5 - r_{12}$), assuming that all components are degraded with a kinetic proportional to their concentration unless a saturation is introduced, while only the non-activated and non-bound proteins will also be produced with a kinetic independent of the concentration. Although the biological mechanisms are, of course, totally different for producing and degrading pathways, we combine them into one apparent net rate for convenience (turnover rates with arrowheads on both ends).

A turnover is essential because we would like to evaluate the steady state behaviour with a focus on bistability. We consider proteolytic reactions, which are essentially irreversible (Eckelman et al., 2006). Negligence of protein turnover would inevitably lead to a complete activation of proteases in the presence of positive feedback once a single molecule would be activated, e.g. by a minor input U.

Irreversibility, turnover and inhibitors distinguish the models investigated in this chapter from well studied examples, e.g. the MAPK cascade. These differences also prevent the straightforward application of new powerful methods developed in the framework of monotone systems (Angeli, 2006; Angeli et al., 2004). Although simplifications as derived in Section 3.2.1 can render some of the models introduced in this chapter monotone, we will rely on classical phase plane analysis, which is related but much more widely known.

If not indicated otherwise, we do not explicitly consider the input U but rather evaluate the behaviour of the system with $U \equiv 0$. If we consider U as an impulse, we account for the molecules

activated by U in the initial conditions of the system without input. Thus, we only explicitly have to account for U when considering a different kind of input signal like a constant stimulus.
We denote the kinetic rate constants by k_{jr}, whereby the index j describes the class the parameter belongs to, i.e. k_{cr} for catalytic constants involved in the cleavage reactions, k_{fr} and k_{br} for the forward and backward reaction constants of binding reactions, k_{dr} and k_{pr} for degradation and production terms and k_{zr} for zymogen mediated cleavage reactions. The subscript index r corresponds to the reaction rate number as given in Figure 3.1. At the point where we consider saturation effects, we use Michaelis-Menten instead of mass action kinetics and denote the Michaelis-Menten constant with K_{Mr} and the maximal rate constant with k_{mr}.
Parameter values are explicitly only used in the normalized models introduced in Section 3.2. Due to this normalization, Michaelis-Menten constants correspond to a normalized concentration, n is dimensionless, and all other parameters are in one per unit of time. If not specified otherwise we assume the nominal parameter values $p = (k_{cr}, n, k_{fr}, k_{br}, k_{dr}, k_{pr}, k_{mr}, K_{Mr}) = (0.01, 2.5, 1, 0.001, 0.003, 0.003, 0.003, 0.01)$. The choice is per se arbitrary but will be evaluated and motivated in Chapters 4 and 5. The models were implemented in Mathematica® (Wolfram Research[1], Inc., Champaign, IL) and the Mathematica dynamical systems package (DynPac[2]) for analytical and phase plane analysis. XppAut[3] (Ermentrout, 2002) was used for numerical bifurcation analysis (steady state continuation).

3.2 Steady state and bistability analysis

A simple cooperative model is derived in Section 3.2.1 and the concept of phase plane analysis is illustrated. The cooperative model is compared to an inhibitor and a zero-order model in Section 3.2.2 with respect to enabling bistability. Section 3.2.3 explores how reversible and irreversible switches can be generated. Section 3.2.4 evaluates the influence of zymogenicity on the three models.

3.2.1 Steady states and their stability in a cooperative model

We consider a simple model including two mutually activating proteases that exist in an active and inactive form, as outlined in Section 3.1. We start with the general description of the model considering a cooperative action of n molecules X_a to activate Y (r_2, Figure 3.1). A simpler model without cooperativity can be obtained by setting $n = 1$. We introduce the external input U needed for some considerations in Section 3.2.3, but otherwise neglect it in the following. Using the introduced modelling approach and assumptions, we obtain the following system of coupled nonlinear ODEs

$$\dot{X}_a = k_{c1} \cdot X_i \cdot Y_a - k_{d5} \cdot X_a + U \cdot X_i, \tag{3.1}$$

$$\dot{Y}_a = k_{c2} \cdot Y_i \cdot X_a^n - k_{d6} \cdot Y_a, \tag{3.2}$$

$$\dot{X}_i = -k_{c1} \cdot X_i \cdot Y_a - k_{d9} \cdot X_i + k_{p9}, \tag{3.3}$$

[1] http://www.wolfram.com/
[2] http://www.me.rochester.edu/∼clark/dynpac.html
[3] http://www.math.pitt.edu/∼bard/xpp/xpp.html

$$\dot{Y}_i = -k_{c2} \cdot Y_i \cdot X_a^n - k_{d10} \cdot Y_i + k_{p10}. \tag{3.4}$$

Introducing the vector $x = (X_a, Y_a, X_i, Y_i)$ the ODE system can be written in the compact form $\dot{x} = f(x) + g(x) \cdot U$.
In the following, we show an approach to visualize the steady states of the full system in the phase plane. Then, we introduce simplifications not affecting the qualitative behaviour of the system, before providing a phase plane analysis.

Steady state analysis of the full system. The above ODE system (3.1)–(3.4) is nonlinear. The coupling of the ODEs makes the determination of steady states non-trivial. We assume $U \equiv 0$. To obtain the steady states we can partly solve the equation system at steady state and visualize the solution in the phase plane. To eliminate two equations we can solve $f_3(x) = 0$ for X_i and substitute the solution into f_1 and similarly solve $f_4(x) = 0$ for Y_i and substitute the solution into f_2. The two equations left provide nullclines in the phase plane whose intersections are steady states

$$X_a = \frac{k_{c1} \cdot k_{p9} \cdot Y_a}{k_{d5} \cdot (k_{d9} + k_{c1} \cdot Y_a)}, \tag{3.5}$$

$$Y_a = \frac{k_{c2} \cdot k_{p10} \cdot X_a^n}{k_{d6} \cdot (k_{d10} + k_{c2} \cdot X_a^n)}. \tag{3.6}$$

In the general case, this procedure is possible if the equation to be eliminated can be solved for the variable to be eliminated.

Simplifications and normalisation. The above equations (3.5) and (3.6) contain several parameters but the derivation of general steady state solutions is still straightforward. To further reduce the complexity, we will now introduce a simplified system and afterwards show the similarities to the full system.
Assuming equal degradation rates for active and inactive proteases, i.e. $k_{d5} = k_{d9}$ and $k_{d6} = k_{d10}$, the ODEs for the total concentrations $X_t := X_a + X_i$ and $Y_t := Y_a + Y_i$ are decoupled

$$\dot{X}_t = \dot{X}_a + \dot{X}_i = -k_{d5} \cdot X_a - k_{d9} \cdot X_i + k_{p9} = -k_{d9} \cdot X_t + k_{p9} \tag{3.7}$$

$$\dot{Y}_t = \dot{Y}_a + \dot{Y}_i = -k_{d6} \cdot Y_a - k_{d10} \cdot Y_i + k_{p10} = -k_{d10} \cdot Y_t + k_{p10}. \tag{3.8}$$

The system (3.1)–(3.4) is equivalent to the system (3.1)–(3.2), (3.7)–(3.8), i.e. we replace the ODEs for the inactive components by those of the total concentrations. Assuming the total concentrations to be in steady state, we obtain $X_t = k_{p9}/k_{d9}$ and $Y_t = k_{p10}/k_{d10}$. With these concentrations as initial conditions, X_t and Y_t are constant over time and the system can be reduced to two ODEs, (3.1) and (3.2). An equivalent system is obtained by considering relative concentrations, namely $X_r := X_a/X_t$ and $Y_r := Y_a/Y_t$. As an additional simplification, we assume $k_{d9} = k_{d10} = k_d$ and define $k_x := k_{c1} \cdot Y_t$ and $k_y := k_{c2} \cdot X_t^n$ in order to get

$$\dot{X}_r = k_x \cdot (1 - X_r) \cdot Y_r - k_d \cdot X_r, \tag{3.9}$$

$$\dot{Y}_r = k_y \cdot (1 - Y_r) \cdot X_r^n - k_d \cdot Y_r. \tag{3.10}$$

The nullclines of this system are

$$X_r = \frac{k_x \cdot Y_r}{k_d + k_x \cdot Y_r}, \tag{3.11}$$

$$Y_r = \frac{k_y \cdot X_r^n}{k_d + k_y \cdot X_r^n}. \tag{3.12}$$

Notice, these nullclines are equivalent to equations (3.5) and (3.6) considering the assumptions introduced. Also notice, we started of with mass action kinetics and the steady state solutions have the same form as the well known Michaelis-Menten or Monod equation (3.5) and (3.11) and Hill equation (3.6) and (3.12) (Ferrell and Xiong, 2001).
In the following, we will proceed using the simplified system (3.9)–(3.10). The results obtained can be derived similarly for the more general case. The simplifications mainly affect the exact dynamics rather than the steady state behaviour.

Phase plane analysis. Equation (3.11) is the nullcline to (3.9), and (3.12) is the nullcline to (3.10). In steady state, they also correspond to stimulus-response curves of two isolated subsystems, e.g. for (3.9) the steady state relation between the input (stimulus) Y_r and the output (response) X_r is given by (3.11). The steady states of the combined system (3.9)–(3.10) are characterized by the intersection of nullclines (3.11)–(3.12).
The X_r nullcline (3.11) is depicted in Figure 3.2(b) for $k_x = 0.01$ in black and for $k_x = 0.005$ and 0.05 in grey. The Y_r nullcline (3.12) is depicted in Figure 3.2(c) for $n = 2.5$ in black and for $n = 1$ and 4 in grey (computed with $X_t = Y_t = 1$). Note that the Y_r nullcline for $n = 1$ and the black X_r nullcline are symmetric with respect to the line $Y_r = X_r$ as $k_x = k_y$. Figure 3.2(a) shows the superposition of the two nullcline plots. The intersections of the different nullclines provide the steady states as indicated by the three dots for the black lines. We number the steady states along the nullcline starting at the origin from 1 to 3 as indicated in the figure.
The classical approach for determining the local stability properties of steady states is to calculate the eigenvalues of the dynamic matrix of the linearised system (employed in this work) or by finding a Lyapunov function in a neighbourhood of the steady state. Alternatively, simple graphical tests for phase plane plots exist for special system classes (Piccardi and Rinaldi, 2002).
The black nullcline corresponding to $n = 2.5$ is typical for the case $n > 1$. The grey dots in Figure 3.2 correspond to stable steady states (1 and 3) and the black dot corresponds to an unstable steady state, which is a saddle (2). Thus the system is bistable. In bistable systems, two stable steady states are often separated by a third unstable steady state (Tyson and Othmer, 1978). Figure 3.2(d) shows in black the unstable manifold of the saddle connecting the three steady states and the stable manifold separating the two areas of attraction. In addition, trajectories for different initial conditions are depicted in grey. Unlike for the case $n > 1$, there are at most two steady states for $n = 1$ as can be seen in Figure 3.2(a). Thus bistability is not possible, irrespectively of the other parameters.

3.2.2 Ways of generating bistability

In Section 3.2.1, we derived the steady states and their stability properties for a reaction system of two mutually activating proteases. If the reaction system is modelled using mass action kinetics

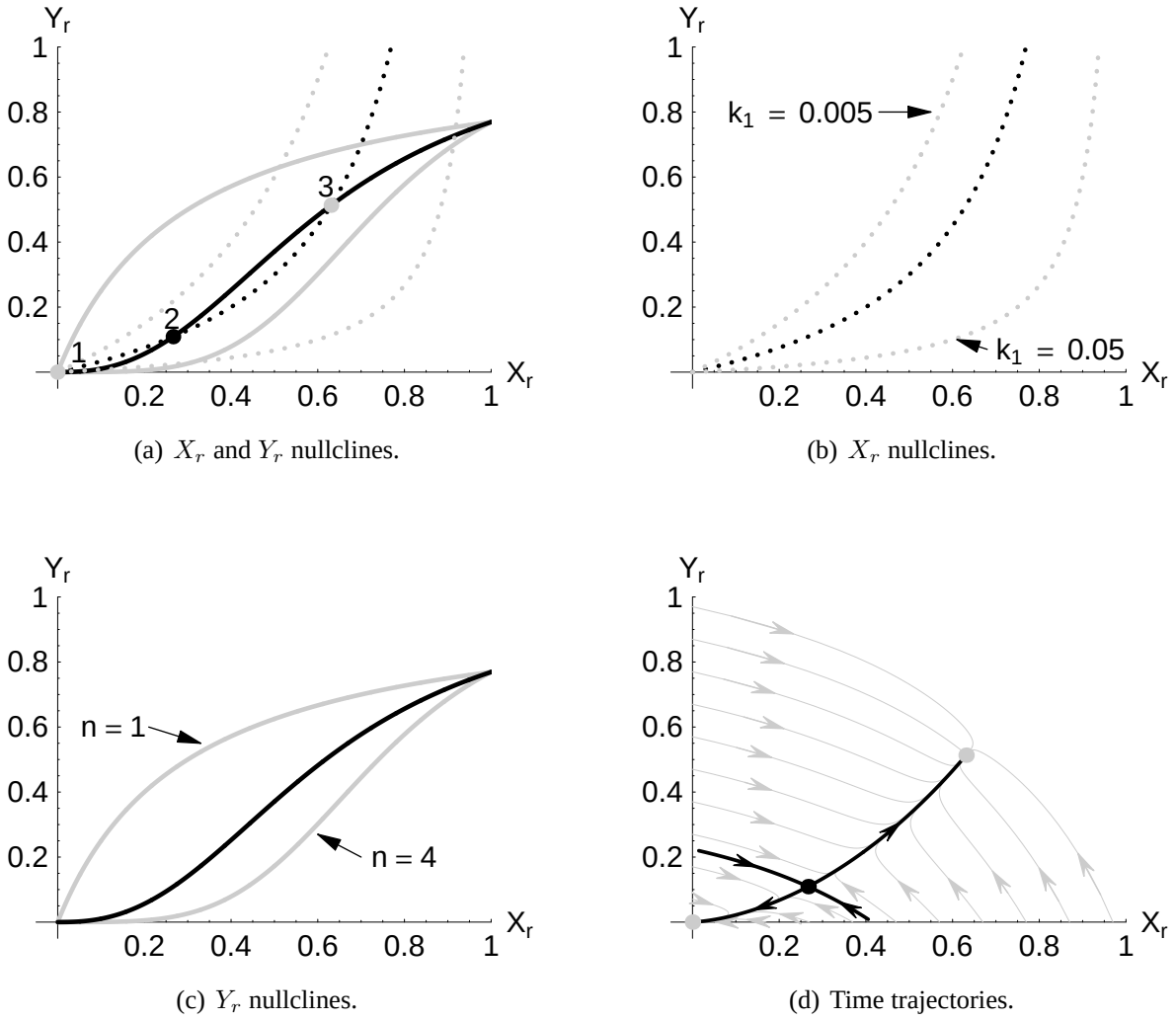

(a) X_r and Y_r nullclines.

(b) X_r nullclines.

(c) Y_r nullclines.

(d) Time trajectories.

Figure 3.2: Phase plane analysis. Figure 3.2(a) is a superposition of Figure 3.2(b) and 3.2(c) giving nullclines of (3.9) and (3.10), respectively. The numbered dots indicate steady states for the nominal parameters. Figure 3.2(d) illustrates trajectories of the system.

without cooperative steps, it is not able to produce a bistable behaviour. Key in generating bistable behaviour was the introduction of an ultrasensitive mechanism which was achieved through cooperativity. This results in a sigmoidal curve instead of a hyperbolic curve. In the following, we will outline additional ways of generating a bistable behaviour in similarly simple reaction schemes. Two well described cases are zero-order ultrasensitivity and inhibitor ultrasensitivity for which we directly show the simplified solution derived according to Section 3.2.1. Additionally, more complicated mechanisms have been investigated as will be discussed.

Zero-order ultrasensitivity. Zero-order ultrasensitivity has so far mainly been studied in the context of kinase/phosphatase reaction schemes (Goldbeter and Koshland, 1981, 1984; Lisman, 1985). When the phosphatase kinetics are described by Michaelis-Menten kinetics instead of mass action kinetics and the system is operating near saturation, this can lead to an ultrasensitive stimulus-response curve and thus to bistability in combination with positive feedback. Such a saturation behaviour is not possible for protease cleavage reactions due to their irreversibility. However, a closer comparison of the involved equations easily reveals that the scenario can be ob-

tained when introducing a saturation in the degradation. To our knowledge there are no conclusive biological data available, but a saturation in the degradation can be envisioned as the degradation is usually carried out by the proteasome and either this machinery or upstream tagging enzymes could become saturated. A saturation in the degradation was recently also proposed to generate oscillations in the NFκB pathway and other signalling pathways (see Krishna et al., 2006 and references therein). We evaluate a saturation in the degradation of Y_r assuming a constant concentration of the degrading enzyme E_d and define $k_m = k_{m6} \cdot E_d/Y_t$ and $K_M = K_{M6}/Y_t$ to obtain

$$\dot{Y_r} = k_y \cdot (1 - Y_r) \cdot X_r - \frac{k_m \cdot Y_r}{K_M + Y_r}, \tag{3.13}$$

where (3.9) as the second ODE remains unchanged. This yields the nullclines (3.11) and

$$Y_r = \frac{k_y \cdot X_r \cdot (1 - K_M) - k_m}{2 \cdot k_y \cdot X_r} + \frac{\sqrt{(k_y \cdot X_r \cdot (1 - K_M) - k_m)^2 + 4 \cdot K_M \cdot k_y^2 \cdot X_r^2}}{2 \cdot k_y \cdot X_r} \tag{3.14}$$

as well as a second negative and thus non-physical solution. The Y_r nullcline is depicted in Figure 3.3(c) for $K_M = 0.01$ in black and for $K_M = 1$ and 10^{-4} in grey (computed with $X_t = Y_t = 1$). As can be seen, although the biological interpretation differs from previously described cases, saturation effects in combination with positive feedback can also produce a bistable behaviour in the setting described here. Saturation in either of the cleavage reactions will contrariwise not be able to produce a bistable behaviour (data not shown).

Inhibitor ultrasensitivity. Inhibitor ultrasensitivity refers to the case where an inhibitor shapes the stimulus-response curve sigmoidal (Ferrell, 1996; Thron, 1994). This setup appears especially relevant for protease cascades as several specific inhibitors have been described for various proteases, e.g. IAPs inhibiting caspases (Danial and Korsmeyer, 2004) or Tissue Factor Pathway Inhibitor (TFPI) and antithrombin regulating important steps in the blood clotting cascade (Dahlbäck, 2000). We evaluate an inhibition where the inhibitor I_i binds to and thereby inactivates the active protease Y_a. We define the relative amount of complex $IY_r = IY/Y_t$, $k_f = k_{f3} \cdot Y_t$ and $k_b = k_{b3}$. With I_t as the total amount of inhibitor, the ODEs for the complex and for Y_r are given by

$$\dot{IY_r} = k_f \cdot (\frac{I_t}{Y_t} - IY_r) \cdot Y_r - k_b \cdot IY_r - k_d \cdot IY_r, \tag{3.15}$$

$$\dot{Y_r} = k_y \cdot (1 - Y_r - IY_r) \cdot X_r - k_d \cdot Y_r - k_f \cdot (\frac{I_t}{Y_t} - IY_r) \cdot Y_r + k_b \cdot IY_r. \tag{3.16}$$

Assuming the inhibitor and its complex to be in a quasi steady state, a substitution of IY_r into (3.16) yields

$$\dot{Y_r} = k_y \cdot (1 - Y_r) \cdot X_r - k_d \cdot Y_r - \frac{k_f \cdot I_t \cdot Y_r \cdot (k_d + k_y \cdot X_r)}{(k_f \cdot Y_r + k_d + k_b) \cdot Y_t} \tag{3.17}$$

and in addition we keep (3.9) unchanged. This yields nullclines described by (3.11) and an equation for Y_r omitted here due to its length[4]. As can be seen in Figure 3.3(b) (computed with $X_t = Y_t = 3 \cdot I_t = 1$), this mechanism can also efficiently produce a bistable behaviour. The Y_r nullcline is depicted for $k_f = 1$ in black and for $k_f = 0.1$ and 10 in grey. Compared to the cases where bistability is achieved through cooperative or zero-order ultrasensitivity the activation in the activated steady state is somewhat lower.

[4] http://www.sysbio.de/projects/tnf/biosystems06/

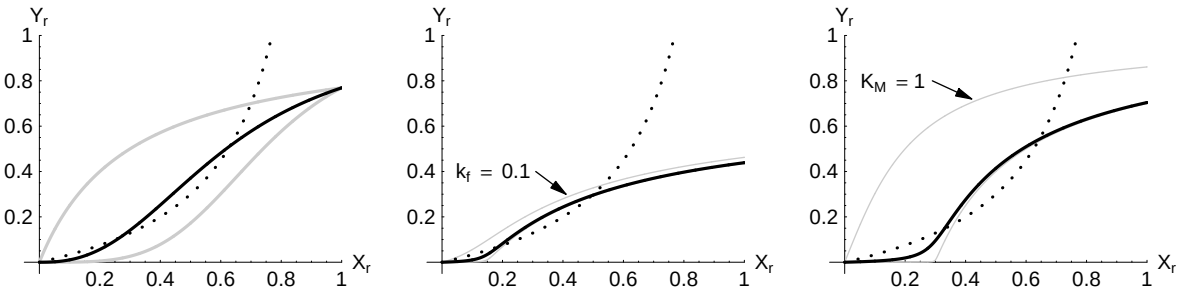

(a) Cooperative. (b) Inhibitor. (c) Zero-order.

Figure 3.3: The three basic mechanisms to produce bistability: Figure 3.3(a) cooperative, 3.3(b) inhibitor and 3.3(c) zero-order ultrasensitivity.

Additional mechanisms and combinations. There are many additional system configurations that can lead to bistability. Here we focus on positive feedback, however double negative feedback or more indirect or implicit forms of feedback can also yield a bistable behaviour (Angeli et al., 2004; Legewie et al., 2007; Markevich et al., 2004; Ortega et al., 2002, 2006). Recently, this was also described for the mitochondrial pathway of apoptosis, where IAP proteins can inhibit both initiator and executioner caspases (Legewie et al., 2006). For monotone systems it was shown that any kind of feedback, which in the sum is positive can give rise to a bistable behaviour (Angeli et al., 2004). As can be seen in Figures 3.2 and 3.3, all these structural requirements are necessary but not sufficient for bistability in the given systems. The parameters have to be balanced in order to generate bistability.

It is easy to envision that a combination of the different mechanisms can produce steeper sigmoidal curves (data not shown). Also, if the forward and the backward part of the reaction system contain a mechanism generating an ultrasensitive response this balance is more easily achieved, e.g. if not only Y_a is inhibited by an inhibitor I_i but also X_a is inhibited by an inhibitor I_e (data not shown, compare Sections 4.3 and 5.4).

3.2.3 Bifurcation and hysteresis

The dependence of the bistable behaviour on the parameters can be more efficiently studied by analysing bifurcations (Section 2.2.2) instead of phase plane analysis. We choose the model considering inhibitors as introduced in Section 3.2.2. The results are easily transferable to the other described scenarios.

Location and stability properties of steady states in dependence on parameters are usually evaluated in bifurcation diagrams. Such diagrams can be seen in Figure 3.4. However, the qualitative picture can already be derived from Figure 3.3(b). For example, we fix the solid black line and shift the dotted black line by changing k_x (as indicated for two values by the dotted grey lines in Figure 3.2(b)) corresponding to the positive feedback activation of X by Y. For decreasing k_x, the value of steady state 3 becomes smaller and that of steady state 2 becomes larger until they finally meet and directly afterwards disappear (saddle-node bifurcation). If the feedback is too weak, a high activation state of the proteases cannot be sustained. On the other hand, for increasing k_x, steady state 2 becomes smaller until it finally reaches steady state 1 with which it exchanges its stability properties, before disappearing into the non-physical negative orthant (transcritical bi-

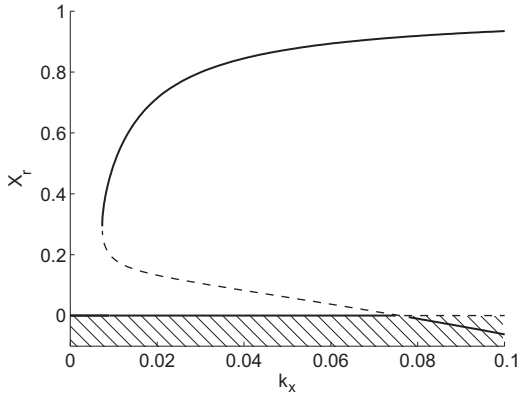

(a) k_x bifurcation without input.

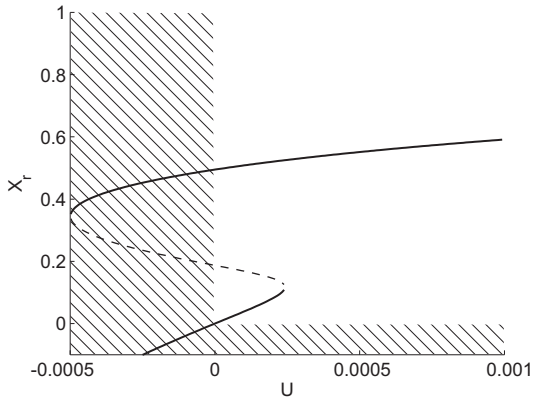

(b) Input bifurcation with $k_x = 0.01$.

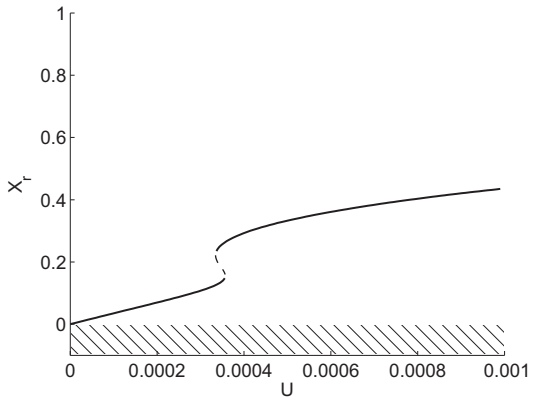

(c) Input bifurcation with $k_x = 0.005$

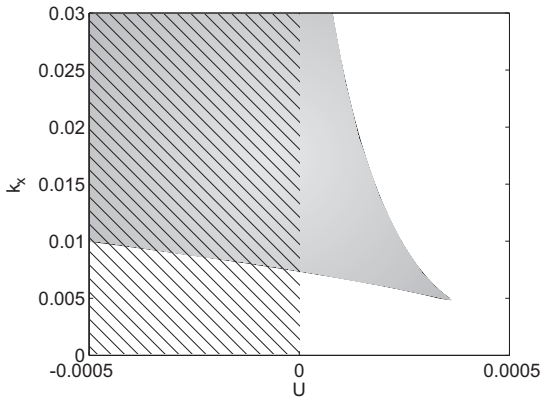

(d) Two parameter bifurcation.

Figure 3.4: Bifurcation analysis. Physically irrelevant areas are hatched. In 3.4(a) – 3.4(c) solid lines depict stable, dashed lines unstable steady states. In 3.4(d) the bistable region is filled in grey.

furcation). If the feedback is too strong even the weakest activation causes the almost complete activation of the proteases (illustrated in Figure 2.4). This behaviour is more quantitatively described in Figure 3.4(a) where stable steady states are depicted as solid lines and unstable steady states as dashed lines. The physically irrelevant areas are hatched.

So far we considered that an external stimulus affects the initial conditions of the systems without explicitly considering the stimulus, e.g. X_a is produced by some impulse stimulus. We now explicitly take the input into account and consider the stimulation of the system by a constant external stimulus. As can be seen in Figure 3.4(b) the bifurcation diagram changes. The steady state 1 is now not always at zero but depends on the external stimulus. The bifurcation diagram basically corresponds to a steady state response curve. When we slowly increase U the system response also rises slowly as steady state 1 rises slowly. Once steady state 1 vanishes, the system jumps into steady state 3 and then again slowly rises further. If we now slowly lower U we remain in steady state 3 and would only return to steady state 1 for negative U, i.e. the hysteresis is large. If we only allow $U \geq 0$, the system is basically trapped in steady state 3 – corresponding to a bistable behaviour of the system with $U \equiv 0$. The bifurcation diagram shows two saddle-node bifurcations.

If we now choose a smaller k_x as done for Figure 3.4(c) we find the same behaviour but with a smaller hysteresis allowing the system to jump back to steady state 1 for small but positive values of U. The system is still bistable for some values of the constant input U but is not irreversibly trapped for $U \geq 0$. Therefore, the system with $U \equiv 0$ is not bistable (compare Figure 3.2(a) and Figure 3.3(b) for $k_x = 0.005$).
Figure 3.4(d) provides a two parameter bifurcation diagram. The two branches do not correspond to steady states any more, but indicate bifurcation points. The lower branch represents the left saddle-node bifurcation and the upper branch the right saddle-node bifurcation (compare to Figures 3.4(b) and 3.4(c)). Between those branches, i.e. in the upper left part, the system is bistable, and it is monostable otherwise. As can be seen, the system is bistable for a large range of k_x for $U \equiv 0$. However, there is only a small range of k_x allowing for a reversible switching in dependence on U, i.e. where both bifurcation events occur for $U \geq 0$. While a normal cell irreversible switches to cell death execution, reversible switching could be of relevance in the other protease cascades introduced.

3.2.4 The influence of zymogenicity

So far we have assumed that the inactive form, also called pro-form or zymogen, of the protease does not possess any catalytic activity. However, it is well know that most zymogens have a residual activity. This activity is called zymogenicity and is defined as

$$z = \text{zymogenicity} = \frac{\text{activity of processed protease}}{\text{activity of zymogen}} \tag{3.18}$$

with known values ranging from 2 to 10^5 for different proteases (Stennicke and Salvesen, 1999). Next, we would like to evaluate the influence of zymogenicity as a pertubation on the system behaviour. To simplify the perturbation, we only consider that X has a zymogen activity. The ODE for Y_r for the cooperative model can be modified according to the definition of zymogenicity to give

$$\dot{Y_r} = k_y \cdot (1 - Y_r) \cdot X_r^n + \frac{1}{z} \cdot k_y \cdot (1 - Y_r) \cdot (1 - X_r)^n - k_d \cdot Y_r. \tag{3.19}$$

Proceeding accordingly for the different ODEs for Y_r (3.13) and (3.17) and again performing a phase plane analysis shows that this disturbance can affect the bistable behaviour of the system.
Figure 3.5 shows how the Y_r nullclines are shifted when increasing zymogen activity (corresponding to decreasing zymogenicity) from $z = \infty$ (grey line), corresponding to the previously evaluated case with no zymogen activity, to $z = 100$ and $z = 10$ (black lines). For the inhibitor (Figure 3.5(b)) and the zero-order setup (Figure 3.5(c)) the shift for $z = 100$ is so minor that the nullclines bury the $z = \infty$ nullcline. Clearly, the cooperative case is most severely affected (Figure 3.5(a)).

3.3 Summary and discussion

In this chapter we reviewed how a bistable behaviour can be generated in a small network of interacting proteins. Specifically, we chose two mutually activating proteases as encountered in apoptosis, blood clotting and several other signalling pathways (Section 2.1). Despite their widespread

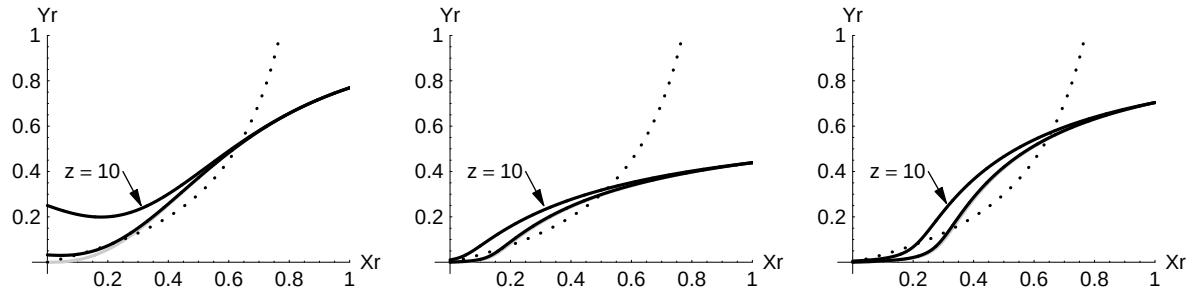

(a) Cooperative. (b) Inhibitor. (c) Zero-order.

Figure 3.5: The three basic mechanisms to generate bistability in the presence of zymogen activity: cooperative (Figure 3.5(a)), inhibitor (Figure 3.5(b)) and zero-order (Figure 3.5(c)) ultrasensitivity. All plots show the X_r nullcline in dashed black. The respective Y_r nullclines are depicted for $z = \infty$ (no zymogen activity) as solid grey lines. These are buried by the solid black lines in Figure 3.5(b) and 3.5(c) giving the Y_r nullclines for $z = 100$ and $z = 10$.

use in biological signalling networks, protease cascades have so far received little attention with respect to the generation of bistable switches. The irreversibility of the involved reactions, as well as the need to consider protein turnover, distinguish the examples from other well studied systems such as the MAPK cascade. Interestingly, the turnover can also be interpreted as a substitute for a back reaction. Whereas in the classical case of zero-order ultrasensitivity the back reaction has to be close to saturation in order to generate bistability, the same has to hold for the degradation in our example. We have focused on two interacting proteases producing a bistable behaviour. It is easy to envision that even a single protease can generate a bistable switch similar to kinases (Ferrell and Xiong, 2001), when an autocatalytic mechanism is introduced. In fact, such a mechanism was also proposed for the blood clotting cascade (Beltrami and Jesty, 1995; Jesty et al., 1993, 2005).

We employ phase plane and bifurcation analysis to illustrate the bistable behaviour from different viewpoints. Phase plane analysis generally relies on the reduction of the reaction system to second order. This reduction is not always possible. One interesting new concept routed in the theory of monotone systems is readily applicable to larger systems but restricted to special system classes as has already been mentioned (Angeli, 2006; Angeli et al., 2004). Both these graphical methods are mainly meant to get a qualitative picture, whereas bifurcation studies can be efficiently used to evaluate the parameter range for which the system actually does display a bistable behaviour. Bifurcation studies generally rely on continuation methods and numerical efficiency is the main limit. These studies can be performed in dependence on one or two parameters. Theoretically, the number of dimensions can be extended. The main restrictions are computational power and our visual conception.

Despite the primarily qualitative nature of phase plane analyses, these can already outline principle robustness features of the models evaluated here. The robustness of the three models compared in Figure 3.3 appears to mainly rely on the steepness of the ultrasensitive reaction component. In the models described here, this steepness is mainly depending on the number of molecules cooperating and their binding characteristics, the strength of the inhibitors binding or the saturation level as indicated by the Michaelis-Menten constant, respectively. However, the steepness is also affected by the chosen set of approximations (Blüthgen et al., 2006; Goldbeter and Koshland, 1981). In principle, none of the investigated mechanisms appears especially robust compared

to another, although Bagci et al. (2006) report that the cooperative mechanism outperforms the inhibitor mechanism in a similar setup regarding the robustness of bistable behaviour with respect to parameter variations. When considering zymogenicity, a class of perturbations so far mostly ignored, especially the behaviour of the cooperative model is affected and thus the model structure appears very fragile (Figure 3.5). To clarify this discrepancy, quantitative robustness considerations based on bifurcations will be presented in Section 5.3.

From a biological point of view, all three mechanisms appear reasonable. Although there are several evidences, further experiments are needed to prove the existence of a protease switch within the cell. Which mechanism is employed by nature and for what reason also awaits experimental elucidation. Clearly, many proteases are known to come along with specific inhibitors, e.g. caspases and IAPs. However, sometimes cooperative mechanisms appear to be involved in their activation, e.g. cytochrome c release and possibly apoptosome assembly in the mitochondrial apoptotic pathway (Rehm et al., 2006).

In the following chapter the inhibitor model introduced in this chapter will be detailed to satisfy the specific requirements of the direct pathway of receptor induced apoptosis. For this pathway, the many biochemical details known, support a mechanism where bistability is achieved via inhibitor ultrasensitivity. As zymogenicity has only a minor impact for that setting, we will ignore it in the following.

Chapter 4

Modelling and Bistability of the Direct Apoptotic Pathway

In this chapter mathematical models of the direct pathway of receptor induced apoptosis are derived and analysed. Section 4.1 provides details on these models. The 'basic' model closely resembles the inhibitor model introduced in Chapter 3. Extended bifurcation analyses of the basic model reveal inconsistencies in the current literature view of this pathway (Section 4.2). The analyses indicate the need for an additional inhibition of the initiator caspases, which we account for in an 'extended' model, and which is now supported by recent experimental data. Simulation studies show that this model qualitatively resembles current knowledge of caspase signalling on the single cell level (Section 4.3). The extended model shows no activation below a threshold input, while inputs above the threshold lead to a fast and irreversible activation of executioner caspases after a lag phase, which is inversely related to the input strength. An investigation of the involved rates reveals that interlinked feedback loops are responsible for this typical and interesting switching feature. During the lag phase IAP proteins efficiently block the caspase feedback loop, thereby sacrificing themselves. When the IAP pool is depleted, the caspase loop rapidly accelerates, leading to an almost complete activation of executioner caspase. Parts of the results presented in this chapter are published in Eissing et al. (2004).

4.1 Models of receptor induced apoptosis

Two different models are detailed in this section, which will be analysed in the following sections and chapters. The 'basic' model resembles the core processes of the direct pathway of receptor induced apoptosis. It will be analysed in Section 4.2. As we will describe in more detail, these analyses reveal the necessity of a slight but important model extension. The 'extended' model will be analysed in Section 4.3. The equations for both models are summarized in Figure 4.1.

Direct and mitochondrial pathway of apoptosis – motivating considerations. A model capturing the reactions outlined in Figure 2.1 was developed (52 reactions, data not shown; detailed in Conzelmann, 2003) to include both the mitochondrial and the direct pathway of receptor induced

apoptosis (Section 2.1). Several million simulations with random sets of parameters within a large range were performed. In each set, the parameters describing molecule synthesis were chosen to balance the degradation of the respective compounds when no active caspases were introduced. Thus, without an external trigger the system was in steady state (corresponding to the fixed initial conditions), showing no changes in the concentrations of the participating components. The parameter sets were then selected based on the behaviour towards different levels of active caspase 8 as an input. First, it was demanded that, after a delay in the range of 30 minutes to hours (Scaffidi et al., 1998), the majority of caspase 3 becomes activated within less than 30 minutes when the system is triggered with 200 molecules of active caspase 8 (Goldstein et al., 2000; Rehm et al., 2002; Tyas et al., 2000). Second, it was demanded that caspase 3 activation does not occur significantly without the mitochondrial pathway, but to occur when the input of active caspase 8 was elevated 10 fold. Third, with only 20 molecules of active caspase 8 as an input, it was required that caspase 3 does not become significantly activated even when the mitochondrial pathway was involved. Within a total time-scale of 8 hours only a few parameter sets fulfilled these requirements, but all of those also proceeded to full caspase activation with only 20 molecules of caspase 8 (and even without the mitochondrial pathway) on a longer time scale (data not shown).
Recapitulating, not a single parameter set could reconcile fast activation kinetics at higher inputs with tolerance to a few molecules of activated caspase 8. As many sets fulfilled the requirements posted on the mitochondrion-linked signalling part, e.g. regarding Bid cleavage, cytochrome C- and Smac-release, the results obtained in this initial work indicated a problem in the pathway (model) independent of mitochondrial signalling.
It is known that cell lines differ in their dependence on the mitochondrial pathway (Section 2.1). Whereas in type II cells the mitochondrial pathway is the primary route of apoptotic signals initiated at the DISC, type I cells primarily signal via the direct pathway and go into apoptosis even if the mitochondrial pathway is blocked (Scaffidi et al., 1998, 1999). Therefore the mitochondrial pathway was removed from the model, to perform more detailed analyses on the direct pathway of receptor induced apoptosis (see below) relevant in type I cells. By now, several studies more closely investigating the behaviour of the mitochondrial pathway with the help of mathematical models, independent of the direct pathway, have been reported (Bagci et al., 2006; Legewie et al., 2006; Rehm et al., 2006).
The problem to control caspase activation is further indicated by the calculations presented in Section 2.2.1. In the following, details on the direct pathway model will be provided, before a formal approach to more closely investigate possible causes for the observed phenomena are presented.

Basic model. The type I cell (Scaffidi et al., 1998) model reflects the pathway as generally accepted in the literature and is constructed with the purpose of being as simple as possible without neglecting essential steps concerning our analyses, i.e. simplifications represent conservative estimations regarding the analysis presented in Section 4.2. The model closely resembles the inhibitor model introduced in Section 3.2.2.
As a model input we consider an inflow of activated caspase 8, which is produced by the DISC formed at the membrane after death receptor stimulation (Lavrik et al., 2003; although the initial steps seem to be more complex in the case of TNFR1; Micheau and Tschopp, 2003; Schneider-

Brachert et al., 2004). We assume a pulsed inflow, which allows the input to be represented as an initial concentration of C8a. The model contains the following reactions:

$$C8a + C3 \rightharpoonup C8a + C3a \tag{4.1}$$

$$C3a + C8 \rightharpoonup C8a + C3a \tag{4.2}$$

$$C3a + IAP \rightleftharpoons C3aIAP \tag{4.3}$$

$$C3a + IAP \rightharpoonup C3a \tag{4.4}$$

$$\text{plus six degradation and turnover reactions.} \tag{4.5}$$

Pro-caspase 3 (C3, standing for the executioner caspases in general, e.g. caspases 3, 6 and 7) is cleaved and activated by activated caspase 8 (C8a; standing for both initiator caspases, caspases 8 and 10; reaction (4.1); Stennicke and Salvesen, 1999; Stennicke et al., 1998). Activated caspase 3 (C3a) positively feeds back onto pro-caspase 8 (C8; reaction (4.2); Cowling and Downward, 2002; Slee et al., 1999; Sohn et al., 2005; Van de Craen et al., 1999). Here we neglect the presumably amplifying effect of caspase 6 within this feedback loop. Activated caspase 3 binds to and is inactivated by XIAP, here for simplicity termed IAP (inhibitor of apoptosis protein), as cIAP-1 and cIAP-2 also have the capacity to block caspase 3 *in vitro*. However, the efficiency of binding is lower for cIAPs, and, as structural evidences indicate, the primary mechanism of inhibition is likely not by directly binding to C3a *in vivo* (as is the case for XIAP) but by facilitating its degradation (Eckelman et al., 2006; Ekert et al., 1999; Salvesen and Duckett, 2002). IAP-bound, activated caspase 3 may form a pool (reaction (4.3)). Furthermore, in parallel IAP molecules can be cleaved by the activated caspase 3 (reaction (4.4)). The cleavage products of XIAP have been described to exert only minor effects on caspase 3 (Deveraux et al., 1999), so these are neglected. Also, the two cleaved forms of caspase 3 are not distinguished, as both have been described to possess similar catalytic activities (Sun et al., 2002). Further on, activated caspases, as well as activated caspase 3 complexed with IAPs, are continuously degraded and pro-caspases as well as IAPs are subjected to a turnover (reactions (4.5)). Again we combine production and degradation terms into one apparent net rate for ease of notation (see Section 3.1). This provides ten reaction rates which can be balanced in six ODEs. The model equations are detailed in Figure 4.1. Table 4.1 provides nominal parameter values and below further technical assumptions are described.

Extended model. The extended model is, as the name suggests, an extended version of the basic model, which in addition incorporates a novel reaction as discussed in detail in Section 4.3.1. It includes all reactions described above (reactions (4.1) – (4.5)) and additionally considers molecules named CARP to bind to and inhibit C8a in a similar fashion to IAP inhibiting C3a:

$$C8a + CARP \rightleftharpoons C8aCARP \tag{4.10}$$

$$\text{plus two additional degradation and turnover reactions.} \tag{4.11}$$

The biological motivation and justification will be discussed in Sections 4.3 and 4.4. The extended model consists of 13 reaction rates and eight ODEs. Again, the model equations are detailed in Figure 4.1. Table 4.1 provides nominal parameter values and further technical assumptions are described below.

For the direct pathway of receptor induced apoptosis, we consider a basic model based on literature knowledge (to the left) which we analyse in Section 4.2 and an extended model (to the right) suggested by the analysis of the basic model. The extended model is analysed in Section 4.3.

For the basic model, we consider the rates

$$\begin{aligned} v_1 &= k_1 \cdot [C8a] \cdot [C3] \\ v_2 &= k_2 \cdot [C3a] \cdot [C8] \\ v_3 &= k_3 \cdot [C3a] \cdot [IAP] \\ &\quad - k_{-3}[C3aIAP] \\ v_4 &= k_4 \cdot [C3a] \cdot [IAP] \\ v_5 &= k_5 \cdot [C8a] \\ v_6 &= k_6 \cdot [C3a] \\ v_7 &= k_7 \cdot [C3aIAP] \\ v_8 &= k_8 \cdot [IAP] - k_{-8} \\ v_9 &= k_9 \cdot [C8] - k_{-9} \\ v_{10} &= k_{10} \cdot [C3] - k_{-10}. \end{aligned} \tag{4.6}$$

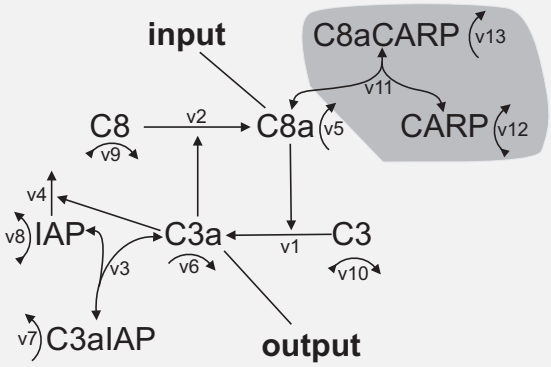

Balancing (4.6) yields (without v_{11})

$$\begin{aligned} \dot{[C8]} &= -v_2 - v_9 \\ \dot{[C8a]} &= v_2 - v_5(-v_{11}) \\ \dot{[C3]} &= -v_1 - v_{10} \\ \dot{[C3a]} &= v_1 - v_3 - v_6 \\ \dot{[IAP]} &= -v_3 - v_4 - v_8 \\ \dot{[C3aIAP]} &= v_3 - v_7. \end{aligned} \tag{4.7}$$

For the extended model we derive the additional rates

$$\begin{aligned} v_{11} &= k_{11} \cdot [C8a] \cdot [CARP] \\ &\quad - k_{-11} \cdot [C8aCARP] \\ v_{12} &= k_{12} \cdot [CARP] - k_{-12} \\ v_{13} &= k_{13} \cdot [C8aCARP], \end{aligned} \tag{4.8}$$

and extending the rates (4.6) by (4.8), the basic model (4.7) is extended by two variables

$$\begin{aligned} \dot{[CARP]} &= -v_{11} - v_{12} \\ \dot{[C8aCARP]} &= v_{11} - v_{13}. \end{aligned} \tag{4.9}$$

Further details on the assumptions, initial conditions and parameter values used can be found in Section 4.1 and Tables 4.1 and 4.2. The math-type font for the states and the squared brackets around them, commonly used to indicate concentrations, are generally omitted for readability in the following.

Figure 4.1: Models of the direct pathway of receptor induced apoptosis.

Assumptions, initial conditions, parameters and units. The basic and the extended model of receptor induced apoptosis are provided in Figure 4.1. The cleavage reactions (4.1), (4.2) and (4.4) are treated as being irreversible and it is assumed that the intermediary cleavage products ('enzyme-substrate complexes') only achieve very low levels and can thus be eliminated – reasonable estimations that have been confirmed by simulation experiments (data not shown; Conzelmann, 2003). The reaction rate equations are deduced according to the law of mass action, which we consider here better suited than other kinetic approaches, like Michaelis-Menten kinetics, whereas theoretical considerations show that the results would be very similar in our case (data not shown). From

Table 4.1: Nominal parameters used in the models summarized in Figure 4.1. Calculations are performed in the unit 'molecules per cell' (mpc). In parentheses the values are shown in more common units to enable a direct comparison with literature values presented in Table 4.2.

	Value	**Unit**		**Value**	**Unit**
k_1	$5.8 \cdot 10^{-5}$ $(5.8 \cdot 10^5)$	$mpc^{-1}min^{-1}$ $(M^{-1}s^{-1})$	k_{-1}	–	
k_2	10^{-5} (10^5)	$mpc^{-1}min^{-1}$ $(M^{-1}s^{-1})$	k_{-2}	–	
k_3	$5 \cdot 10^{-4}$ $(5 \cdot 10^6)$	$mpc^{-1}min^{-1}$ $(M^{-1}s^{-1})$	k_{-3}	0.21 (0.0035)	$min^{-1}(s^{-1})$
k_4	$3 \cdot 10^{-4}$ $(3 \cdot 10^6)$	$mpc^{-1}min^{-1}$ $(M^{-1}s^{-1})$	k_{-4}	–	
k_5	$5.8 \cdot 10^{-3}$ (120)	min^{-1} (min)	k_{-5}	–	
k_6	$5.8 \cdot 10^{-3}$ (120)	min^{-1} (min)	k_{-6}	–	
k_7	$1.73 \cdot 10^{-2}$ (40)	min^{-1} (min)	k_{-7}	–	
k_8	$1.16 \cdot 10^{-2}$ (60)	min^{-1} (min)	k_{-8}	464 $(1.3 \cdot 10^{-11})$	$mpc\, min^{-1}$ $(M\ s^{-1})$
k_9	$3.9 \cdot 10^{-3}$ (180)	min^{-1} (min)	k_{-9}	507 $(1.4 \cdot 10^{-11})$	$mpc\, min^{-1}$ $(M\ s^{-1})$
k_{10}	$3.9 \cdot 10^{-3}$ (180)	min^{-1} (min)	k_{-10}	81.9 $(2.3 \cdot 10^{-12})$	$mpc\, min^{-1}$ $(M\ s^{-1})$
k_{11}	$5 \cdot 10^{-4}$ $(5 \cdot 10^6)$	$mpc^{-1}min^{-1}$ $(M^{-1}s^{-1})$	k_{-11}	0.21 (0.0035)	min^{-1} (s^{-1})
k_{12}	10^{-3} (693)	min^{-1} (min)	k_{-12}	40 $(1.1 \cdot 10^{-12})$	$mpc\, min^{-1}$ $(M\ s^{-1})$
k_{13}	$1.16 \cdot 10^{-2}$ (60)	min^{-1} (min)	k_{-13}	–	

this, molecular balances can be derived for each considered molecular species resulting in the ODE systems (4.7) for the basic model and (4.9) for the extended model.

We take the average concentrations in an unstimulated cell as initial conditions. For caspase 8 and 3 these were quantified in HeLa cells to be 130,000 and 21,000 molecules per cell (mpc), respectively, using quantitative western blot analyses (unpublished data, Institute of Cell Biology and Immunology, University of Stuttgart; Eissing, 2002). The average concentration of IAPs was estimated to be 40,000 mpc. Other reported concentrations are 30 nM, 200 nM and 30 nM for caspase 8, caspase 3 and XIAP respectively (Stennicke et al., 1998; Sun et al., 2002). Estimating a cell volume of 1 pl yields that 600 mpc is equivalent to 1 nM. Thus, the values are in the same order of magnitude and were used as initial concentrations. The other compounds were considered not to be present in the absence of a stimulus. In the extended model, the concentration of the newly introduced molecule CARP was assumed to be 40,000 mpc (corresponding to the IAP concentration). We consider the unit mpc more illustrative for cellular concentrations than the unit M, but on the other hand we prefer and use units such as $M^{-1}\ s^{-1}$ for K_m/k_{cat} ratios.

Table 4.1 lists the parameters as used in simulations (unless indicated otherwise). The respective values are also provided in more common units (in brackets). For the reaction rates v_3 and v_5 – v_{10} the parameter values were taken from the literature as stated in the model description. The respective references are summarized in Table 4.2. For the reaction rates v_1, v_2 and v_4 values were chosen that are in accordance with the desired kinetics and the requirement for bistability (as deduced from bifurcation analyses, see below). The values for v_{11} were fixed under the assumption of a similar binding affinity as reported for v_3. The values for the v_{12} and v_{13} represent estimated turnover rates.

The models were implemented in MATLAB® (The MathWorks[1], Inc., Natick, MA) for simulation

[1] http://www.mathworks.com/

experiments, Mathematica® (Wolfram Research[2], Inc., Champaign, IL) for analytical analysis, and XppAut[3] (Ermentrout, 2002) for numerical bifurcation analysis (continuation).

4.2 Bistability evaluation of the basic core model

In Sections 2.2.2 and 4.1 it was motivated why the caspase model should exhibit a bistable behaviour. Recognizing the close relationship of the basic model to the inhibitor model introduced in Section 3.2.2, the model should allow for bistability. In this section we will analyse for what parameters bistability is possible and compare the results to experimental literature data. In Section 4.2.1 we will summarize our steady state and stability calculations as well as bifurcation results for the basic model. We do not elaborate on the latter, as they closely resemble the results obtained for the inhibitor model analysed in Section 3.2.3. Instead, we will present additional results in Section 4.2.2 that are able to illustrate parameter dependences in a three dimensional parameter space.

4.2.1 Steady states, stability and bifurcations

We first explain a possible way to calculate the steady states and their stability for the basic model and then summarize 'classical' bifurcation analysis results.

Steady state derivation and stability analysis. The steady states were derived under the steady state condition $\dot{x} = 0$ (for all compound concentrations x). A consecutive elimination of variables leads to a third order polynomial in C3a, whose solutions present the steady state concentrations of C3a from which the steady state concentrations of the other molecular species can be derived. The 'life' steady state, corresponding to the standard initial conditions where no active caspases are present, can be factored out leaving a quadratic equation of the general form $ax^2 + bx + c = 0$ for the basic model. Interestingly, the coefficient c is the same as the coefficient c derived in the stability analysis of the life steady state (see below).
For the life steady state one can easily construct the characteristic polynomial $det(\lambda I - A) = 0$. Here, det refers to the determinant, λ represents the Eigenvalues, I the identity matrix and A the Jacobian matrix of the basic model evaluated at the life steady state. For the nonlinear ODE system to be locally (asymptotically) stable, all Eigenvalues need to have negative real parts. The Hurwitz criterion provides conditions for stability based on the coefficients of the characteristic polynomial. The most restrictive condition for the basic model is that the coefficient c

$$c = k_5(k_3k_7IAP + k_6(k_7 + k_{-3})) - k_1k_2(k_7 + k_{-3})C3C8 \tag{4.12}$$

is positive. The stability of the steady states other than the life steady state can easily be evaluated numerically.

[2]http://www.wolfram.com/
[3]http://www.math.pitt.edu/∼bard/xpp/xpp.html

Classical bifurcation analysis. Classical bifurcation analysis can be performed using above knowledge or standard numerical continuation tools. The bifurcation diagrams look similar to the bifurcation diagram for the inhibitor model (Section 3.2.3, Figure 3.4). In fact, an exemplary result with bifurcation parameter k_1, where all parameters apart from k_1 were fixed according to Table 4.1, is shown in Figure 2.4(c) (Section 2.2.2). The transcritical bifurcation occurs at $k_1 \approx 3.2 \cdot 10^3\ M^{-1}s^{-1}$. A stable life steady state is only possible below this value, which is more than 300 times lower than reported in literature (Stennicke and Salvesen, 1999; Stennicke et al., 1998).
However, the situation might look different when assuming different values for the parameters that are kept constant. Generally, the high dimension of the parameter space makes conclusive statements difficult using traditional methods. Therefore, in the following section we will use the knowledge derived above to conduct an 'untraditional' bifurcation and bistability analysis in higher dimensions.

4.2.2 Higher dimensional bistability analysis

Classical continuation approaches for tracing bifurcation points in three (or higher) dimensions are numerically and computationally very demanding. Below, we will outline how alternative bistability constraints can be derived exploiting the special systems structure outlined in the last section. While we have to rely on a three dimensional analysis for visualisation, we complement the analysis by a Monte Carlo approach and thereafter shortly discuss the special role of IAPs.

Bistability within a small parameter domain. For visualization we group our parameters into three classes, which also allows a simultaneous variation. The parameters were grouped according to biological considerations and relations were chosen based on the literature summarized in Table 4.2:

- caspase activation: $k_1 = 2 \cdot k_2$,
- turnover (half-life time): $k_7 = k_8 = 2 \cdot k_5 = 2 \cdot k_6 = 4 \cdot k_9 = 4 \cdot k_{10}$,
- IAP cleavage: k_4.

For the parameters k_3 and k_{-3} thermodynamic binding affinities are available that can be considered more reliable than values for the other parameters, which were estimated by experimental techniques that have to be considered less accurate. Consequently, v_3 was kept fixed in the following analysis. In fact, the binding affinities only determine the ratio of the two parameters. However, association rates have also been reported and as long as the binding is fast, as reported, the exact values exert a minor influence (see Sections 5.1 and 5.4.3).
Figure 4.2 shows the transcritical bifurcation point in dependence of the three parameter classes (red surface, transcritical bifurcation manifold). The surface can be constructed by setting (4.12) to zero corresponding to a stability change of the life steady state. A stable life steady state is possible below the red surface. The two additional steady states besides the life steady state provide further information. Theoretically, one additional steady state within the positive concentration range is sufficient to achieve bistability (because other phenomena than an unstable steady state could

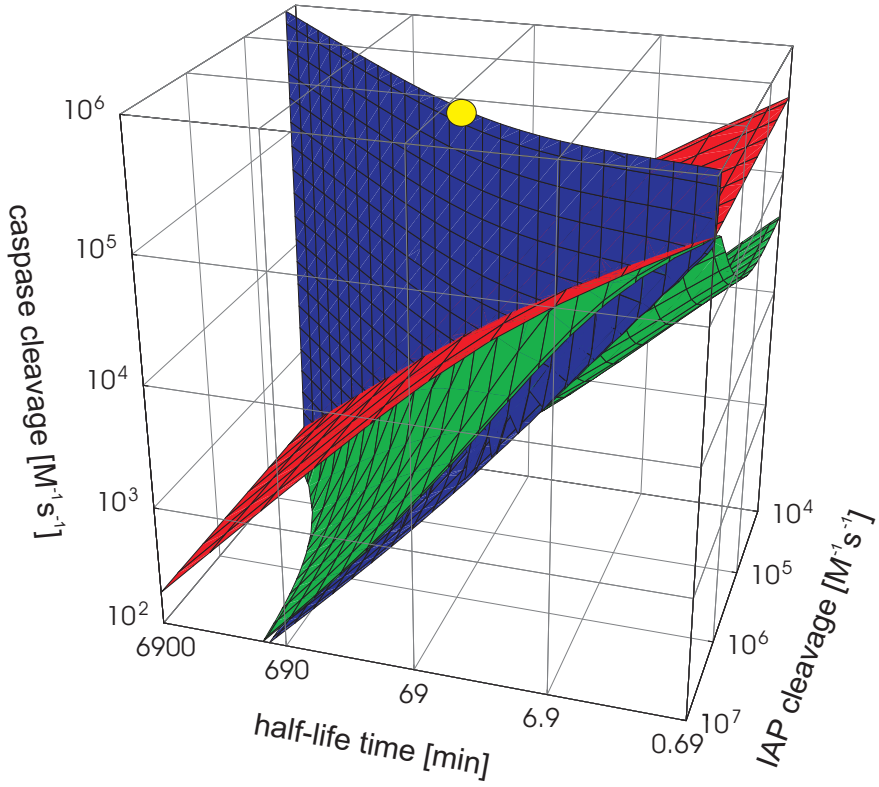

Figure 4.2: (Bi-) Stability analysis. Stability aspects of the basic model were evaluated over wide parameter ranges. For the three-dimensional visualization the following parameter ratios were chosen as axis: for caspase activation $k_1 = 2 \cdot k_2$, for half-life time $k_7 = k_8 = 2 \cdot k_5 = 2 \cdot k_6 = 4 \cdot k_9 = 4 \cdot k_{10}$, and for IAP cleavage k_4; v_3 was fixed according to literature values. The yellow dot indicates values as expected from literature data (although the IAP cleavage reaction parameter can only be estimated, see Table 4.2). Above the red area no stable life steady state exists, below the blue area no second stable steady state within the positive concentration range can exist and below the green area the solutions are complex numbers. Thus, bistability requires parameter combinations below the red AND above the blue AND above the green area.

separate the two stable steady states). However, in our model this configuration is only possible above the red surface and for that setting the life steady state is unstable. Accordingly, bistability is only possible if both additional steady states are within the positive concentration range, which is the case above the blue surface in Figure 4.2 on which the coefficient ratio $-b/a$ from the quadratic equation for C3a is zero. Another restriction is imposed by our biological system as the solutions must contain real numbers, which is the case above the green surface in Figure 4.2 on which $b^2 = 4ac$ (saddle-node bifurcation manifold).

The parameter combinations that can be deduced from literature are indicated by a big yellow dot. Thus, bistability is only possible in a very restricted parameter region far away from values reported in literature (Figure 4.2). Please note the logarithmic axes. In accordance with general considerations on this topic (Section 2.2.2) the feedback from caspase 3 onto caspase 8 is necessary for bistability (data not shown).

To further evaluate our results, we lift the restrictions imposed by the parameter relations and conducted several million simulations with small inputs and random sets of parameters taken from the

Table 4.2: Instability ranges. Parameter ranges that do not provide parameter combinations enabling a stable life steady state. The k_- column indicates whether a reaction is assumed to be reversible or not. If reversible, the values can be calculated with the help of the provided explanations. The last column also provides literature parameter values and respective references.

	k_+min $[M^{-1}s^{-1}]$	k_+max $[M^{-1}s^{-1}]$	k_- $[s^{-1}]$	**Explanations and References**
v_1	$3 \cdot 10^4$	$5 \cdot 10^6$	no	*in vitro* $K_M/k_{cat} = 10^6\ M^{-1}s^{-1}$ (Stennicke and Salvesen, 1999; Stennicke et al., 1998)
v_2	$2 \cdot 10^4$	$5 \cdot 10^6$	no	C3a faster than C8a using fluorogenic substrates (Garcia-Calvo et al., 1999; Stennicke and Salvesen, 1999; Van de Craen et al., 1999)
v_3	$1 \cdot 10^5$	$5 \cdot 10^6$	yes§	§ to obtain: *in vitro* K_i = 0.7 nM (Deveraux et al., 1997; Ekert et al., 1999)
v_4	$1 \cdot 10^3$	$5 \cdot 10^6$	no	estimation
	$t_{1/2}$min $[min]$	$t_{1/2}$max $[min]$	k_- $[M\ s^{-1}]$	$k_+\ [min^{-1}] = \ln 2/t_{1/2}$
v_5	30	300	no	$t_{1/2} \approx 180\ min$ for caspases; $t_{1/2}$ = 30 - 40 min for DIAP (Ditzel and Meier, 2002; Yoo et al., 2002); production rate to establish the initial concentration
v_6	30	300	no	
v_7	30	300	no	
v_8	30	300	yes	
v_9	60	500	yes	
v_{10}	60	500	yes	

parameter ranges shown in Table 4.2. All combinations resulted in significant caspase activation with very small input signals (i.e. an unstable life steady state), although the onset time varied greatly (data not shown).

IAPs and their cleavage. Interestingly, by and large the stability of the life steady state seems to be independent of the IAP cleavage reaction (Figure 4.2). This is not expected and indeed dynamic simulations show that, upon faster IAP cleavage, the onset of caspase activation is achieved more rapidly for parameter combinations where the life steady state is unstable (data not shown). However, for parameter combinations where the life steady state is stable, a slower reaction stabilizes the life steady state by enlargement of its area of attraction. Without this reaction, the life steady state is globally stable. This can be explained by the fact that we assumed higher concentrations of IAPs than that of caspase 3, in order to make a conservative estimation concerning the stability of the life steady state. If we assume lower numbers of IAP molecules and require the turnover not to exceed that of caspases significantly, we can achieve bistability even in the absence of this cleavage reaction, as demonstrated in Section 3.2.2. However, the parameters where a stable life steady state is possible, would be even further away from those values reported in literature (data not shown). Summarizing, the model indicates that the IAP cleavage reaction is important for a decisive switching.

Further analysis of the model reveals that apoptosis can only proceed after the IAP pool is exhausted, as otherwise most of the active caspase 3 molecules become neutralized (data not shown). As the binding of active caspase 3 to IAPs is a reversible reaction, a slower degradation of the com-

plexes would elevate the levels of free active caspase 3 and therefore promote apoptosis. Thus, our results also argue for the view of IAPs as altruistic proteins, sacrificing themselves to prevent cell death (Ditzel and Meier, 2002). In our investigations we did not change the initial concentrations in order to restrict the number of free parameters. The effects of changed initial concentrations will be evaluated in Section 5.1. Further, looking at the model equations it can be seen that changing certain parameter values, as done above, has a similar influence as changing certain initial concentrations.

In summary, the above analysis reveals a major problem in the known biochemistry of apoptosis (Hengartner, 2000), as outlined in the many reviews on this topic. However, the problem is not observable in a static diagram (as commonly drawn in biological reviews) but only unfolds in an analysis also considering system properties and dynamic aspects. Either, the *in vitro* caspase activity measurements provide values that are several orders of magnitude away from the true *in vivo* activities to allow for bistability, which could then, however, also no longer explain the fast activation kinetics observed *in vivo*. Or, the model structure assumed, and therefore current knowledge, is missing important regulatory elements.

4.3 Model extension and simulation studies

As outlined in the previous section, the known components and reactions of the much studied apoptosis pathway cannot explain experimental measurements when evaluated from a systems perspective. In this section, we will first discuss possibilities to resolve the observed discrepancies. A single hypothesis cannot be excluded but is supported based on a critical evaluation of literature and using insights gained through modelling and analysis. We extend our basic model accordingly and show that this extended model is in good agreement with key features observed in experiments (Section 4.3.2). In Section 4.3.3 we then use our mathematical model to reveal the key processes shaping the observed behaviour.

4.3.1 Possible model extensions

An inherent problem of the described basic model of caspase activation is that relatively fast activation kinetics must be realized in order to be consistent with parameter values from literature and observations in various experimental setups (Fladmark et al., 1999; Goldstein et al., 2000; Krippner-Heidenreich et al., 2002; Luo et al., 2003; Rehm et al., 2002, 2006; Tyas et al., 2000). However, only if the kinetics are slow, the system displays the desired bistability, which allows for a threshold to filter out small accidental stimuli. Thus at low concentrations of activated caspases the reactions should be slow, but fast for high concentrations. There are several possibilities how a model extension could reconcile those facts. The basic idea is ultrasensitivity as discussed in Chapter 3. A common way in cell biology to achieve such a behaviour is cooperativity (Section 3.2.1), which could also be assumed to exist for caspases, as they are known to act as heterodimers. However, experimental results by Donepudi et al. (2003) indicate that the monomer is just as bioactive as the dimer, arguing against this possibility. Another mechanism could be zero-order ultrasen-

sitivity (Section 3.2.2): at low concentrations the active caspases are quickly degraded but the degradation machinery becomes saturated and is not able to handle larger amounts of activated caspases. However, there are no evidences in literature supporting such a mechanism.
Alternatively, one might suggest a mechanism where the amount of free active caspases is limited by inhibitors. Such mechanisms are well known to exist for caspases 3 and 9, where IAPs lower the effective concentration of active proteases. Similar mechanism have recently been promoted for caspase 8 but have not found a wide appreciation yet. It has been reported that activated caspase 8 can be functionally inactivated in mitochondrial membranes. There, the molecule BAR (bifunctional apoptosis regulator) has been proposed to bind to activated caspase 8 via its pseudo death effector domain leading to effective neutralization of its proteolytic activity. However, conflicting results exist (Breckenridge et al., 2002; Qin et al., 2001; Stegh et al., 2002; Zhang et al., 2000). More recently, caspase 8- and 10-associated RING proteins (CARPs) were identified in a high-throughput screen as binding to the receptor-associated initiator caspase. Their suppression results in apoptosis sensitisation and inhibition of tumour cell growth and homologies to IAPs are indicated (McDonald and El-Deiry, 2004). Apart from an inhibitor for C8a, an inhibitor for caspase 6 could also solve part of the problem by introducing a double seal in the feedback loop. However, there are no hints for this mechanism in literature and it could also not explain how some cells can live with partially activated caspase 8 – an inhibitory mechanism that is more active in these settings on the other hand could. Also, simulation studies of our basic model show that even without this positive feedback loop, minor amounts of C8a can activate caspase 3 quite fast. Further on, it is intuitive to control such a deadly mechanism at the front end. Certainly, regulators like FLIPs are know to control caspase 8 activation. However these cannot control C8a itself.
Therefore, we hypothesise that inhibitors of C8a must exist. We include a corresponding mechanism into our model and name the molecules CARP in this thesis, as they present the most reasonable candidates based on current knowledge. (In our original publication the molecules were named BAR as the discovery of CARPs was only published after the initial submission of our manuscript.) The extended model is described in Section 4.1 and analysed in the following.

4.3.2 Executioner caspase activation

The extended model equations allow for five steady states, two of which contain negative concentrations for the evaluated parameter range and are thus not of interest. Importantly, stability of the life steady state and bistability of this extended model is possible with kinetic values close to those described in literature (data not shown: transcritical bifurcation point at $k_1 \approx 5.9 \cdot 10^5 M^{-1} s^{-1}$ for the other parameters as shown in Table 4.1). Generally, the extended model also allows for additional complex dynamics like limit cycles for more extreme parameter values (e.g. turnover of caspases in the range of seconds to minutes, data not shown). In accordance with our findings, Carotenuto et al. (2007b) also present formal proofs of the steady state and stability properties of the extended model and discuss the oscillation behaviour.
We performed simulations with input signals of different strength (Figure 4.3) for the parameters outlined in Table 4.1, which allow for bistability and which we consider biologically reasonable. In each case, caspase activity remains low for a certain time, inversely proportional to the stimulus strength, followed by a steep rise in activity if the input exceeds the threshold (about 75 molecules

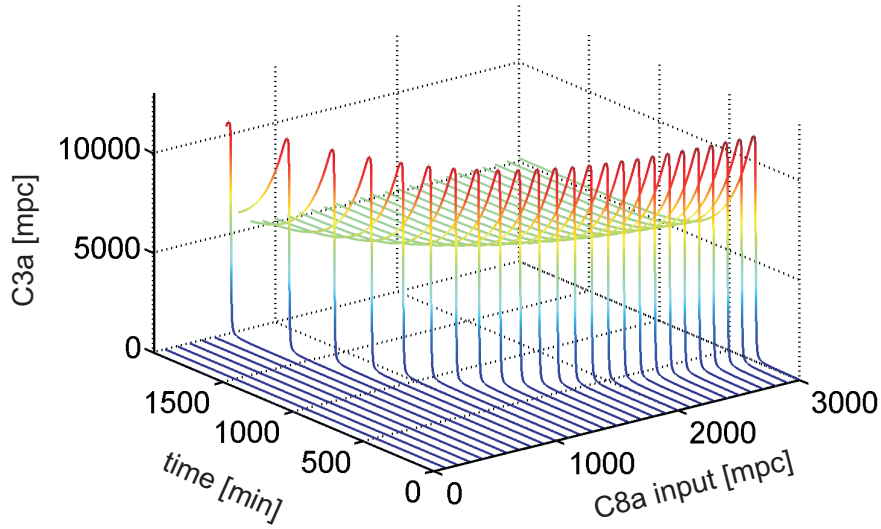

Figure 4.3: Bistable behaviour of the extended model. Simulation experiments with varying inputs (initial C8a concentrations) and C3a over time as output are shown. Above a certain input threshold ($\sim$75 molecules of C8a) the system becomes fully activated, while sub-threshold activation results in recovery. The two stable steady states can be envisioned, with the life steady state corresponding to the blue area and the apoptotic steady state corresponding to the green area achieved after longer times.

of activated caspase 8 per cell). After reaching a maximum, caspase activity ceases again, due to our assumption of higher degradation rates for the activated caspases as compared to the production rates of the pro-caspases. Similar to the model without the molecule CARP, the IAPs again play a critical role (see below). Although the exact quantitative behaviour depends on the choice of parameters (which cannot be properly identified from the available data), these simulations display the desired characteristics like bistability and fast activation kinetics combined with prolonged lag phases, inversely related to the strength of the apoptotic trigger, as observed in experiments (Rehm et al., 2002).

4.3.3 Concentration and rate time evolution

As outlined above, the extended model reproduces available biological data. We will now more closely evaluate the processes happening within the model that allow for the characteristic time courses shown in Figure 4.3. Figure 4.4(a) and (b) show how the different molecular species evolve over time for an input stimulus of 5,000 mpc C8a. Figure 4.4(c) to (f) show how the different rates, as detailed in Figure 4.1, evolve in the same time frame. Thereby, the rates of reversible reactions were divided into a forward and backward reaction part indicated by '+' and '-' signs. Six of the 13 reactions are reversible, resulting in 19 partial rates. Four of those are constant production terms of which only one is shown as an example and for comparison (v_{-9}, Figure 4.4(e)). All solutions are given in both absolute units (dashed lines) and in relative units where each rate was normalized to its respective maximum to allow a better comparison (solid lines). The components and rates were grouped and coloured to reveal redundant information, and enable an insight into cause and

consequence. The most important aspects will be discussed in the following, primarily focussing on the relative quantities.

Initial phase. The C8a input is applied as an initial condition corresponding to a pulse stimulation. Rapid processes happen as a direct consequence within the first minute. Several rates peak at the very beginning never again returning close to their maximal relative rates at the value 1. Although this can hardly be seen directly, it becomes evident by the fact that these rates do not reach their maximum in the remaining time interval (or by more specifically inspecting the relevant time frame, data not shown). The binding of C8a to CARP, v_{-11} (f) peaks leading to an initial fast but small decrease of CARP which captures most of the available C8a. The formation of the complex leads to a sharp increase of the rates proportional to this concentration, v_{13} (d) and v_{-11} (f), corresponding to complex degradation and dissociation, respectively. Also, the caspase 3 cleavage rate, v_1 (e) peaks at the very beginning before C8a is complexed to CARP. Due to the extremely short peaking, only a limited amount of C3a is produced, most of which is directly captured by IAP (b).

Lag phase and switching transition. Probably the most interesting and relevant phase is the lag phase, during which mainly slow processes occur, and the transition to the rapid caspase activation phase. During the lag phase IAP dominates C3a leading to the degradation of most active caspase 3. In fact, the amount of C3a left is not able to activate enough caspase 8 to allow an increase of its concentration. For almost one hour C8a is slightly decreasing (data not shown/visible). However, C3a increases slowly but steadily, finally again causing a slow increase of C8a. Still, enough IAP is left to hold C3a down. However, IAPs are thereby sacrificing themselves as well (Ditzel and Meier, 2002). While the IAP concentration is slowly but significantly decreasing (a), C3a starts to very slowly increase (b). When the IAP concentration becomes small (a), more C3a is left unbound to activate caspase 8 v_2, (e), consequently also leading to a faster increase of v_1, (e), consequently leading to a faster increase of C3a (positive feedback). Thus, the mutual caspase activation rates very slowly rise conversely causing a slow increase of the active caspases. These are controlled by their respective inhibitors. Finally, in the switching phase, C3a assumes control by cutting the remaining IAP molecules (peaking of v_4, (e)). The crucial role of this reaction enabling bistability has been discussed in Section 4.2.2 and holds for the extended model. Finally, the caspase activation loop efficiently peaks clearly dominating this phase (v_1 and v_2, (e)). Consequently, active caspases suddenly increase while their pro-forms suddenly almost vanish. And from then on the high amount of C3a (b) keeps IAP down (a) – the switch has tipped and apoptosis is inevitable. The dominance of the activated caspases over their pro-forms and inhibitors is reflected in the degradation rates, which go up for the activated caspase (v_5 and v_6, (d)) and down for the other proteins (v_8, v_9, v_{10} and v_{12}, (c)). Only the complexes of the caspases and their inhibitor are further degraded at a high rate (v_7 and v_{13}, (d)) reflecting that newly produced inhibitors are now 'captured' by the caspases and consequently degraded.
Figure 4.4 also reveals that caspase 3 activation generally precedes caspase 8 activation where the majority is activated as a consequence, (a) and (b). Likewise, IAP depletion precedes CARP depletion. This reflects the faster forward part of the positive feedback loop as well as the additional cleavage of IAP by C3a. The higher production rate of C8 compared to C3 in combination with a smaller k_2 value compared to k_1 allows a higher apoptotic steady state for C8 compared to C3. This

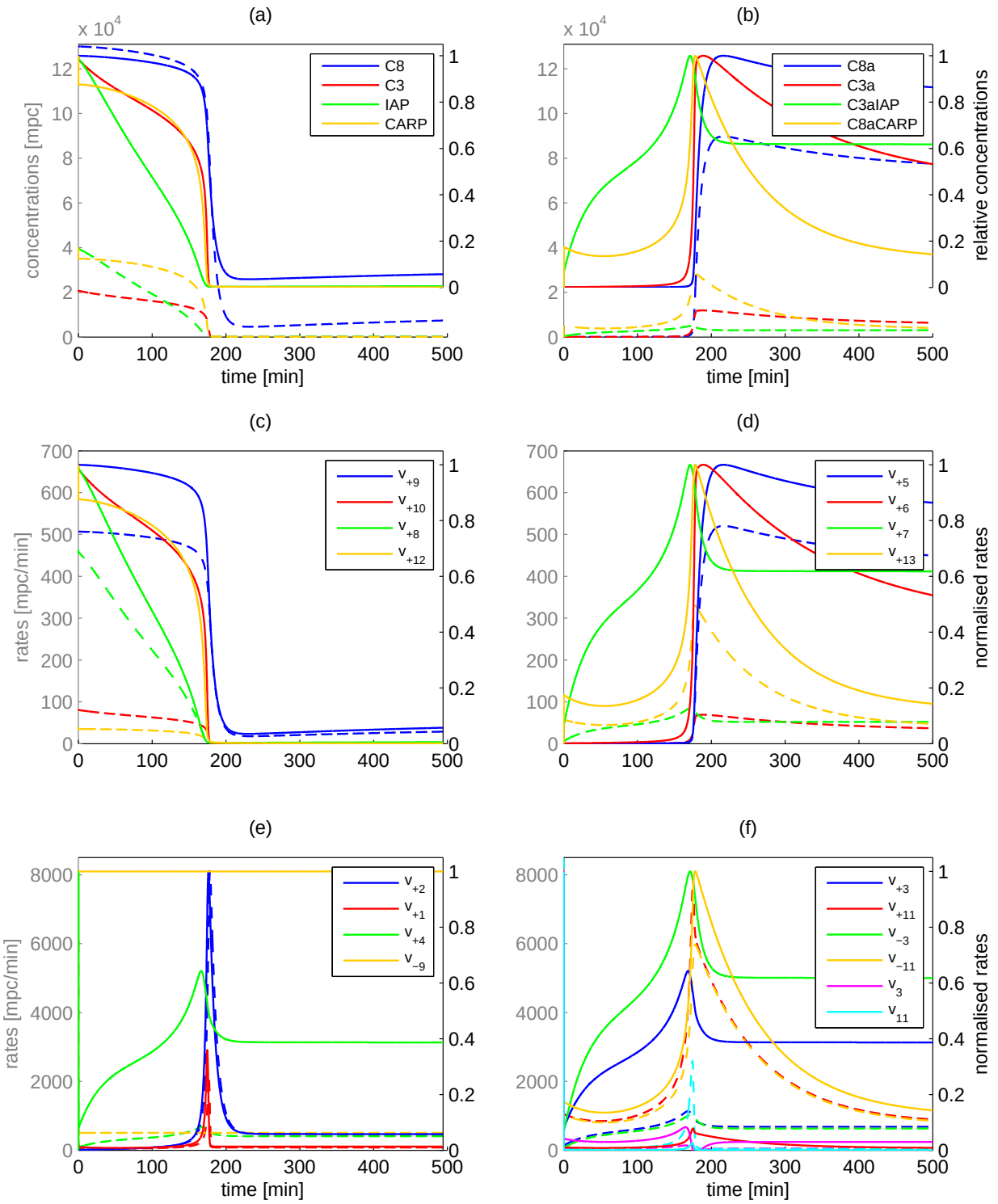

Figure 4.4: Concentration and rate trajectories. Shown is the time evolution of all system components ((a)-(b)) and non-constant rates ((c)-(f)) after an input stimulus of 5,000 mpc C8a. The absolute values are shown as dashed lines with their axis on the left-hand side. The axis on the right hand-side corresponds to the relative component concentrations or rates (solid lines), where each time course was normalized to its corresponding maximum.

higher amount of C8 also causes a larger rate v_2 compared to v_1 although the associated kinetic parameter values show an opposite relation.

A feedback perspective. Recently, the usefulness of representing biological networks as incidence graphs has been employed to reveal network elements responsible for complex nonlinear behaviour such as bistability and oscillations (see Angeli et al. 2004 and the supplementary material thereof for the methodology in a biological context). Although the full approach cannot be applied to our model (the system is not monotone), such a representation reveals another interpretation of the inhibitor binding reactions (data not shown): the edge in the incidence graph from C3a to IAP is negative, as is the edge in the opposite direction. (The same is true for C8a and CARP.) Two negative edges in a loop have been classified as positive feedback. In fact, the incidence graph reveals even more positive feedback loops in our network. However, under the above considerations the two most critical loops appear to be those centred on C3a. From this point of view, it can be argued that the double negative (positive) feedback is responsible for the lag phase and for stabilizing the two different cellular states (before and after switching), while the (true) positive feedback is responsible for the fast switching between those states.

Summarizing, the mutual caspase activation is directly responsible for the fast switching observed, while the IAPs allow the long delay by keeping the positive feedback down during this lag phase.

4.4 Summary and discussion

In this section we provided simplified models of the core reactions of apoptosis, with a special focus on the direct pathway initiated by death receptors. While simplified, the proposed basic model already represents the relevant steps of the signalling pathway based on the current literature view (Ashkenazi, 2002; Hengartner, 2000; Thornberry and Lazebnik, 1998). Simplifications mainly include conservative estimations with respect to the subsequent analysis. Because the molecular events occurring at the level of the receptor induced signalling complex are only in part understood (Micheau and Tschopp, 2003; Scaffidi et al., 1998; Schneider-Brachert et al., 2004), the input signal of the model is represented by a given number of molecules of activated initiator caspase, excluding the pathways how this initial caspase activation is mediated.
The bifurcation analysis reveals that the network is able to fulfil the principle requirement of allowing a bistable signalling as motivated in Section 2.2.2. However, additionally taking kinetic information from various sources into account reveals that the system cannot produce the dynamic requirements observed. For bistability, kinetic parameters are required that are far away from those reported in literature. For example, the kinetic properties of the caspase must be orders of magnitudes smaller than measured in biochemical experiments. However, when postulating such small caspase activities, the resulting system cannot execute as rapidly and decisively as has been observed on the cell biological level.
Our model analysis suggest that activated initiator caspases have to be controlled in a similar way as IAPs control executioner caspases. Critically evaluating the literature with respect to possible additional control mechanisms, we find that indeed most alternatives can be ruled out, but now

find support for our hypothesis in a recent publication, where CARPs are identified as molecules binding to and inactivating receptor associated initiator caspases (McDonald and El-Deiry, 2004). We extend our model accordingly and show that it allows a behaviour, which reproduces observed kinetics and is in agreement with reported kinetic values. Importantly, it is in agreement with three key features described for this signalling pathway: *i)* a rapid development of the executive phase of apoptosis, i.e. executioner caspase activation; *ii)* resistance towards small, unintended activating signals, a mandatory prerequisite to prevent accidental apoptosis, and *iii)* a prolonged delay phase before the activation of the executioner caspases, the length of which is inversely dependent on the strength of the apoptotic signal.

Additional explanations for the long lag phases have been proposed recently. A certain delay is introduced in TNF induced apoptosis by the formation of the signalling complex 2 (Section 2.1, Micheau and Tschopp, 2003; Schneider-Brachert et al., 2004). However, this is not evident for TRAIL and FAS induced apoptosis and our studies demonstrate that caspase 8 and 3 inactivation is a likely mechanistic explanation for the observed lag period followed by fast effector caspase activation. Whereas this lag phase might be largely controlled at the level of the mitochondria in type II cells (Goldstein et al., 2000; Rehm et al., 2002, 2006), a similar behaviour was also observed for type I cells, where the initial activation of caspase 8 usually takes place immediately after stimulation (Lavrik et al., 2003; Scaffidi et al., 1998).

In an even more recent study, it is indicated that CARPs act as ubiquitin ligases promoting p53 degradation (Yang et al., 2007). Based on this finding it could be speculated that CARPS might not primarily act by directly binding and inhibiting C8a but by binding and promoting its rapid degradation, as is indicated for cIAPs action on C3a. These steps would also open the opportunity to integrate zero-order ultrasensitivity as investigated in Section 3.2.2. Based on the results presented in the last two chapters, this could contribute to the observed switching but would only underscore our primary result, which demands for additional regulation. Likely, the near future will provide more conclusive data on the exact regulatory mechanism of action.

We further analysed what processes are responsible for the different characteristics observed. Clearly, the system as a whole shapes its performance. The CARP molecules were responsible for allowing a realistic description in the first place. However, our analysis outlines another interplay as pivotal. The mutual caspase activation is directly responsible for the fast switching observed, while the IAPs allow the long delay by keeping the positive feedback down during this lag phase. From a systems perspective, this can be interpreted as interlinked positive and double-negative feedback loops, which provide the cell with time to counteract apoptosis if desired (Section 7.2), but allow a rapid and decisive execution if required. Whether this underlying design is repeatedly employed by biological signalling networks remains to be established. Interestingly, a recent report describes interlinked fast and slow positive feedback loops as a reoccurring motif to drive reliable cell decisions by creating ‘dual-time’ switches which are both, rapidly inducible and resistant to noise in the upstream signalling system (Brandman et al., 2005). In our setting none of the two feedback loops appears to be especially fast compared to the other. While the double negative feedback loop is slightly more active for most of the time, it is crucial for the fast switching that the positive feedback provides a decisive peaking. During the switching a high amount of free and active caspase 3 is produced which is conserved by the positive feedback, while the double negative feedback ensures that IAPs remain down – a composition that inevitably leads to apoptosis.

In a deterministic model, of course, the inevitability of apoptosis or not is already determined by the initial conditions including the input. However, it is reasonable to argue that *in vivo* processes not considered in the model can influence and fine tune the final outcome during the lag phase (see Section 5.1.1 and Section 7.2).
The observed fast and slow kinetics can also be used to reduce the model complexity. Much of the relevant behaviour of the system is occurring on the unstable manifold of the separating steady state, which is a slow manifold of the system as can already be seen in similar representations to Figure 3.2(d). The behaviour of the extended model in this respect was analysed in detail by Bullinger (2005). Different procedures for systematic model reduction will be shortly outlined in Section 7.2. These are based on robustness considerations – a topic we will consider in the following chapter. These analyses will reveal how dependent the quantitative and qualitative behaviour is on the different parameters.

Chapter 5

Sensitivity and Robustness Aspects

This chapter extends the sensitivity and robustness considerations for the different models introduced in the two previous chapters. Robustness as an important property of biological systems was introduced in Section 2.2.3. Using standard approaches, Section 5.1 evaluates the sensitivity of the extended model for receptor induced apoptosis. The results indicate the relative significance of the different parameters emphasising an important role of the IAP molecules and providing interesting insight regarding potential pharmaceutical intervention (Eissing et al., 2006, 2007a). Section 5.2 introduces a Monte Carlo (MC) based method to determine the region in higher dimensional parameter space allowing for complex behaviour such as bistability. Principal Component Analysis furthermore can characterize the bistable parameter space and reveal parameter relationships. The volume of the region can be used as a robustness measure. The MC procedure is applied to the models proposed in Chapter 3 and compared with other established robustness measures. The analyses reveal that the different mechanisms for generating ultrasensitivity and thereby bistability allow a similarly robust bistable performance as detailed in Section 5.3 (Eissing et al., 2007b), which is in contrast to another report (Bagci et al., 2006). In addition, the procedure is applied to the basic and the extended model introduced in Chapter 4. Section 5.4 describes that the model extension also leads to a significant increase of robustness, further arguing for the proposed model extension (Eissing et al., 2005a).

5.1 Sensitivity of the apoptosis model

In Section 4.3, a model for the direct pathway of receptor induced apoptosis was established. The model nicely captures qualitative and semi-quantitative data available. This section evaluates the dependence of the model behaviour on initial conditions and kinetic parameter values.

5.1.1 Simulation studies mimicking NFκB

As outlined in Section 2.1, IAP and FLIP are key regulatory molecules negatively controlling caspase activity and activation, respectively. Interestingly, both molecules are up-regulated by NFκB, the transcription factor also activated by the death ligand TNF (Section 2.1). Therefore, these molecules represent potential key signals linking pro- and anti-apoptotic pathways (crosstalk) as also discussed in Section 7.2.

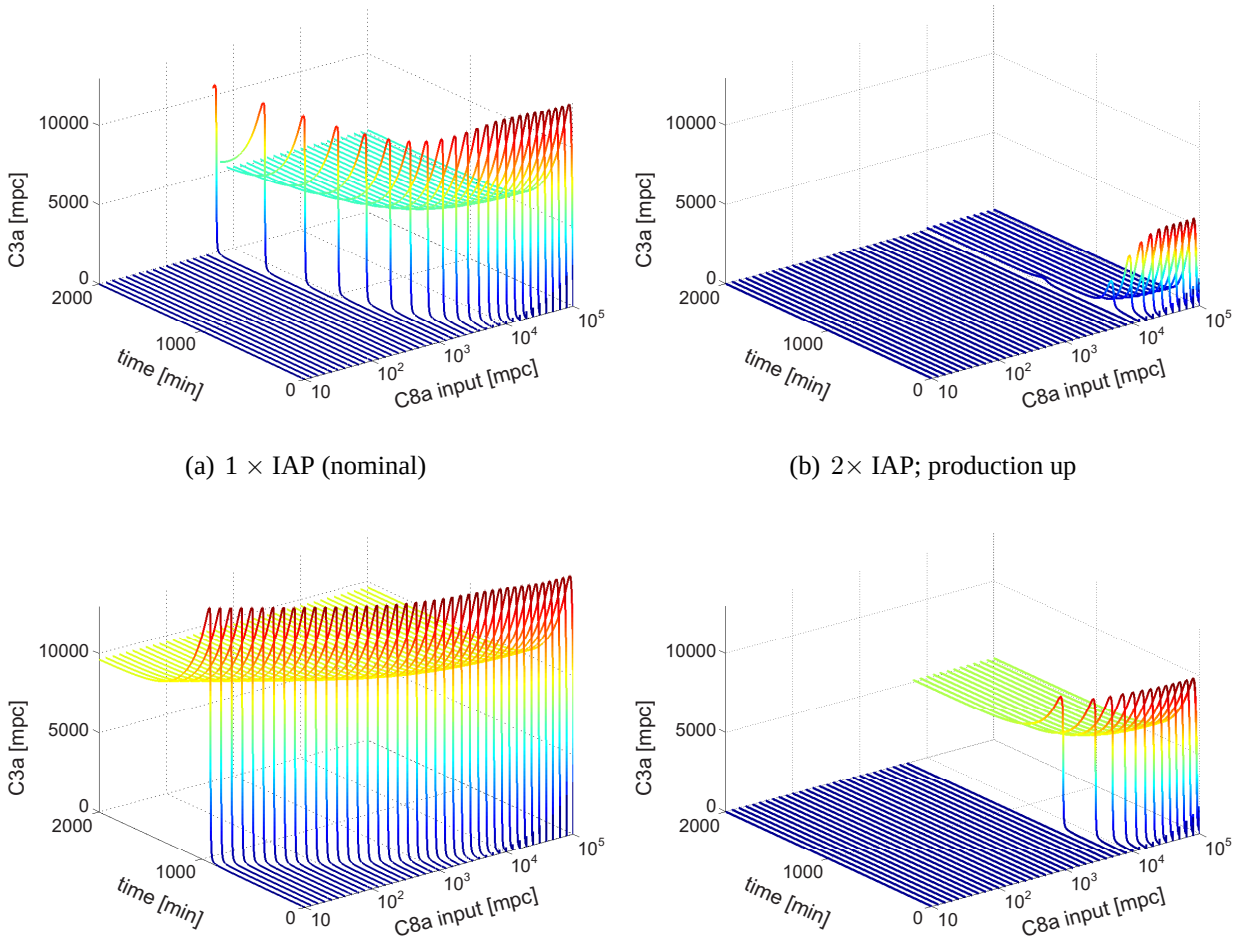

(a) $1\times$ IAP (nominal)

(b) $2\times$ IAP; production up

(c) $0.5\times$ IAP; production down

(d) $2\times$ IAP; degradation down

Figure 5.1: Simulation experiments showing C3a over time as an output for various inputs C8a. The different figures correspond to different IAP levels. 5.1(a) describes the nominal case, as also depicted in Figure 4.3, but with a logarithmic input coordinate. 5.1(b) corresponds to a two fold IAP up-regulation through increased production whereas 5.1(c) corresponds to a two fold IAP down-regulation through decreased production. 5.1(d) also corresponds to a two fold IAP up-regulation but achieved through a decreased degradation.

To mimic the effect of NFκB regulation, simulation studies were performed with modified protein concentrations. Changed FLIP levels directly affect the input, and the input dependent threshold behaviour has already been discussed (Section 4.3). Altered IAP concentrations were simulated by changing the initial condition and the respective production rate constant to give a steady state with zero input to account for altered gene expression.

As can be seen in Figure 5.1, the effects of a two fold up- or down-regulation (Figure 5.1(b) and 5.1(c), respectively) of the effector caspase inhibitor IAP are strong. A down-regulation leads to an earlier onset of significant effector caspase activation for comparable inputs. Both the peak and the death steady state level of activated caspases are increased. Further, the threshold below which no caspase activation occurs virtually vanishes (below one molecule C8a input). This is in contrast to XIAP knock out mice, which hardly show a phenotype. However, this can be explained by the redundancy of IAP molecules *in vivo*, represented as a single pool *in silico* (Eckelman et al., 2006; Harlin et al., 2001). The up-regulation almost completely abolishes effector caspase activation

even for high inputs, only allowing for a temporal activation of a much lower magnitude. Not only the peak but especially the death steady state level of activated caspases is decreased yielding a signal that is almost only transient (almost returning to zero C3a). This is interesting as it not only shows how cells can be protected against weaker apoptotic signals, but it also indicates that for large inputs temporarily restricted caspase activation can occur. In certain cancers IAP proteins are up-regulated (Nakagawa et al., 2005; Ramp et al., 2004; Yamamoto et al., 2004; Yan et al., 2004). In the light of the above observations, it can be suggested that the up-regulation not only shifts the apoptotic threshold, thereby preventing on efficient removal of cancerous cells as suggested by experimental studies. In addition, these cells might be damaged by partial caspase activation when encountering strong apoptotic triggers. Partial executioner caspase activation might lead to partial DNA cleavage favouring further mutations or to damages in the cytoskeleton potentially making the tumour cell more invasive, both being hallmarks of cancer progression (Aplan, 2006; Hanahan and Weinberg, 2000; Samejima and Earnshaw, 2005). In support of this hypothesis, an increased aggressiveness of XIAP over-expressing tumours has been reported recently (Li et al., 2007; Nakagawa et al., 2006; Oudejans et al., 2005; Takeuchi et al., 2005). However, a causative role of temporal partial caspase activation has not been demonstrated experimentally to our knowledge.
Modifying the level of the third inhibitor CARP, which might also be controlled by NFκB, qualitatively yields the same results (data not shown). The inhibitors strongly shift the input dependent threshold up or down, depending on whether they are up- or down-regulated, respectively. Therefore, NFκB can efficiently influence the apoptotic outcome.

The simulations clearly indicate an important role for IAP molecules in controlling the apoptotic pathway. In addition, they indicate how these molecules might contribute to cancer progression. Further, the simulation studies not only hint to the effects of NFκB but also indicate what effects mutations or pharmaceutical effectors, i.e. drugs might have. We extend these studies to all possible reactions and components in the apoptotic pathway in the following.

5.1.2 Wide range sensitivity analysis

While the previous studies were able to provide a dynamic and clear insight into the system behaviour when certain system properties are altered, the approach is cumbersome to provide a survey for the effects of all different rates and components. Therefore, we employ a systematic analysis for all parameters of the system.
Figure 5.2 shows how certain output characteristics change when varying a kinetic parameter or an initial condition. When varying an initial condition, in addition either the degradation rate constants or the production rate constants have been varied accordingly, denoted by the subscript ‘deg’ and ‘prod’ respectively, so that the initial condition is in steady state without input. For parameter changes the ratio is kept constant, i.e. only the forward rates have been varied, and if the reactions were reversible, the back rates have been changed in the respective way to preserve the ratio. As output characteristics we choose the following, evaluated for an input signal of 5,000 mpc:

a) t(C3a$>$500) – the time until the number of activated effector caspases exceeds 500 mpc corresponding to the length of the lag phase,

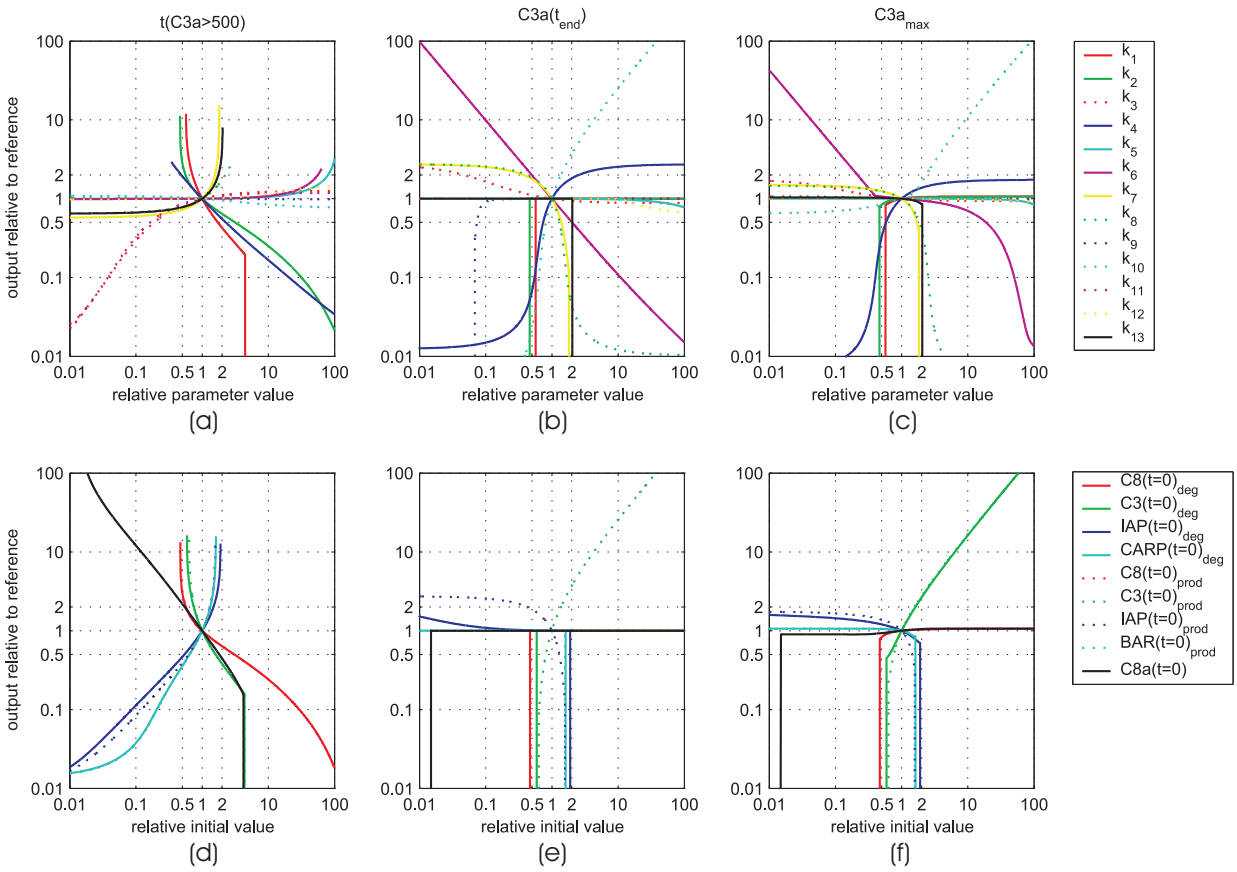

Figure 5.2: Sensitivity plots. The dependence of the three characteristic outputs t(C3a>500) (a, d), C3a(t$_{end}$) (b, e) and C3a$_{max}$ (c, f) on the kinetic parameter values (A-C) and the initial conditions (D-F) is shown. Both axes are in logarithmic scale and the values normalized to the nominal case.

b) C3a($t_{end} = 10^5\ min$) – the number of caspase molecules at the end of the simulation corresponding to either the life or death steady state depending on whether the input signal is above or below the threshold for the given conditions, and

c) C3a$_{max}$ – the maximal effector caspase activation achieved.

Both the fold parameter or initial condition change as well as the output characteristic are normalized to the nominal system (i.e. all curves intersect in the middle of the plot and, for example, a relative initial value of two indicates a two fold up-regulation). The choice of a double logarithmic scale is also motivated by the fact that wet lab experiments often proceed in fold changes. A 100 fold down-regulation nearly corresponds to a knock out, whereas a more than 10 fold up-regulation might be considered as physiologically irrelevant (although applied in certain experiments).
The length of the lag phase (Figure 5.2, left column) is mainly determined by the kinetics of the mutual caspase activation (k_1 and k_2), the degradation of the activated caspase-inhibitor complexes (k_7 and k_{13}) and the turnover of IAP molecules (k_4 and k_8). Unexpectedly, the reactions involving the IAP binding to C3a itself (k_3), the reactions involving CARP, but also the caspase turnover (Figure 5.2(a)) only have a minor impact. The effects are clearly nonlinear and also asymmetric, i.e. a two fold up-regulation does not have the quantitatively inverse effect of a two fold down-regulation. All initial conditions exert a strong effect on the length of the lag phase (Figure 5.2(d)).

The effect of CARP up-regulation is slightly more pronounced when compared to the effect of IAP up-regulation. This can be explained by the fact that the same inhibition kinetics were assumed, but the CARPs are inhibiting the more potent caspase. However, as pointed out in the model description, more experimental details regarding the CARP kinetics are needed to confirm this point. Interestingly, both CARP and IAP have a stronger impact on the caspase activation than the input. This points to the relevance of FLIP, and therefore its role might not be as dominant as that of the inhibitors IAP or CARP. The discontinuities at about one fifth of the nominal time for certain parameters or initial concentrations can be explained by the appearance of a second earlier peak, which is already visible in Figure 5.1 for high inputs (the vertical connecting lines are plotting artefacts and have not been removed because they are helpful in the interpretation). This early peak is derived from the initial activation before C8a molecules become bound to the CARPs. Whether a change in the initial concentration is accompanied by a corresponding change in the production or degradation rate hardly influences the length of the lag phase.

Regarding the final values of activated caspase 3 molecules (Figure 5.2, middle column) the parameters and initial concentrations can be divided into two groups: those that have no impact on the location of the steady states, but influence whether the life or death steady state is accomplished (i.e. giving a 1 or 0 output as can be seen in the discontinuous output; again the vertical connections were not removed) and those parameters, which also influence the location of the steady state. The latter group contains the rates that affect the turnover of (activated) caspase 3 molecules as well as the corresponding initial concentration (k_6 and k_{10} in Figure 5.2(b), $C3_{prod}$ in 5.2(e)). Interestingly, an up-regulation through increased expression strongly increases the final C3a value, while an up-regulation through decreased degradation reveals no such effects. This can be explained by the fact that in the apoptotic case, i.e. after a significant caspase activation was achieved, almost all caspase molecules will become activated. And whereas the degradation of pro-caspases is proportional to their concentration, the production is independent of this. The same effect can be seen for IAP molecules (Figure 5.2(e)). An up-regulation through production lowers the final value of C3a. Contrary, an up-regulation through a reduced degradation has no impact on the final value, although at high IAP concentrations the activation is completely abolished for the given input signal. This can be explained by the fact that in the apoptotic case the majority of IAP molecules are degraded by the cleavage reaction, independent of the degradation rate. This feature is shown in Figure 5.1(d). As described in Section 5.1.1, the up-regulation through increased *in silico* expression yields an almost transient signal for high inputs. The same fold up-regulation through decreased degradation only shifts the threshold but not the principle form of the original signal. Thus, while apoptosis prevention via increasing IAP expression might lead to pathological cellular states as described in the previous section, this might not be the case if the up-regulation is achieved via a decreased degradation (e.g. through interference in the proteasomal degradation pathway) pointing to an interesting feature, that awaits experimental validation. The maximal effector caspase activation (Figure 5.2, right column) is similarly influenced. The information in these plots can also be used to fine tune the parameters when more quantitative experimental data become available.

In summary, analysing the dependence of the systems behaviour to wide range parameter varia-

tions indicates that many parameters can significantly influence the systems behaviour. The direct inhibitors of active caspases, IAP and CARP, appear especially powerful.

5.1.3 Local sensitivity analysis

So far the analyses have focused on the influence of parameters on a single output. However, molecules such as IAP members are also important in other pathways. It is therefore interesting to investigate the effects of parameter changes on other state variables. To do this, we applied different local sensitivity analyses. We consider our system (4.7) plus (4.9) (Figure 4.1) in form $\dot{x} = f(x, p)$ as introduced in Section 1.1 with $x \in \mathbb{R}^n$ and $p \in \mathbb{R}^q$.

Steady State sensitivities. We evaluated the dependence of the stable apoptotic and the unstable decision steady state to 1% parameter changes (Δp). The sensitivities were calculated using the Matlab Systems Biology Toolbox[1] (Schmidt and Jirstrand, 2005). The results provide a normalized output relative to the nominal steady state (x_{SS}) and parameter values (p), i.e. the sensitivity of state x_{SSi} with respect to parameter p_j is defined as

$$S_{SSij} = \frac{p_j}{x_{SS_i}} \cdot \frac{x_{SS_i}(p_j + \Delta p_j) - x_{SS_i}(p_j)}{\Delta p_j} \qquad i = 1...n, \quad j = 1...p. \tag{5.1}$$

Figure 5.3(a) shows the local sensitivities of the death steady state. The C3a-column is related to the tangents in Figure 5.2(b) point (1,1), although for the local analysis the parameter ratios have not been kept constant and thus a direct comparison is only possible for unidirectional reactions. Indeed, k_7, dictating the degradation speed of the C3aIAP complex, is strongly negative in Figure 5.3(a) and also has a steep negative slope in Figure 5.2(b). For bidirectional reactions the sum of the two local values should roughly (locally) provide results comparable to the analysis shown in Figure 5.2(b). For example, strong but opposing effects are exerted by the parameters k_{-8} and k_{-10} describing the IAP and C3 production, respectively. For these, the local analysis shows that the steep slopes in Figure 5.2(b) almost completely derive from the back reaction rate constant and not from the forward degradation rate constants. Opposing effects for the rate constants within one reaction can be seen for reaction 3. Although the slope in Figure 5.2(b) indicates a minor impact, the local analysis reveals a strong but opposing effect of the association and dissociation constant. While the results of the wide range sensitivity analysis were surprising, they can now be easily understood as this reaction corresponds to the reversible inhibition of C3a by IAP molecules. A stronger binding acts anti-apoptotic lowering the concentration of C3a.
Apart from activated caspase 3, the most sensitive states are IAP and C8. Regarding IAP, a strong interdependence with C3a can be seen. The interplay of C3a and IAP highlighted in Section 4.3.3 manifests in this sensitivity analysis. The two state variables are influenced by the same parameters to comparable extends. However, the effects of the different parameters are always opposite. Parameters that positively influence C3a, negatively influence IAP and vice versa, reflecting the mutually negative influence as discussed in Section 4.3.3. For example, the most sensitive parameter for IAP is k_{-8} corresponding to its own expression rate – while a faster expression intuitively has a positive influence on the IAP concentration, it negatively influences C3a. Interestingly, C8 most

[1] http://www.sbtoolbox.org/

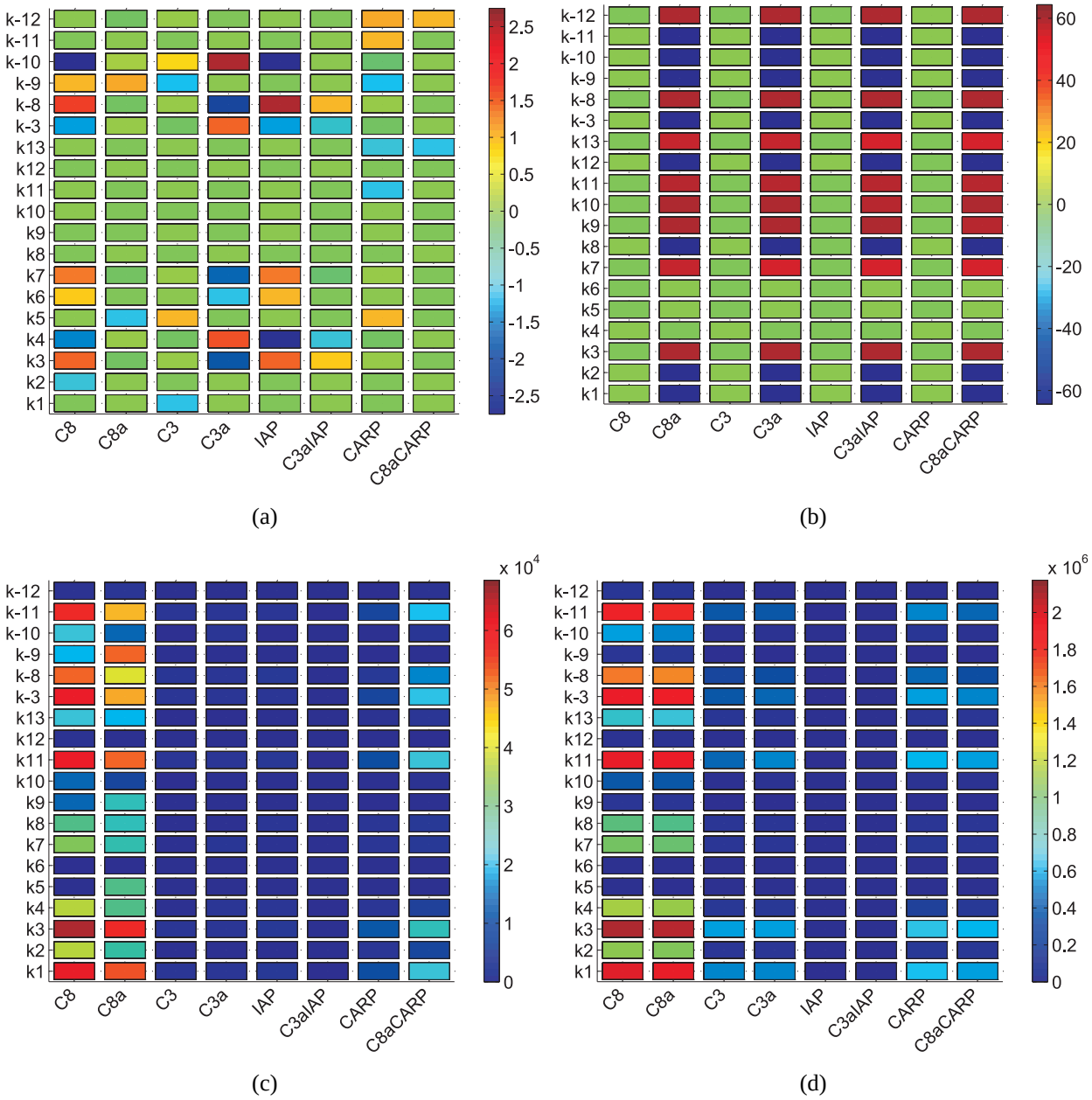

(a) (b)

(c) (d)

Figure 5.3: Normalized first order sensitivities. 5.3(a) shows normalized sensitivities of the stable apoptotic, 5.3(b) of the unstable separating steady state according to (5.1). 5.3(c) shows the mean, and 5.3(d) the maximum normalized sensitivities along the trajectories, which were calculated according to (5.2).

strongly depends on rate constants, which do not directly influence the state (k_3, k_4, k_{-8}, k_{-10}). From a dynamic systems point of view, this behaviour can easily be envisioned for a nonlinear system containing feedback loops; however, for biologists this can provide valuable unexpected insight. Another important point to notice is that these local analyses are obviously not able to predict non-local behaviour. For example, both the local and the wide range sensitivity analysis predict that varying k_1 or k_{13} will have no impact on the final C3a concentration, but only the wide range analysis shows that this is only true for a restricted parameter interval. Outside of this interval, the system completely changes its behaviour.

Figure 5.3(b) shows the local sensitivities of the decision steady state. As we illustrated in Sec-

tion 3.2, such an unstable steady state is generally required to generate bistability. Its stable manifold separates the areas of attraction for the two stable steady states. It is therefore directly influencing the model behaviour. As can be seen, the sensitivities are highly structured. While the concentration of the pro-caspases and inhibitors are hardly influenced by any parameter, the activated caspases and their complexed forms are highly sensitive to all parameters but k_4, k_5, and k_6. From this viewpoint, the pro-caspases and their inhibitors are not required as dynamic states for generating bistability. Indeed, this is supported by analysing the relevance of the states by a method proposed by Schmidt and Jacobsen (2004). These results outline a possibility for model reduction, and indeed as shown by Waldherr et al. (2007) the number of states of the extended model can be halved. Further, Waldherr showed that the combination of local sensitivities and states relevance, both based on a local linearisation, enables similar robustness measures as proposed by Ma and Iglesias (2002), which is based on a more global analysis of bifurcations (Eissing et al., 2007a; see Section 5.3.1 for the method of Ma and Iglesias, 2002).

Dynamical sensitivities along the trajectories. Dynamical sensitivities along the trajectories were calculated according to

$$\dot{S}(t) = \frac{\partial f(x,p)}{\partial x} S(t) + \frac{\partial f(x,p)}{\partial p} \qquad S(t_0) = 0, \tag{5.2}$$

where S is the $n \times q$ dimensional sensitivity matrix (Khalil, 2002), which is the sensitivity of the solution of the ODE system with respect to variations in the parameter p. The sensitivities were calculated using a Matlab toolbox developed by Bullinger (unpublished), which employs algebraic derivatives and simultaneously solves the nominal solution and (5.2). The obtained solutions can again be normalized by multiplying with the nominal, time dependent state values and dividing by the nominal parameter values.

The mean and maximum of the absolute values of the normalized sensitivities are shown in Figures 5.3(c) and 5.3(d), respectively. Clearly, C8 and C8a are most strongly influenced by various parameters. Interestingly, the binding of IAP to C3a (k_3), more strongly impacts on caspase 8 than 3 again mirroring the importance of the positive feedback in the system. A closer dynamic inspection also reveals that many parameters only influence certain states during specific time instances. However, for the extended model, no further conclusions can be derived than already presented above.

Comparing the different local sensitivities, it becomes evident that these do not necessarily provide comparable results when evaluating complex nonlinear phenomena. One has to be careful when deducing conclusions from a single evaluation. Similar dynamic sensitivities, evaluated at different locations in parameters space, were also used to define robustness measures (Stelling et al., 2004a). However, in the following we will consider an alternative approach that we consider more revealing for the models investigated in this thesis. Beforehand, we will shortly summarize the parameter dependencies uncovered in this section.

5.1.4 Discussion and summary

Our results demonstrate that local sensitivity analyses can reveal a useful overview, but also have to be complemented because they cannot capture the nonlinear and asymmetric effects of parameter

changes as observed. These can be captured to some extend by wide range parameter changes and, in more detail, by simulation studies. However, time course raw data become excessive when used to study all state and parameter dimensions. Overall, the extended model of apoptosis appears to be rather sensitive to several parameter changes. This is somewhat in contrast to observations for other biological processes (Barkai and Leibler, 1997; Stelling et al., 2004b). One has to keep in mind though that additional processes increasing the robustness of the model have been neglected in order to enable a better insight into the principal behaviour (see Section 5.5 and Chapter 7). The results of our analysis outline the importance of controlling activated caspases for prevention of apoptosis. Here, it appears to be more efficient to inhibit activated caspases (i.e. IAPs and CARPs) than to inhibit the activation (i.e. FLIP). Especially the role of the NFκB induced IAP molecules appears to be critical in the regulation of apoptosis. Thereby, the analyses indicate how tumours over-expressing IAPs might not only become resistant to apoptotic stimuli but can become more aggressive. IAPs are currently investigated as potential drug targets (Devi, 2004; Nachmias et al., 2004; Schimmer and Dalili, 2005; Schimmer et al., 2006). Our results indicated that for anti-cancer therapy, drugs slowing down IAP production (e.g. by interfering with transcription or translation), should be more promising than increasing the degradation through the proteasomal pathway, or just inhibiting the inhibitors (e.g. by small molecules). Decreasing the production of IAPs should not only sensitise cells to apoptotic signals but could in addition prevent tumour progression. Vice versa, for drugs aiming to prevent excessive apoptosis, it should be more promising to interfere with proteasomal degradation rather than up-regulating IAPs through expression. In addition, these analyses provide valuable insight for extending the model of receptor induced apoptosis to include additional pathways as outlined in Section 7.2 because they in detail show how the major points of cross-talk influence the apoptotic program.

5.2 A Monte Carlo approach to approximate a bistable region

In Chapters 3 and 4 different methods for evaluating parameter regions for bistability were introduced. Bifurcation analyses allow a nice visual interpretation but are most powerful in one or two dimensions only. The three dimensional bistability analysis presented in Figure 4.2 was depending on the special form of the basic model equations. Therefore, different approaches are desirable in order to evaluate complex behaviour like bistability in higher dimensional parameter spaces.

In the following, we will introduce a different approach to approximate bistable regions. The method is suitable for higher dimensional spaces and based on a Monte Carlo procedure. Random parameter sets are evaluated for whether they produce a bistable behaviour (hits) or not (non-hits). The ratio of hits versus total sets evaluated is an estimate of the relative volume allowing for a bistable behaviour and can be used as a quantitative robustness measure.

In this section the method will be applied to the simple inhibitor model introduced in Section 3.2.2. Choosing three free parameters allows a visualisation of the hit and non-hit distribution. The three dimensional point cloud is then approximated by an ellipsoid whose volume can provide an alternative robustness measure. The information contained in the ellipsoid can also be formalized by a Principal Component Analysis (PCA). The PCA procedure will be introduced and can be used to characterize point clouds of arbitrary dimensions and to identify parameter relations.

The inhibitor model used in this section presents a simple application example of the MC approach open to visualization. The true power of the approach will be unfolded in Sections 5.3 and 5.4, where selected aspects of the whole procedure will be applied to compare the robustness of different model structures in higher dimensions.

5.2.1 Monte Carlo approach for volume estimation

Due to nonlinearities and the dimensionality of the systems under investigation, a closed solution for the bistable volume in higher dimensional space does not exist. Therefore, we choose a MC approach to approximate this volume as its convergence rate is not affected by the dimension of the problem, making it particularly suited for large and complex systems (Lafortune, 1996). A robustness measure is then defined as the size of the parameter region leading to bistability.
For the approach, parameter vectors are randomly selected from predefined ranges, such that each parameter is uniformly distributed on a logarithmic scale, similarly to, for example, Barkai and Leibler (1997) and Blüthgen and Herzel (2003). For each parameter vector the model is checked for the presence of two stable steady states having non-negative concentrations – one steady state without activated proteases and one with activated proteases. The procedure is fast in the examples investigated in this thesis, as both the location and the stability of the steady states can be evaluated numerically without simulation in time.
The approach is applied to the simple inhibitor model introduced in Section 3.2.2. For visualization reasons, $k_f = 10$ and $k_b = 0.001$ are fixed and parameter vectors $[k_x\ k_y\ k_d]$ are randomly generated from the interval $[10^{-5},\ 1]$ to give a uniform distribution for each parameter on a logarithmic scale. Evaluating 10,000 parameter vectors yielded 1,821 parameter vectors for which the model is bistable (hits) and 8,179 parameter vectors for which the model is not bistable (non-hits). Thus, the relative volume allowing for a bistable behaviour is 0.18. The chosen number of parameter sets provides a value whose asymmetric binomial confidence interval for a 95% confidence spans 2% around the value provided.
Figures 5.4(a) and 5.4(b) show the distribution of the hits (blue dots) and non-hits (yellow dots) in the three-dimensional parameter space from two different perspectives. A visual inspection of Figure 5.4(b) indicates that the hits nicely cluster into one region without holes (simply connected, maybe even convex). We also observe that the region might be nicely approximated by an ellipsoid. In the following, we will fit the hit point cloud by an ellipsoid and then evaluate the quality of the achieved fit to justify our procedure.

5.2.2 Ellipsoid fitting as a geometric interpretation of point clouds

An ellipsoid is a relatively simple geometric object whose shape can provide additional information about the distribution of the hits. Due to the efficiency of the MC approach, the sample size allows the direct estimation of an ellipsoid via the calculation of the covariance matrix (Σ), defining the ellipsoid's axis directions (eigenvectors of Σ) and the ratio of their lengths (square root of the eigenvalues of Σ). The Mahalanobis distances (Bard, 1973; Johnson and Wichern, 1992), which measure the distance between each point and the centre, relative to the corresponding ellipsoid radius, are then used to scale the ellipsoid to contain 95% of the points. Formally, the Mahalanobis

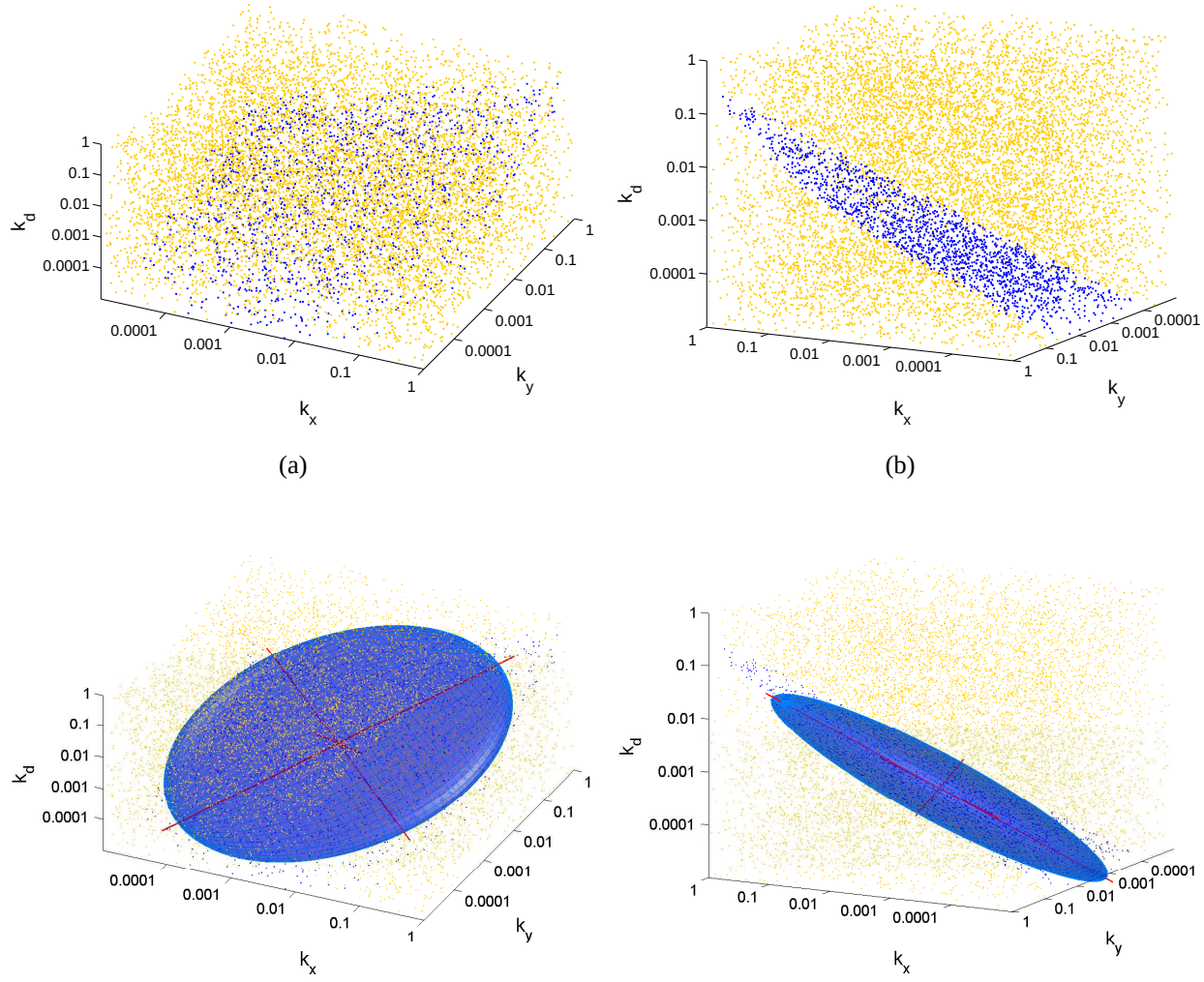

Figure 5.4: Distribution of hits (in blue) and non-hits (in yellow) for the simple inhibitor model from two different views (5.4(a) and 5.4(b)). 5.4(c) and 5.4(d) show the same viewpoints but in addition also show the 2 standard deviations ellipsoids whose main axes are depicted (in red). In the figure, the axis length was chosen 1.1 times the length of the true ellipsoid axis.

distance D for a point p is defined as

$$D(p) = \sqrt{(p-\mu)^T \Sigma^{-1} (p-\mu)} \tag{5.3}$$

where μ is the mean of the sample. The Mahalanobis distance differs from the Euclidean distance in that it takes into account the correlations of the data set and is scale-invariant.
For visualization, Figures 5.4(c) and 5.4(d) show ellipsoids whose axis are scaled to two standard deviations of the covariance matrix. A visual inspection indicates that the ellipsoid well separates hits and non-hits. However, for higher dimensions such an inspection is generally not possible. In the following, we will introduce procedures also allowing to evaluate the quality of the ellipsoid fit in higher dimensional spaces.

Quality evaluation of the ellipsoid fit. Of course, the true distribution of hits will rarely have the exact form of an ellipsoid. To evaluate the quality of the ellipsoid fit, we first use the non-hits and calculate how many of these are contained within the ellipsoid. For the inhibitor model

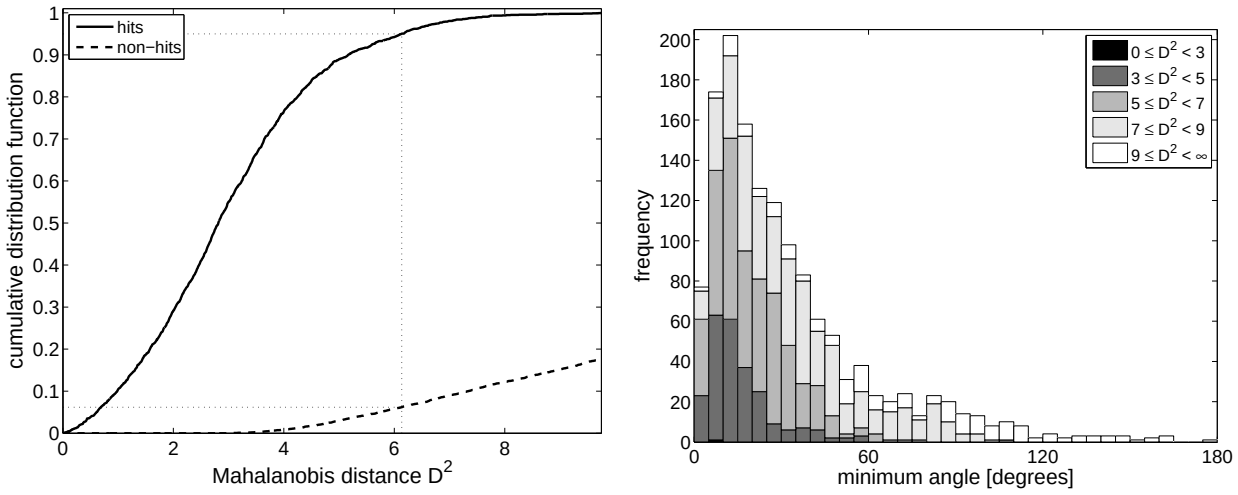

(a) (b)

Figure 5.5: Figure 5.5(a) shows the cumulative sum for hit and non-hit points of the relative fraction having a larger Mahalanobis distance D^2 than shown on the x-axis.The distances are calculated from the centre of the fitted ellipsoids. The dotted lines indicate how the percent of non-hits contained in the ellipsoid, that is, the relative fraction contained in the 95% ellipsoid times 100, can be obtained. Figure 5.5(b) shows the distribution of minimum angles according to (5.4). The patch colour indicates the distance of the respective non-hit points from the center of the ellipsoid.

shown in Figure 5.4, 6% of the non-hits are contained in the ellipsoid fitting 95% of the hits (Figure 5.5(a)). Secondly, for each non-hit point, we calculate the smallest angle (minimum angle) between any hit point further away from the centre of the ellipsoid (both in the Mahalanobis and Euclidean distance), the centre and the non-hit point itself according to

$$\text{minimum angle}_n = \min_{h \in H_n} \angle(n, h), \tag{5.4}$$

with n corresponding to a non-hit and H_n to the set of all hits h further away from the centre than n. If H_n is empty, n has no associated minimum angle. In the case of holes within the bistable domain, a significant number of small minimum angles is to be expected.

In the inhibitor model data set, 17% of the non-hits have certain hit points that are further away from the center of the ellipsoid. The distribution of minimum angles is shown in Figure 5.5(b). The smallest minimum angle obtained is 1.5°. Further, it can be seen that several minimum angles are rather small. The figure also indicates the Mahalanobis distance of the corresponding non-hit points. As can be seen, all non-hits possessing a minimum angle as defined in (5.4) are rather far away from the center of the ellipsoid. Further, the distribution of the distances for small angles is similar to the distribution for larger angles. This indicates that the non-hits with a small minimum angle do not correspond to holes as otherwise one distance range should be accumulated (unless the hole is narrow in the direction parallel to the ellipsoid surface and wide orthogonal to it). If these are holes, the holes are small and distributed at the edge of the ellipsoid.

Therefore, our true geometric object, defining the area that allows bistable behaviour, is likely a simply connected region in the space (i.e. does not contain holes), as one would otherwise also expect to find more angles close to zero. Furthermore, the areas not allowing bistable behaviour contained within the ellipsoid are mostly at the edge of the ellipsoid. The statistical evaluations

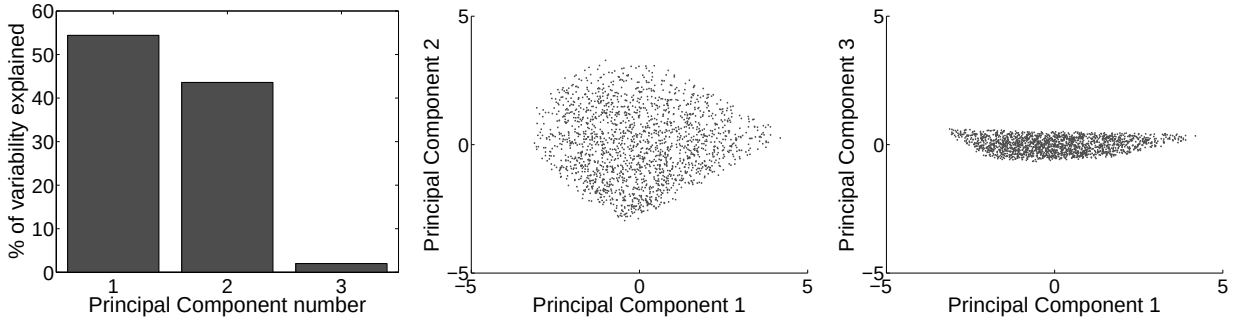

(a) (b) (c)

Figure 5.6: Principal Component Analysis. Figure 5.6(a) shows the % variability explained (corresponding to normalized eigenvalues of Σ) by the different principal components for hits as shown in Figure 5.4. Figures 5.6(b) and 5.6(c) show two representations of the hit points in two-dimensional principal component spaces, distinguished by the choice of principal components.

could be extended to further clarify this point. However, the visualization already illustrates the quality of the fit and we have derived measures of the quality plotted, which can also be calculated and compared to in higher dimensional spaces where a visualization is not possible.

Principal component analysis and parameter relations. A Principal Component Analysis (PCA) corresponds to a coordinate transformation with the new coordinates corresponding to the main ellipsoid axes. The ellipsoid axes, i.e. principal components, are depicted in Figure 5.4 as red lines. As explained above the direction and length of these axes basically correspond to eigenvectors and eigenvalues of the covariance matrix, respectively.

Generally, the aim of PCA is to detect structure in higher dimensions and to use the gained information to reduce the dimensionality of the data. If one PC does hardly contribute to the total observed variance it can be left out. The remaining principal components are then still able to explain most of the observed total variance. The principal component analysis was performed using the built-in Matlab function 'princomp'.

The main results of the PCA for the simple inhibitor model are shown in Figure 5.6, where basically ellipses axes lengths are compared to another. Two PCs are dominating whereas one direction has a minor influence reflecting the flat shape already observed by visual inspection. An even simpler measure, also used later on is the 'roundness' of the ellipsoid, which we define as the ratio of the minimal to the maximal ellipsoid axis radius. The measure corresponds to the inverse of the condition number sometimes used in literature. The roundness for the illustrated example is 0.19. Clearly, certain directions in parameter space are more robust with respect to preserving bistability (along the first two PCs) than others (along the third PC).

The PCA information not only provides further insight into the problem but can also be used to reduce the dimension of the parameter space. For example, if we want the simple inhibitor model to be bistable, an elementary approach would be to require the parameter vector to be on the plane spanned by the first two PCs (which is orthogonal to the third PC). This leaves out the shortest ellipsoid axis, i.e. the third PC with the smallest eigenvalue associated, and corresponds to the best fit of the three dimensional point cloud by a two dimensional plane. In original coordinates this plane is given by $k_x + 1.2 \cdot k_y - 2 \cdot k_d - 1.9 = 0$, which leaves only two free parameters. The

parameter choice could be further restricted requiring the parameter vector to be not only on the plane but additionally be contained in the two dimensional ellipse.
These analyses not only allow quantitative measures of robustness, but could also be used to choose parameters – the parameter set, which is at the centre of the ellipsoid, can be considered maximally robust. As will be pointed out in Section 5.3.3, the choice of a reference parameter set is a major difficulty for the application of many robustness measures. The centre of the ellipsoid would provide a rational reference to compare different models and methods. Also, the centre of the ellipsoid should be close to the point obtained by a multi-dimensional optimization of the mean of the Ma and Iglesias (2002) measure (introduced in the next section).

5.3 Basic ultrasensitivity mechanisms are similarly robust

Recently, Bagci et al. (2006) published interesting results regarding the mitochondrial apoptotic pathway. While focussing on this pathway, the authors also investigate simplified general reaction mechanisms, which generate bistable behaviour. They state that a cooperative reaction mechanism is superior to other mechanisms, such as inhibitor binding, based on their finding that it is "much more robust" (Bagci et al., 2006). The authors present this result in a general context, as robustness of bistable behaviour is not only relevant to apoptosis, but to (bistable) signal transduction in general. The models investigated by Bagci et al. (2006) are in fact similar to those described in Chapter 3. As discussed in Section 3.3, our qualitative analysis cannot support their findings. Here we compare the robustness of the three models introduced in Chapter 3 using two different quantitative measures of robustness, one proposed by Ma and Iglesias (2002) and the MC approach introduced in Section 5.2 (Eissing et al., 2007b).

5.3.1 Robustness measure according to Ma and Iglesias

A robustness measure based on the distance of the nominal parameter value to a parameter value where a bifurcation occurs has been introduced by Ma and Iglesias (2002). For dynamical behaviour like bistability, the relevant bifurcations are the ones where the unstable steady state turns stable. Precisely, Ma and Iglesias define the degree of robustness (DOR) of the dynamical behaviour for a given nominal parameter vector p with respect to variations in the single parameter k_j as

$$DOR_j = 1 - \max\left\{\frac{\check{k}_j}{\tilde{k}_j}, \frac{\tilde{k}_j}{\hat{k}_j}\right\}, \tag{5.5}$$

where $\tilde{k}_j$ is the nominal value for the parameter k_j and bifurcations occur at $\check{k}_j$ and $\hat{k}_j$, with $0 \leq \check{k}_j < \tilde{k}_j < \hat{k}_j$ and with all other parameters $i \neq j$ held at nominal values. The definition is illustrated in Figure 5.7 at the example of the parameter k_x of the inhibitor model introduced in Section 3.2.2. Bifurcations that abolish bistability appear for $k_x = \check{k}_x$ and $k_x = \hat{k}_x$. k'_x and k''_x indicate two possible nominal parameter values for k_x and for which $\check{k}_x$ and $\hat{k}_x$ are the bifurcation values that determine DOR, respectively. The maximal robustness is obtained for a nominal value of $k_x = \bar{k}_x$, the geometric mean of the bifurcation values.

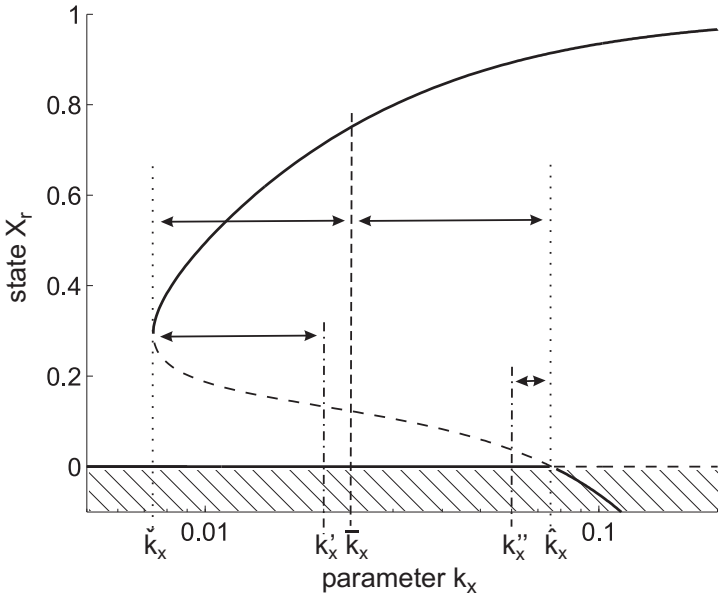

Figure 5.7: Explanation of the robustness measure according to Ma and Iglesias (2002) using the inhibitor model example (Section3.2.2). The bifurcation diagram corresponds to Figure 3.4(a) with a logarithmic scale. Stable steady states are drawn as solid lines, unstable steady states as dashed lines. Physically irrelevant areas are hatched.

Table 5.1: Robustness measures DOR according to (5.5).

Parameter	Cooperative	Inhibitor	Zero-order
k_x	0.214	0.262	0.302
k_y	0.282	0.187	0.171
k_d	0.131	0.119	0.302
n	0.155	-	-
k_f	-	0.879	-
k_b	-	0.967	-
K_M	-	-	0.889
mean	0.196	0.483	0.416

Table 5.3.1 provides the robustness values according to the Ma and Iglesias (2002) measure for the three models investigated and using the nominal parameter values introduced in Section 3.1. It can be seen that for the parameters k_x, k_y (mutual protease activation rate constants) and k_d (degradation rate constant) shared by the three models, the measures are all rather similar, not revealing any mechanism to be especially robust. Interestingly, the measure is especially small for the cooperative setup when considering the parameters unique to each model. For example, the cooperative model with reference parameter values is not bistable for either $n = 2$ or $n = 3$ (with n indicating the degree of cooperativity), but only in-between. Obviously this measure is strongly dependent on the nominal parameter set, which is not always easy to obtain. For example, the robustness measure for the parameter k_x of the inhibitor model is far off the maximal value

Table 5.2: Robustness with respect to parameter variations evaluated by Monte Carlo approach. We generate random parameter sets for k_x, k_y and k_d (the parameters common to all three models when assuming k_m to correspond to k_d), so that each parameter is uniformly distributed in logarithmic space in the interval from 10^{-5} to 1. We evaluate $10,000$ parameter sets for each model. This provides accurate values whose asymmetric binomial confidence intervals for a 95% confidence span about 2% around the values provided.

Cooperative		Inhibitor			Zero-order	
$n = 1$	0.00	$k_f = 0.1$	$k_b = 10^{-2}$	0.00	$K_M = 10^{-1}$	0.02
$n = 2$	0.41	$k_f = 1$	$k_b = 10^{-3}$	0.09	$K_M = 10^{-2}$	0.07
$n = 3$	0.37	$k_f = 1$	$k_b = 10^{-4}$	0.13	$K_M = 10^{-3}$	0.16
$n = 4$	0.35	$k_f = 10$	$k_b = 10^{-3}$	0.18	$K_M = 10^{-4}$	0.21
$n = 5$	0.34	$k_f = 10^2$	$k_b = 10^{-5}$	0.32	$K_M = 10^{-5}$	0.29
$n = 10$	0.29	$k_f = 10^6$	$k_b = 0$	0.37	$K_M = 10^{-10}$	0.36

of 0.686, which can be achieved with a nominal value of $k_x = \bar{k}_x$. Thus, the reference parameter choices for the inhibitor model were not obviously biased to maximize robustness and this measure already provides a first indication that none of the three mechanisms appears to be especially robust compared to another.

5.3.2 Robustness measure using a Monte Carlo approach

We use the MC approach introduced in Section 5.2.1 to measure the bistable volume in parameter space. As can also be proven analytically, Table 5.3.2 shows that for $n = 1$ the system is not able to display a bistable behaviour because ultrasensitivity is a necessary structural requirement (compare Section 3.2.1). The cooperative models for $n > 1$ all allow a bistable performance in a rather large volume of the parameter space. Interestingly, for larger values of n, corresponding to increased cooperativity, the models do not become more robust. The Y_r nullcline becomes steeper with increasing n but is also shifted to the right counteracting an increase of the robustness (see Figure 3.2). Unlike the cooperative model for $n > 1$, the inhibitor and zero-order model strongly depend on the values of their unique constants, i.e. only strong inhibitors or enzymes close to saturation allow a robust bistable performance similar to the cooperative model. Also, the cooperative model achieves slightly larger maximum values due to not having a transcritical bifurcation present in the two other models, limiting their bistable parameter range (see Section 3.2.3).

Relevance for apoptosis – a simple calculation. The potential practical relevance of the theoretical finding can be shown by simple calculations for the apoptosis example. IAPs are known to be rather strong inhibitors of caspases with a reported $K_i = k_b \cdot Y_t/k_f = 7 \cdot 10^{-4}\ \mu M$ for XIAP binding activated caspase 3 (Deveraux et al., 1997; Ekert et al., 1999). A total amount of protein $X_t = Y_t = 3 \cdot I_t = 1\ \mu M$ is within the range of reported values (Stennicke et al., 1998; Sun et al., 2002; Svingen et al., 2004). Then, a k_b/k_f ratio of 10^{-3} or even smaller is a reasonable estimation for the considered reaction in the normalized setup analysed above. Thus, the reference binding values and the strong inhibitors needed to achieve comparable robustness measures in the Monte

Carlo test are not only theoretical hypotheses, but can already be found in apoptosis signalling.

5.3.3 Discussion and summary

We evaluate the robustness of bistable behaviour to parameter variations for different reaction systems where ultrasensitivity, a necessary ingredient for bistability, is generated either via cooperativity, saturation (zero-order) or inhibitors. Using two previously described measures for robustness in bistable systems (Eissing et al., 2005a; Ma and Iglesias, 2002), we find that theoretically all three model structures allow a robust bistable performance. In all cases, the bistable property and its robustness is dependent on the right combination of parameters.
Comparing different models and different methods, we find that all methods tend to give biased results. The method introduced by Ma and Iglesias (2002) is strongly dependent on a reference parameter set. However, experimental data rarely allow an exact choice of parameters. The exact results of the Monte Carlo approach are also affected by the parameter ranges assumed. Allowing for large parameter ranges or varying these ranges can attenuate this effect (Section 5.4; Eissing et al., 2005a). The investigated cases reveal another problem common to both methods employed. All models show a saddle-node bifurcation limiting the bistable parameter range to one side. But only the parameter range of the inhibitor and zero-order model is also limited to the other side by a transcritical bifurcation. For the cooperative model, the unstable steady state asymptotically approaches the life steady state. Therefore, many of the parameter sets evaluated as mathematically bistable in the Monte Carlo approach can hardly be considered 'biologically bistable' as the threshold is smaller than one molecule of activated caspases within a cell. While this explains why the maximal robustness measure of the cooperative model is slightly larger than those of the two other models, it also indicates the need for improved methods. For example, one could extend the Monte Carlo approach to pose additional requirements on the location of the steady states. This indeed reduces the value of the MC measure and especially large MC measurement values are reduced. The different models become even more similar when such a restriction is imposed (data not shown). Other approaches, not directly evaluating the property of bistability, are measuring the degree of ultrasensitivity (Legewie et al., 2005), using overall coefficients developed in the framework of metabolic control analysis (Wolf et al., 2005) or other global measures of robustness (Stelling et al., 2004a,b). Thus the described analysis cannot be considered complete and cannot finally answer the questions of which reaction mechanism confers a better robustness. Also, both the models described here and those investigated by Bagci et al. (2006) neglect residual activities of pro-caspases (zymogenicity; Stennicke and Salvesen, 1999). Especially the bistability in the cooperative model is very susceptible when considering this kind of perturbation (Section 3.2.4; Eissing et al., 2007c).
In conclusion, our results provide clear indications that none of the mechanisms evaluated here appears to be clearly superior regarding the robustness of bistable behaviour with respect to parameter changes. Both measures described provide comparable results. We find that only the combination of different methods and a critical evaluation of the results enables conclusive insights. Simple calculations highlight the potential importance of (caspase) inhibitors in generating bistable behaviour (during apoptosis). For apoptosis, the importance of inhibitors predicted through mathematical

modelling was recently also confirmed experimentally at the single cell level (Rehm et al., 2006). Additionally, these inhibitors can generate an implicit positive feedback, further enhancing the bistable behaviour (Legewie et al., 2006). Nevertheless, especially in the mitochondrial pathway of apoptosis there are several potential cooperative steps in addition to inhibitors (Rehm et al., 2006). *In vivo*, most likely a combination of different mechanisms will secure a tight switch (Manoharan et al., 2006).

5.4 Model extension by CARPs increases robustness

We apply the Monte Carlo approach as outlined in Section 5.2 to the basic and extended model as introduced in Chapter 4. We distinguish eight computer experiments by the choice of predefined ranges (around 5 orders of magnitude for each parameter, see Figure 5.9). The four parameters specific to the extended model are kept at their nominal values, in order to compare parameter spaces of the same dimension. Further, the initial conditions and the thermodynamic binding constant for IAP binding C3a are kept at their nominal values, thus also the ratios for reversible reactions are retained, leaving ten free parameters.
Robustness has been proposed as a plausibility measure of models and can be used to discriminate between models, as introduced in Section 2.2.3. As described in Chapter 4, there are several evidences to prefer the extended model over the basic model. In Section 5.4.1 we evaluate if the preferences are supported by quantitative measures of robustness, that is the frequency ratio and the volume of the ellipsoid as introduced in Section 5.2. Section 5.4.2 evaluates the quality of the ellipsoid fit and Section 5.4.3 in more detail analyses the distribution of the hits. Finally, Section 5.4.4 provides a three dimensional comparison of the two models providing insight, also into the bistable parameter space of the extended model, as was previously only possible for the basic model.

5.4.1 Model discrimination by frequency ratio and ellipsoid volume

We define and evaluate two model discrimination criteria. Both are ratios of bistable volume measures for the extended and the basic model. For the Monte Carlo approach, we choose 5 million parameter sets for each experiment, which provides a good estimate of the bistability domain. In all cases investigated, the asymmetric binomial confidence intervals for a 99% confidence span less than 1% around the values provided in Table 5.3.
First, we calculate the volume in the 10-dimensional logarithmic parameter space as the relative frequency of hits, see Section 5.2.1, for each experiment and model. The ratio of the volumes of the extended and the basic models is then the first model discrimination criterion (see Table 5.3). Secondly, we calculate the volume of the ellipsoid containing 95% of the parameters resulting in bistability, again in the 10-dimensional logarithmic parameter space. We chose the mean of the data set as a centre for the ellipsoid in Section 5.2. Here, we chose ellipsoids centred at the median to obtain the values displayed in Table 5.3. Comparing the ellipsoids centred in the median versus those centred in the mean (examples centred in the mean are provided in Section 5.4.2), one can observe that the values are comparable. However, the median consistently provides slightly better

Table 5.3: Bistable parameter volumes. Further explanations are provided in the text. Exp.: Experiment; Vol.: Volume; Ext.: Extended.

	Monte Carlo			Ellipsoid						
	Basic model	Ext. model		Basic model			Ext. model			
Exp.	vol.	vol.	Vol. ratio	Vol.	Round-ness	% non-hits in	Vol.	Round-ness	% non-hits in	Vol. ratio
1	0.0893	0.2195	**2.46**	231.09	0.2767	17.60	498.25	0.4197	31.11	**2.16**
2	0.0205	0.0926	**4.52**	87.00	0.2491	2.97	275.19	0.4453	13.49	**3.16**
3	0.0588	0.1983	**3.38**	15.73	0.2150	9.33	36.74	0.3529	26.99	**2.34**
4	0.0116	0.0597	**5.16**	41.10	0.2203	1.48	161.31	0.3806	9.12	**3.92**
5	0.0341	0.0991	**2.90**	164.33	0.2790	4.94	338.15	0.4556	14.51	**2.06**
6	0.0736	0.2159	**2.93**	12.40	0.2492	9.97	26.68	0.3705	27.13	**2.15**
7	0.0030	0.0506	**16.80**	0.53	0.1419	0.40	5.61	0.2641	5.18	**10.58**
8	0.0009	0.0127	**13.43**	3.38	0.1269	0.11	43.70	0.2565	2.33	**12.93**
mean	0.0365	0.1185	**6.45**	69.45	0.2198	5.85	173.20	0.3682	16.23	**4.91**

ellipsoid fits, as it is known to provide more robust estimates not as strongly affected by outliers. The ratio of the ellipsoids' volumes defines the second model discrimination criterion.

Our two measures of robustness yield similar results. The extended model structure has a bistable region in the 10-dimensional logarithmic parameter space, which is on average more than five times larger than the basic one. The reactions added to the basic model, thus, have significantly enlarged the original bistable region, increasing the model robustness. Using the robustness measure for model discrimination favours the extended model, supporting previous indications (Chapter 4).

5.4.2 Quality of the ellipsoid fit

In order to evaluate the quality of the ellipsoid fits obtained in the 10-dimensional space, we evaluate 100,000 non-hit points as described before. On average, the ellipsoids fitting 95% of the bistable parameter points contain only 11% of these non-hits indicating that the true hit distribution can quite well be approximated by an ellipsoid (Table 5.3). Two exemplary computer experiments for the extended model are detailed in Figure 5.8. Unlike in Table 5.3, here the mean, instead of the median was chosen for ellipsoid calculation. The ellispoid fitting 95% of the hits contains 37% or 3% of the non-hit points for Experiment 1 (Figure 5.8(a)) and 8 (Figure 5.8(c)), respectively. For the extended model, Experiment 1 corresponds to the worst case (i.e. the ellipsoid containing the highest fraction of non-hits) and Experiment 8 corresponds to the best fit (compare Table 5.3).

We further calculated the minimum angles according to (5.4) for each of the 100,000 non-hits in those two experiments. The results are shown in Figure 5.8(b) for Experiment 1 and Figure 5.8(d) for Experiment 8. While we obtain significantly more minimum angles for Experiment 1 (87,756) than for Experiment 8 (13,694), the distribution looks very similar. Further, no minimum angles smaller than 5° are obtained in both experiments and most minimum angles derive from non-hits that are rather far out. The distribution looks even less likely to allow for holes than discussed for the simple inhibitor model in Section 5.2, where a graphical inspection was able to underscore the quality of the ellipsoid fit.

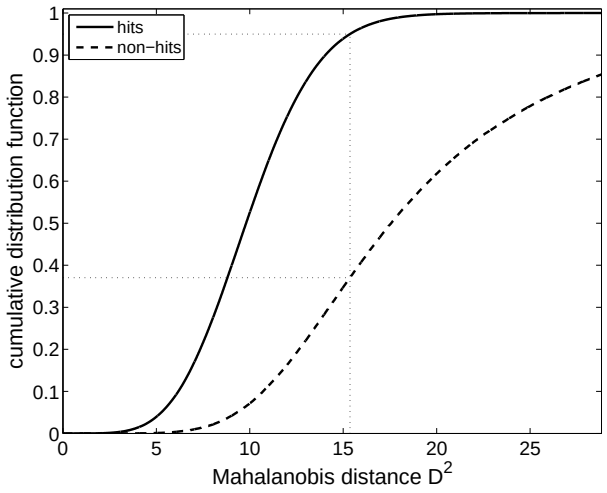

(a) Extended model, Experiment 1.

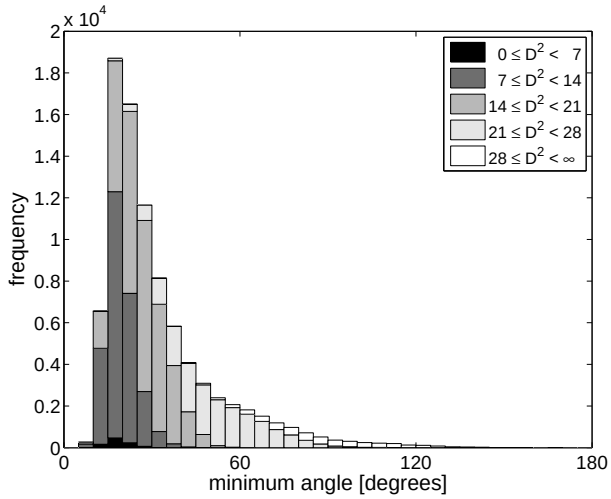

(b) Extended model, Experiment 1.

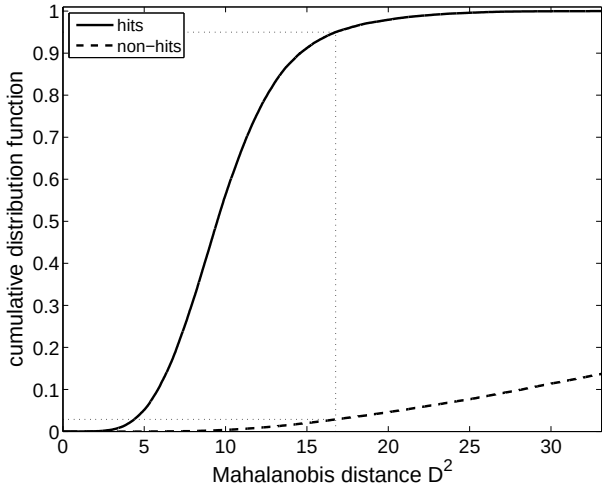

(c) Extended model, Experiment 8.

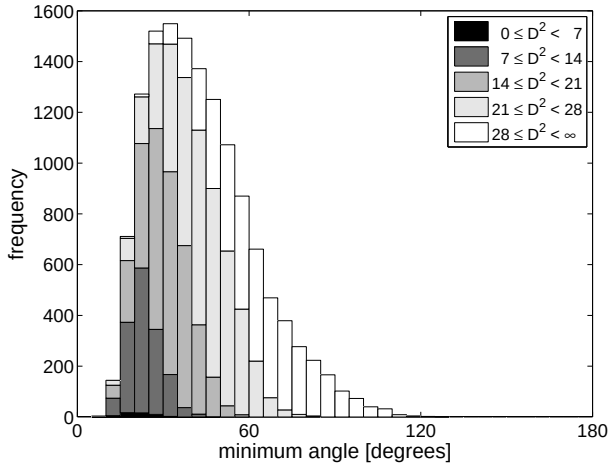

(d) Extended model, Experiment 8.

Figure 5.8: Figures 5.8(a) and 5.8(c) show the cumulative sum for hit and non-hit points of the relative fraction having a larger Mahalanobis distance D^2 than shown on the x-axis. The distances are calculated from the centre of the fitted ellipsoids. The dotted lines indicate how the percent of non-hits contained in the ellipsoid, that is, the relative fraction contained in the 95% ellipsoid times 100, can be obtained. Figures 5.8(b) and 5.8(d) show the distribution of minimum angles according to (5.4). The patch colour indicates the distance of the respective non-hit points from the center of the ellipsoid (see also Figure 5.5(a)).

This indicates that our true geometric object, defining the area that allows bistable behaviour, is a simply connected region in the space (i.e. does not contain holes), as one would otherwise expect to find significantly more angles close to zero. Furthermore, the areas not allowing bistable behaviour contained within the ellipsoid are mostly at the edge of the ellipsoid.

5.4.3 Hit distribution and principal component analysis

A closer look at the spatial distribution of the hits for both models reveals interesting points (Figure 5.9). For almost all parameters, the complete predefined ranges are feasible. The effect of changing a parameter can therefore be compensated by adapting the remaining ones. This only

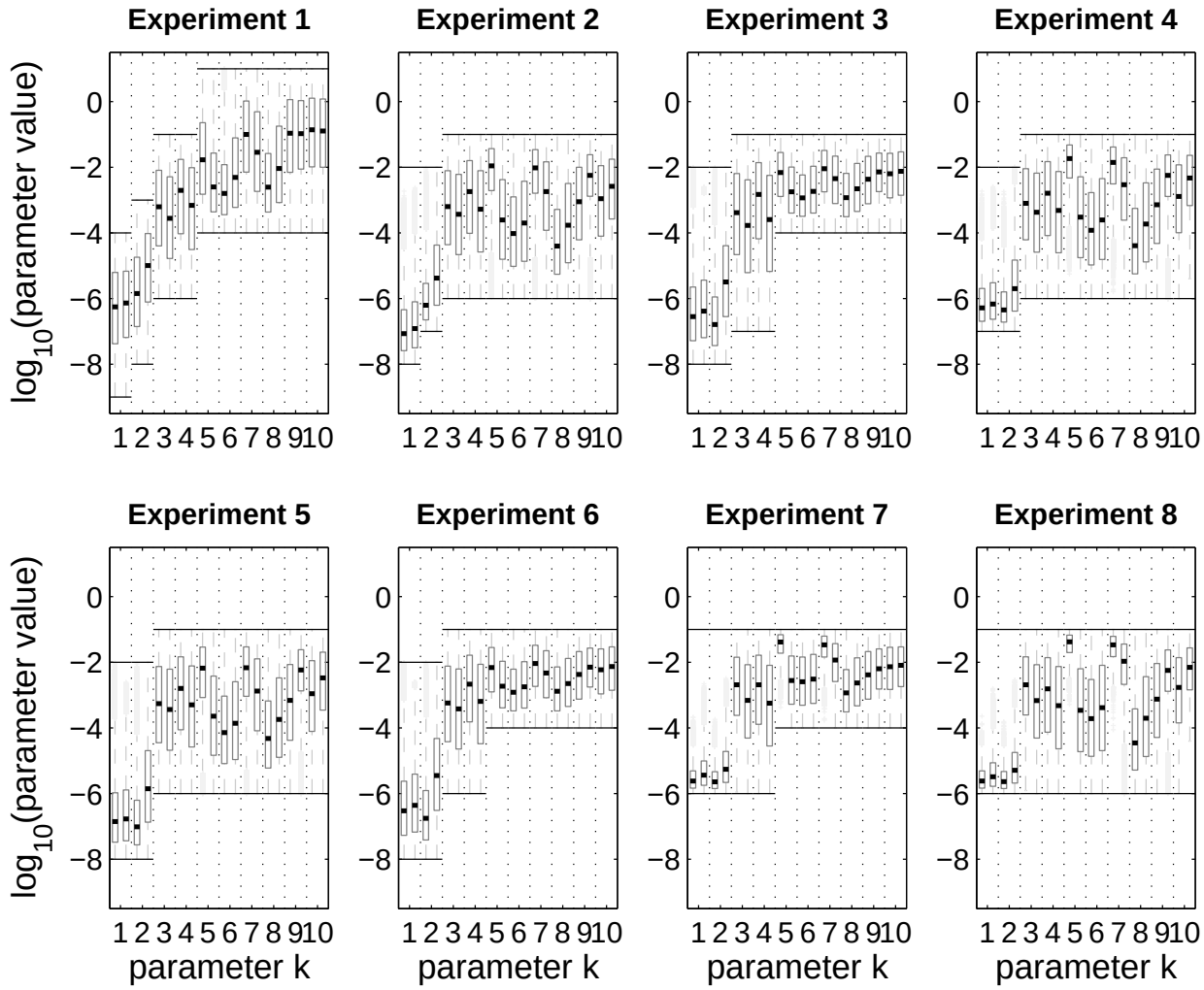

Figure 5.9: Predefined ranges and boxplots of bistable parameter sets. The computer experiments differ by the predefined ranges indicated as longer thin black lines. Each parameter with basic model on the left, extended model on the right; thick black lines indicating the medians, grey boxes from upper to lower quartiles, dashed whisker extensions in light grey at most 1.5 times the boxes, and outliers in light grey represented as '+' signs. The units correspond to the mpc units provided in Table 4.1.

changes when rather unreasonable parameter values are excluded. For example, Experiments 7 and 8 restrict the caspase activation rates to be at least 1% of those estimated in *in vitro* experiments and the turnover for the participating molecules to values at most three times faster than estimated in literature (compare Table 4.2). Although the latter boundary might appear tight, the estimation of turnover rates is less uncertain and an even faster turnover would implicate a higher turnover than e.g. for cyclins known to be quickly degraded to exert their function. In these experiments, the size of the bistable region shrinks and the basic model is more severely affected than the extended model, as can also be seen in the higher discrimination ratios achieved (Table 5.3). Further, the majority of hits are less centred within the predefined ranges, especially the mutual caspase activation and, for the basic model, also the turnover. A bistable performance is thus favoured by slow caspase activation rates and high protein turnovers.

When comparing the two models, the overall differences are not as large as possibly expected. Only the distributions for k_2 and k_5 differ significantly in all experiments. Interpreting the differ-

ence for k_5 is easy as this describes the turnover of C8a, which can be slower in the extended model where the additional reactions buffer exactly that component. More interesting is the difference for the kinetic constant k_2 in the feedback loop, which can be faster and more flexible in the extended model. Although the additional reactions in the extended model directly inhibit only the forward part of the loop, the reason can be traced back to the inhibition reaction: the feedback liberates C8a, inhibited in the extended model but not in the basic. This compound can then efficiently trigger the forward loop. The forward loop itself is not as significantly affected by the additional reactions, although its input is directly effected, because its output (C3a) is buffered in both models. Thus, the effect seen is rather indirect, again highlighting the importance of feedback. These results also indicate that apparently both the forward and the back part of the activation loop need to be tightly controlled for a robust, bistable performance.
That certain critical reactions are more robust in the extended model is also reflected in the shape of the ellipsoid containing 95% of the hits. The roundness is overall larger in the extended model indicating that the critical parameter combinations have become more robust (Table 5.3). Although the extended model is more robust than the basic model, simple simulations with slightly varied parameters or initial conditions show that the model is far from 'totally' robust (Section 5.1).

Principal component analysis. We performed a principal component analysis as described in Section 5.2. The results are shown in Figure 5.10 confirming the roundness measures, which already reveal that especially the least robust direction has become less fragile in all experiments. The increased robustness in the fragile direction also makes the hyper-ellipsoid less flat, implying that a larger error will be introduced when neglecting this direction. The regularity of the ellipsoid in the different directions varies considerably for the different experiments. Interestingly, when we restrict our parameter space using biological insight (Experiment 7 and 8, discussed above), the spread along the different directions drifts apart.
As introduced in Section 5.2.2, the PCA information can be used to approximate a higher dimensional space by a lower dimensional one. Thereby, parameter relations can be identified. The Kaiser criterion (Kaiser, 1960) is often applied as a first guideline on how many and which ellipsoid directions (PCs) to retain. The criterion proposes to only retain directions having associated eigenvalues greater than one. Exemplary applying the criterion to the extended model, Experiment 7, suggests to retain two principal components. This corresponds to an approximation of the ten dimensional point cloud by a two dimensional plane. As exemplified in Section 5.2.2, this would allow the derivation of algebraic equalities, in this case for eight parameters, essentially only leaving two parameters free. We could further analyse correlations between the different experiments to confirm the choice of PCs to retain or use other factor analysis techniques to possibly retrieve additional information, a road not further pursued within the framework of this thesis. We consider it more interesting to closer look at the information within the principal components, which is displayed in Table 5.4 for the extended model, Experiment 7.
Table 5.4 displays the different principal components along with their eigenvalues, which indicate the spread observed along the corresponding direction. Principal components 1 and 2 are mainly oriented in the direction of parameter k_4 and k_3, respectively. This indicates, that both the parameters describing the binding kinetics of IAP to C3a, as well as its cleavage by C3a are not critical to achieve a bistable behaviour. This confirms our previous argument (Section 4.2) that the binding

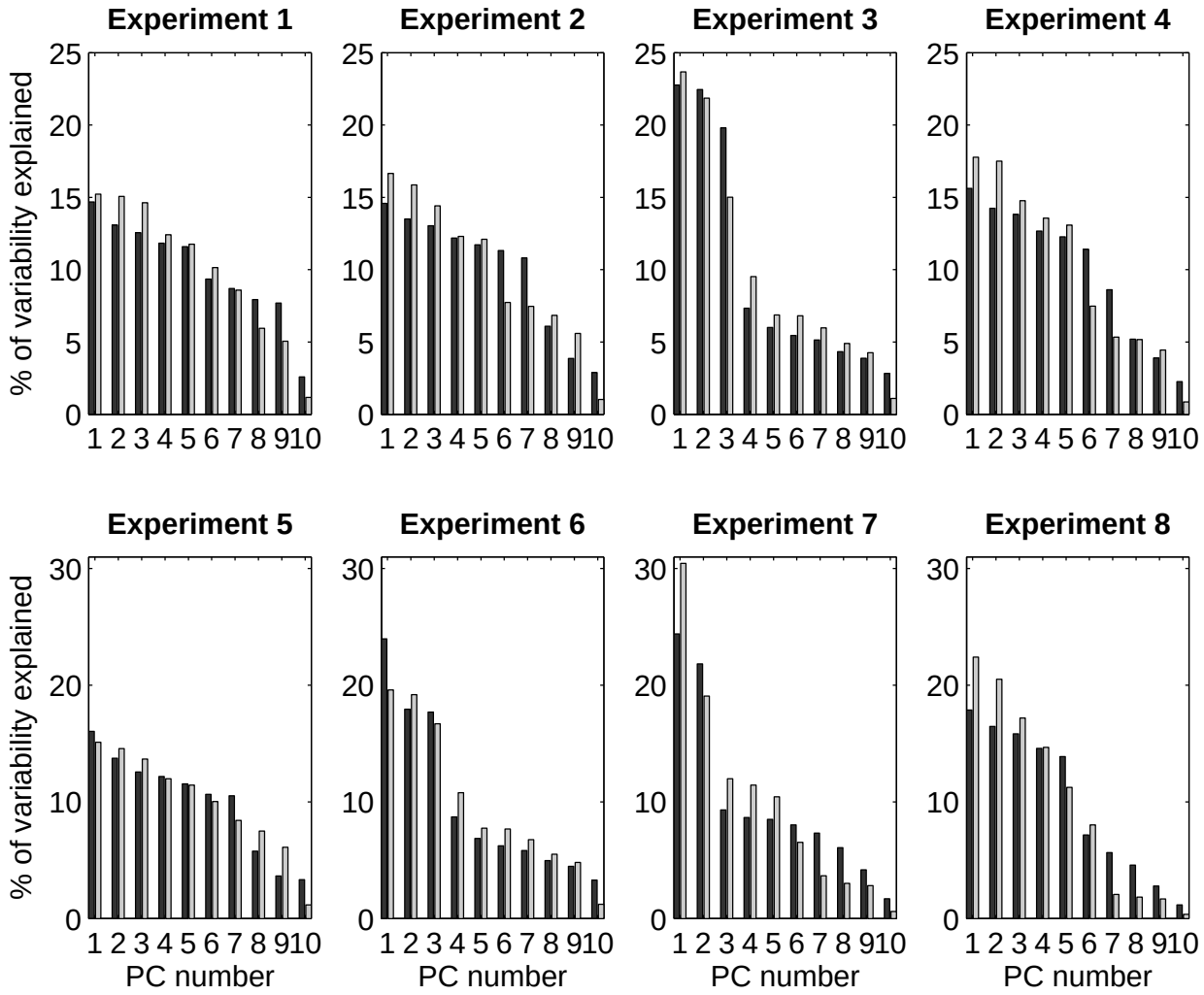

Figure 5.10: Principal component analysis as introduced in Section 5.2. The bars in light and dark grey correspond to the basic and extended model, respectively.

Table 5.4: Principal components of the bistable point cloud, extended model, Experiment 7. The last line indicates the associated eigenvalues measuring the variance along the direction.

$p \backslash PC$	1	2	3	4	5	6	7	8	9	10
k_1	-0.01	0.06	0.01	0.02	-0.16	-0.21	0.25	0.23	-0.52	0.74
k_2	0.00	0.12	0.04	-0.02	0.16	-0.33	-0.50	-0.26	0.50	0.53
k_3	0.06	0.98	-0.04	-0.00	-0.01	0.14	0.04	0.00	-0.02	-0.07
k_4	0.99	-0.06	-0.01	-0.04	0.03	-0.01	0.05	0.04	0.04	0.02
k_5	0.04	-0.00	0.56	-0.21	-0.73	0.12	-0.29	-0.06	-0.04	-0.03
k_6	-0.01	-0.01	-0.65	-0.68	-0.28	-0.13	-0.10	-0.11	-0.07	-0.05
k_7	0.03	0.09	0.15	0.04	0.10	-0.78	-0.24	0.09	-0.34	-0.40
k_8	0.06	-0.02	-0.47	0.69	-0.42	0.03	-0.30	-0.11	-0.11	-0.03
k_9	-0.03	0.00	-0.10	-0.04	-0.01	0.09	-0.34	0.91	0.21	-0.00
k_{10}	-0.05	0.04	-0.03	0.11	-0.40	-0.42	0.57	0.13	0.55	-0.06
EV	2.44	2.18	0.93	0.87	0.85	0.80	0.73	0.61	0.42	0.17

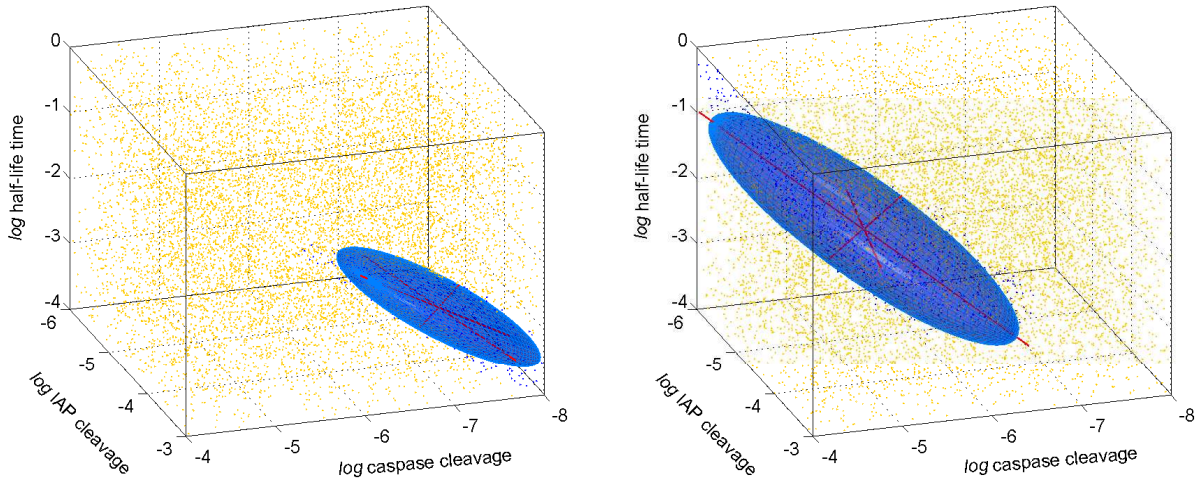

(a) Basic model. (b) Extended model.

Figure 5.11: Bistable parameter domain for the basic and extended model introduced in Chapter 4. Bistable parameter sets are indicated as blue dots and non-bistable parameter sets as yellow dots. The blue surface is marking the two standard-deviation ellipsoids as introduced in Section 5.2. 5.11(a) is also directly comparable to Figure 4.2 – the axis scales are corresponding, only the units differ.

kinetics are less critical, as long as they are fast enough and the thermodynamic equilibrium is retained. Also, the exact rate of cleavage of IAP, though in principal important, is not crucial. On the other end, principal component 10 (and also 9) is directed towards k_1 and k_2, which supports the idea that the mutual caspase activation has to be in a specific ratio that does not allow much freedom.

5.4.4 Visual comparison in three dimensions

The MC approach also allows another visualization form of the problem addressed in Figure 4.2. While the analysis in Section 4.2 was dependent on the special structure of the basic model and did not allow an easy extension to the extended model, the MC approach can be used to visualize a comparison of the basic and the extended model in three dimensions. We again choose the parameter ratios described in Section 4.2.2 to only leave three free parameters to be varied randomly. As predefined ranges we selected those used in Figure 4.2 to allow a comparison. The results are displayed in Figure 5.11(b).

As can be seen from the figure, the model extension clearly enlarges the volume allowing for bistable behaviour. Further, the volume is shifted to allow a faster caspase activation. Thereby, the correlation between the caspase activation and turnover remains: for bistability with fast caspase activation kinetics, comparably high turnovers are necessary. Otherwise, several points discussed in Section 4.2.2 for the basic model, remain true for the extended model, e.g. the IAP cleavage has to fulfil minimum requirements but is less critical in a rather large range.

5.4.5 Discussion and summary

The robustness of the basic and extended model for receptor induced apoptosis, as introduced in Section 4.1, was evaluated in this section. The Monte Carlo approach introduced in Section 5.2 is used to determine robustness measures, which can further be used for model discrimination. Two model discrimination criteria have been formalized. Both use the volume in higher dimensional space allowing for bistable behaviour for comparing different models. They are distinguished by how this volume is calculated: either directly as given by the relative frequency of hits in the MC approach, or indirectly by determining the volume of the ellipsoid fitting 95% of the hits. The extended model has clearly increased robustness measures compared to the basic model and is thus favoured by the formal discrimination criteria. This is in accordance with the additional evidences arguing for a model extension prestented in Chapter 4.
The evaluations show that the Monte Carlo results are dependent on the choice of predefined parameter ranges. While the discrimination criteria are in favour of the extended model for all predefined ranges investigated, the degree of discrimination is better for more restricted parameter ranges, which more closely resemble biological constraints. The partial distribution of the bistable parameter sets reveals that the mutual caspase activation has to be tightly balanced and constitutes a fragile part of the system. Contrarily, the IAP binding to and cleavage by C3a can be considered a robust part of the system. While previous analyses stress the importance of these reactions for the time dependent behaviour, for bistability as such it is important to have those reactions but their rates are not as critical.
Finally, the Monte Carlo approach also allows a visual comparison of the bistable volume of the two models investigated in three dimensions. The results confirm previous indications that the model extension allows for a faster mutual caspase activation combined with a slower protein turnover. Together this indicates that, from a structural point of view, it is favourable to balance both legs of the positive feedback loop through ultrasensitive reaction mechanisms.

5.5 Summary and discussion

The sensitivity of the extended model towards parameter changes is evaluated in Section 5.1. Two different local measures are employed: classical sensitivities for steady state behaviour as well as dynamic sensitivities along the trajectories. We find that the local measures are not always straightforward to interpret when evaluated in isolation. However, these allow compact forms of evaluation, which is required in higher dimensional state and parameter space to guide more detailed analysis. The local analyses reveal several state variables and parameters to be sensitive. The local measures are complemented by an analysis evaluating the change of system characteristics over large parameter intervals. Strong non-local and asymmetric effects become apparent as can be expected for a bistable system. One interesting feature is the unequal behaviour of two mechanisms both resulting in increased IAP levels as observed in certain cancers. When this molecule is up-regulated by increasing its expression, the final value of C3a is significantly lowered. However, when this molecule is up-regulated by decreasing its degradation the final value is unaffected for a certain range of parameter changes. This behaviour is studied in detail in simulation studies. These reveal that the switching from low to high caspase activity is shifted towards higher inputs when

IAPs are up-regulated through a decrease of its degradation. When IAPs are up-regulated through an increased expression, the switching is basically abolished, but a temporally restricted caspase activity is observed. These results are of medical relevance indicating that tumours over-expressing this molecule might not only be less sensitive to apoptotic signals but that this over-expression can further directly contribute to tumour progression (Eissing et al., 2006). Based on these insights, points to take into consideration for drug development, as currently on the way, can be formulated. Increased IAP levels, however, are not restricted to tumour cells but are a natural mechanism to prevented undesired apoptosis. As introduced in Section 2.1, IAPs are up-regulated in response to TNF via the NFκB pathway. Therefore, the analysis performed provide valuable information when extending the model to include these anti-apoptotic pathways as outlined in Section 7.2.

As discussed in Section 5.3.3 and below, sensitivity measures are often also used to evaluate robustness. In Section 5.2 we define a different approach, which focusses on the qualitative behaviour of bistability. A Monte Carlo approach is proposed to evaluate higher dimensional parameter spaces for this characteristic behaviour. Theoretically, comparable results can be achieved by a higher dimensional bifurcation analysis. However, these methods are numerically very demanding. The obtained results are point clouds consisting of bistable parameter sets (hits) and parameter sets, which are not bistable (non-hits). The ratio of hits and total parameter sets evaluated is a direct measure for the relative volume in higher dimensional space allowing for bistable behaviour. While the point clouds can be easily visualized in three parameter dimensions, a statistical analysis can provide further insight in higher parameter dimensions. The point cloud is fitted by an ellipsoid and indicators for the achieved fit are derived. A principal component analysis provides further insight about the length and direction of the ellipsoids' axes and thereby geometrically characterizes the point cloud described by it. Selected aspects of the procedure are employed in Sections 5.3 and 5.4 to further analyse and compare the models proposed in Chapters 3 and 4.

In Section 5.3 the Monte Carlo procedure is applied to the three models proposed in Chapter 3. The analyses are complemented by a robustness analysis according to Ma and Iglesias (2002), which is also based on bifurcations. Both measures provide comparable results. The three mechanisms for generating bistability can all allow for a robust bistable performance. None of the mechanisms evaluated appears especially preferable compared to another (Eissing et al., 2007b) unlike previously reported (Bagci et al., 2006).

In Section 5.4 the Monte Carlo procedure is applied to the basic and extended model of receptor induced apoptosis as detailed in Chapter 4. The relative hit frequency and the volume of the ellipsoid fitting the bistable parameter sets are proposed as quantitative measures for model discrimination. Both measures provide comparable results in favour of the extended model when applied. This supports the proposed model extension, also suggested by our previous analysis (Chapter 4). A more detailed analysis of the distribution of hits in parameter space also supports previous analyses. The model extension clearly allows for faster caspase activation kinetics (Eissing et al., 2005a).

The MC approach proposed to evaluate complex behaviour in higher dimensional parameter space is not restricted to bistability. It can, for example, also be applied to evaluate oscillatory behaviour as in Morohashi et al. (2002) without the restriction of varying only one or two parameters at a time. Random parameter variations as employed here allow the analysis in higher dimensions and of nonlinear effects due to parameter combinations. Only few studies on the robustness of (sig-

nalling) pathways have employed random parameter variations (Stelling et al., 2004b). Examples are the robustness analysis of ultrasensitivity or of adaptation (Barkai and Leibler, 1997; Blüthgen and Herzel, 2003). Both use a continuous output and measure robustness with respect to relative parameter changes.

While the extended model is much more robust than the the basic model, and comparably robust to other bistable signalling models (Bhalla and Iyengar, 2001), especially the different sensitivity analyses indicate that also the extended model is more strongly influenced by parameters than indicated for other biological systems. This is in some contrast to our postulation of robustness in apoptosis (Section 2.2.3). This might reflect our assumptions during modelling. We aimed to keep our model simple making conservative assumptions to simplify analyses and reveal the principle mechanisms responsible for the observed behaviour. Clearly, more robust models of apoptosis signalling can be thought of (see Section 7.2). However, our results might also reflect that apoptosis is not as robust as we desire it to be. For example cancer, where apoptosis is impaired, is a common disease and a leading cause of death, especially in developed nations. But then, on average only 1 out of 10^{15} cells develops into a cancer, which after all is not that common (Hartwell et al., 1999). A unifying perspective on these conflicting results will be presented in Section 7.2, where we argue that the observed sensitivity could be the result of a robustness-performance trade-off due to additional physiological constraints. Either way, the relative character of robustness and what can be considered 'common' or 'rare' requires objective approaches to compare different findings. Therefore, the analyses as proposed are helping to reveal these features in healthy and diseased conditions and can guide medical interference strategies.

The different sensitivity and robustness analysis techniques employed and a critical evaluation of the results obtained thereby, reveals that different measures provide different insight. Therefore, a combination of different techniques is advisable. Further, improved methods are desirable. Several robustness measures rely on the evaluation of first order sensitivities as described in Section 5.1. These provide results, which often only hold in the immediate surrounding of the point considered for linearisation. Although the procedure is often extended to different points in parameter space, the results might still not capture relevant nonlinear behaviour. Several additional measures have been proposed in the literature to quantify parameter dependencies of dynamic properties, such as the integral over a transient or the frequency or amplitude of oscillations (Heinrich et al., 2002; Hornberg et al., 2005a,b; Ingalls, 2004; Wolf et al., 2005). Thereby interesting relations for the obtained measures have been formulated as laws. Similar measures could be considered for the models presented in this study, e.g. defining properties as described in Section 5.1.2. However, the generally local validity of these measures remains an issue. This is of particular relevance, when the models under consideration display nonlinear 'global' phenomena such as oscillations or bistability. For example, the analysis in Section 5.1.2 show that several parameters influence properties in a discontinuous, all-or-nothing fashion. The local nature of these methods is especially problematic as parameters in models of biological processes to date probably only provide rough estimates of the true parameters. Once experimental procedures become more quantitative to allow for a more rigorous identification, the usefulness of the methods could also increase further. To the contrary, bifurcation analyses consider global properties and robustness measures based on bifurcations can be derived. The Monte Carlo approach proposed in Section 5.2 provides a measure based on bifurcations but only considers one qualitative feature introducing limitations

as indicated in Section 5.3. Global measures are generally also harder to compute. Therefore, methods and measures are desirable that rely on local investigations but are able to capture more global characteristics. Promising steps have been made employing ideas routed in robust control as discussed in Section 7.2.

Chapter 6

Stochastic Influences

Stochastic effects are observed during apoptosis. For example, different cells within a population die at different time instances as introduced in Section 2.2.4. Thereby, different delay times due to the stochastic nature of biological systems could enable fast single-cell segments of caspase activation to integrate, forming an overall slow caspase activation at the macroscopic level (compare Figure 2.5). In Section 4.3 we showed that in our model the strength of the apoptotic input stimulus mainly translates into such a delay between the input and significant effector caspase activation. However, stochastic effects are not readily captured using an ODE description. In this chapter, stochastic effects are introduced in two different ways. In Section 6.1, stochastic simulations are used to evaluate how well the considered processes can be approximated by an ODE description. Somewhat surprising, stochastic effects due to the stochastic nature of reactions are small for a relevant and large range of inputs because the inhibitors buffer the activated caspases and thereby filter out noise (Eissing et al., 2005a). In Section 6.2, kinetic parameter and input distributions are applied. These introduce a pronounced variability into the model behaviour and allow the reconciliation of the different kinetics observed in single cells and populations in terms of understanding and modelling (Eissing et al., 2004).

6.1 Stochastic simulations and inhibitors as noise filters

The mathematical models introduced in Section 4 consist of deterministic ODEs. Therefore the underlying assumption is that the stochastic nature of the reactions can be neglected. However, deterministic simulations show that even for large inputs, the activated caspases remain at very low concentrations corresponding to a few molecules per cell for long time intervals (decision or lag phase) before suddenly being activated (activation phase; e.g. Figure 4.3). Therefore the impact of the stochastic nature of the reactions, also called intrinsic noise (Elowitz et al., 2002), should be investigated. Models with significantly more molecules are known to be influenced by the inherent stochasticity of reactions. Generally, species with low numbers determine the stochasticity, and the relative magnitude of molecular fluctuations (determined by the ratio of steady state standard deviation and mean) increase quadratically with decreasing numbers of reacting molecules (Fall et al., 2002; Rao et al., 2002).

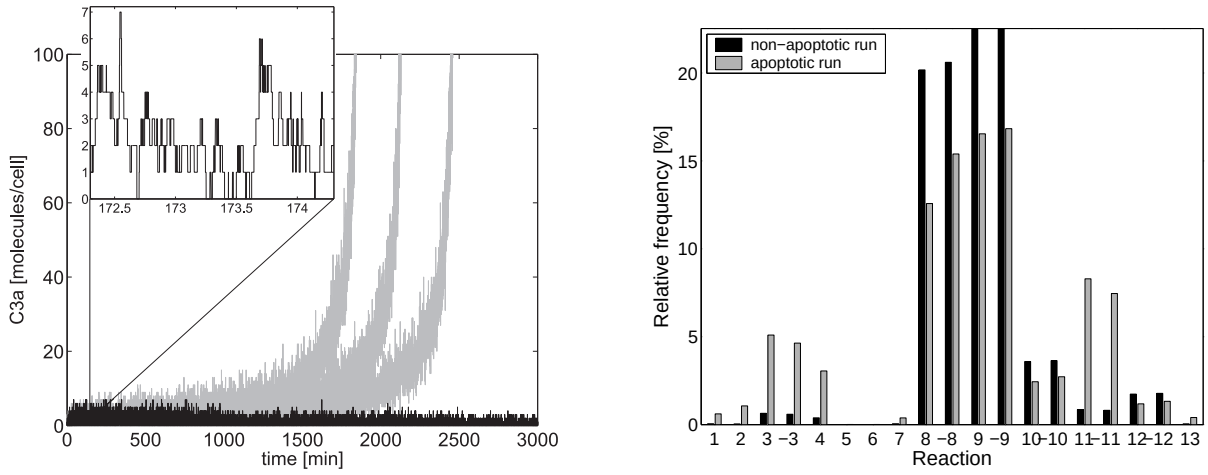

(a) Single stochastic simulations

(b) Statistics

Figure 6.1: Non-apoptotic and apoptotic stochastic simulations of the extended model for the input $[C8a]_{t=0}$=443 mpc (using standard parameters, Table 4.1). 6.1(a) shows two obtained non-apoptotic (black) and three apoptotic (grey) stochastic simulations, with the inlet representing a zoom into one of the apoptotic runs. 6.1(a) shows the relative frequency of the different reactions occurring during the simulation for one representative apoptotic run and one representative non-apoptotic run.

Stochastic simulations. The stochastic apoptosis models are similar to the deterministic ones described in Section 4.1, except that the concentrations are now a discrete number of molecules and the deterministic rate constants k become transition probabilities. This corresponds to a description as a Markov process. Both the extended and the basic model were simulated using the next reaction algorithm (Gibson and Bruck, 2000). In our examples, this algorithm speeds up the simulations by several orders of magnitude compared to the 'traditional' approach proposed by Gillespie (1975, 1976) without introducing approximations.

As in the deterministic simulations (Figure 4.3), stochastic simulations also show low concentrations of the key molecule C3a during the decision phase, as exemplarily shown in Figure 6.1(a). The high turnover of the molecules and the length of the simulations require many stochastic simulation steps (Figure 6.1(b)).

To more quantitatively evaluate the impact of intrinsic noise, the models were simulated 5,000 times for each of 55 C8a input concentrations, log-uniformly distributed between 10 and 15,013 mpc. The simulations finish when one of the following three conditions holds:

1. The concentration of C3a exceeds 8,000 mpc, i.e. at that time point the cell is irreversibly committed to apoptosis and even in the stochastic setting does not return to 'life' due to the hysteresis and irreversibility in the switch (Rao et al., 2002). A weaker hysteresis as for example seen in Acar et al. (2005) can lead to basin hopping, i.e. the stochastic system switches between its stable steady states. We define the time point when C3a exceeds 8,000 mpc as the end of the activation phase. This phase is itself very short and follows the much longer decision phase. The input strength strongly affects the length of this decision phase, whereas the activation phase is always very short.

2. No free or bound active caspases are left in the system, i.e. also in the stochastic setting no further caspase activation can occur without an additional input.

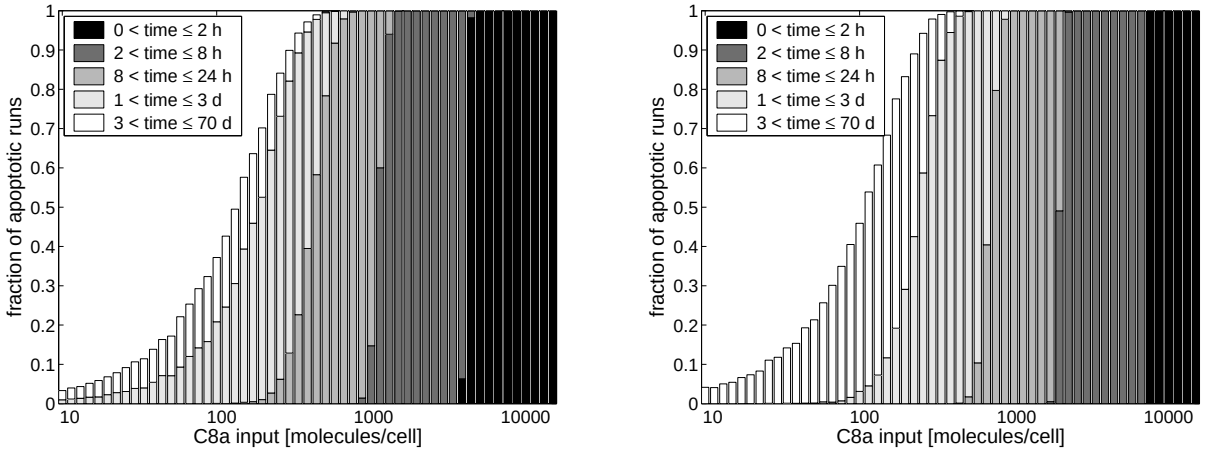

(a) Basic model

(b) Extended model

Figure 6.2: Stochastic simulations: fraction and time point of apoptotic runs. For the time points, only a rough interval resolution indicated by the patch colour is shown. Notice the different time units within the legend: h – hours; d – days.

3. 100,000 minutes (∼10 weeks) simulation time has passed – a time frame far beyond the biological validity of the model.

While the nominal parameters were used for the extended model, these do not allow for bistability in the basic model. For comparing the models regarding the influence of stochasticity on the bistable behaviour, a bistable parameter set for the basic model was chosen allowing for a similar bistable threshold[1].

Inhibitors as noise filters. For larger inputs, almost all simulations show a high concentration of C3a after some time corresponding to apoptosis. Unlike the deterministic case, no sharp threshold separating the areas of attraction of the two stable steady states exists. Figure 6.2 shows the fraction of apoptotic runs for each initial condition and the results are very similar for both models. Even for the smallest possible input, a single C8a molecule, certain stochastic simulations lead to apoptosis (data not shown). A closer look at low input concentrations reveals that the duration of the decision phase is in the order of several days or even weeks (Figure 6.2, patch colour). Similar durations can be observed in the deterministic case for inputs slightly above the threshold. Biologically, the prediction of such long decision phases is meaningless as the model ignores many processes occurring on this time scale within the cell, e.g. gene induction or simply dilution due to cell division.

Figure 6.3 shows the distribution of the time between stimulus and apoptosis in the stochastic case and compares it to the deterministic case. Again the results are similar for both models. For low inputs we see a large variability for the time point of cell death. Above an input of about 300 mpc C8a, both the median and the mean (not shown) are very close to the deterministic results. Above approximately 1,000 mpc, the stochastic responses are narrowly distributed around the deterministic solution. As only large inputs lead to apoptosis within a meaningful time, the stochastic effects

[1] http://www.sysbio.de/projects/tnf/IEE05/

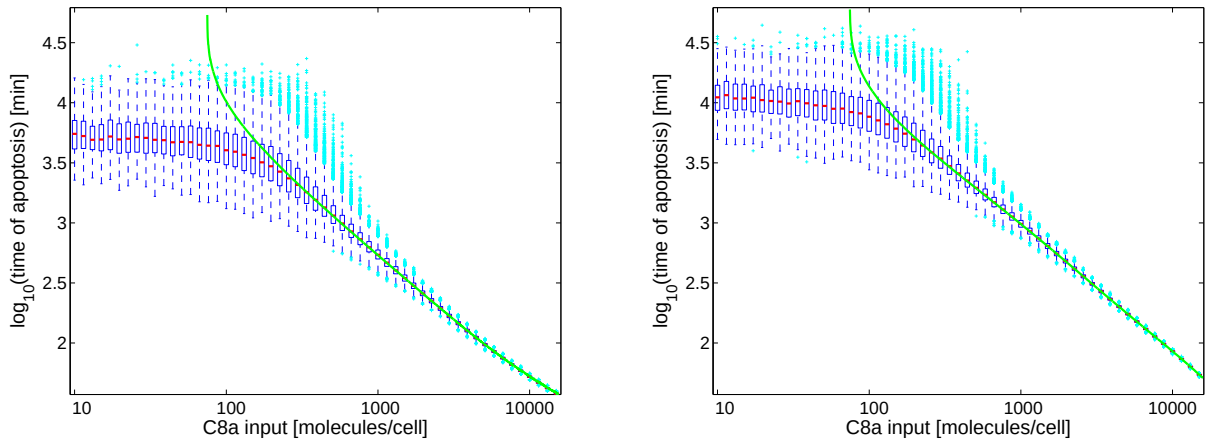

(a) Basic model

(b) Extended model

Figure 6.3: Stochastic simulations: variation and comparison to deterministic run. Boxplot of the apoptotic runs, with red lines indicating the medians, blue boxes from upper to lower quartiles, dashed whisker extensions in blue at most 1.5 times the boxes, and outliers in cyan represented as "+"-signs. Deterministic simulation results shown as green lines.

can be neglected. In the light of the scarcity of key molecules shown in Figure 6.1(a), this finding is rather surprising.

The reason for the minor impact of intrinsic noise on the performance is given by the inhibitors. During the decision phase, the activated caspases are almost exclusively present as complexes with their inhibitors (Figure 4.4(b)). The corresponding reactions 3 and 11 are therefore very frequent, with only the turnover of the inhibitors taking place more often, see Figure 6.1(b) (compare also to Figure 4.4(f) where the forward and backward parts of the reactions occur at a high absolute rate, while the overall rate is small). This pool of bound molecules serves as a buffer, dampening the stochastic fluctuations by maintaining a dynamic balance between the activated molecules and the inhibited ones, similar to a chemical buffer maintaining a constant *p*H value. This effect can be seen in both models, as both contain inhibiting reactions. Interestingly, the extended model containing two such buffers hardly outperforms the basic model only containing one. Apparently, the slower mutual activation kinetics of the caspases in the basic model poses lower demands on the system in this respect, such that intrinsic noise can well be handled by only one buffering system.

In conclusion, this section evaluates the influence of the intrinsic stochastic nature of reactions. Due to the scarcity of key molecules during simulation, rather strong stochastic effects could be expected. However, the stochastic simulations show that the models behave almost deterministically for a relevant and large range of inputs, because the inhibitors buffer the activated caspases and thereby filter out noise (Eissing et al., 2005a). While this is in support of ODE investigations, the stochastic nature of reactions cannot explain the stochastic effects observed in experiments (Section 2.2.4).

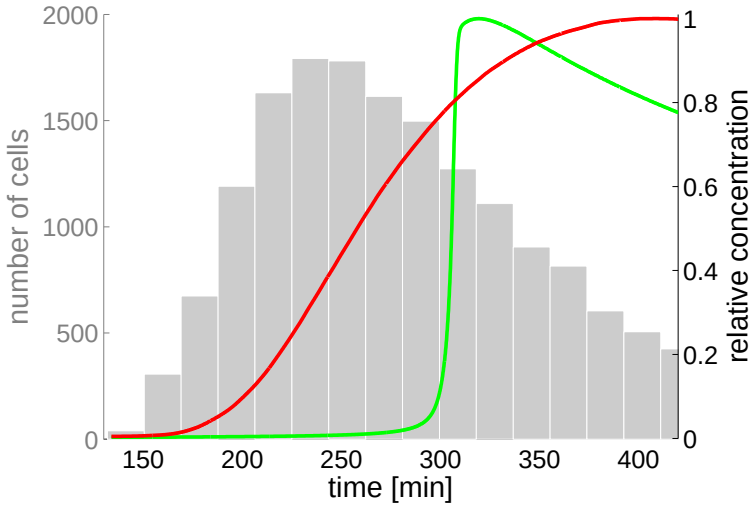

Figure 6.4: Population behaviour (red) and nominal single cell behaviour (green) as relative concentrations of C3a for $[C8a]_{t=0}$=3,000 mpc. The light grey bars indicate how many cells in the relevant time frame exceed a threshold of 500 mpc C3a. 20,000 cells were simulated, each with parameters randomly chosen from a uniform distribution between 90 and 110% of its nominal value.

6.2 Kinetic parameter and input distributions

The model derived in Section 4.3 has the aim to reproduce certain aspects of apoptosis induction at the single cell level such as a fast effector caspase activation. However, most experimental studies have been performed using cell populations where effector caspase activation is typically observed within a range of a few hours (Fotin-Mleczek et al., 2002; Hentze et al., 2002; Scaffidi et al., 1998). This can be linked to different cells dying at different time instances. Thus, as introduced in Section 2.2.4, apoptosis shows stochastic characteristics. However, the intrinsic stochastic nature of reactions cannot explain the stochasticity observed (Section 6.1). In the following two simple and intuitive ways relying on distributed model parameters are illustrated that can reconcile the observed single cell differences both in terms of understanding and modelling. The effects of distributed model parameters are already indicated in Section 5.1. We first consider a random variation of all kinetic parameters and then a distribution of the initial concentration of C8a corresponding to the model input.

Distributed parameters. Figure 6.4 illustrates how a population of 20,000 cells, where each parameter of each cell was randomly chosen form a uniform distribution between 90 and 110% of its original value, can yield a completely different picture at the population level. Whereas the single cells show a rapid caspase 3 activation at different time points, the caspase 3 activity is increasing much slower on the population level. These qualitative differences reflect observed differences in single cell and population experiments.

Distributed input. Above, single cell simulations with random parameters were averaged to describe the behaviour of a population. In the following, we will exemplarily proceed the other way around and calculate a distribution needed to produce a given population behaviour. Based on the simulations of the deterministic single cell model described in Figure 4.3, we can describe

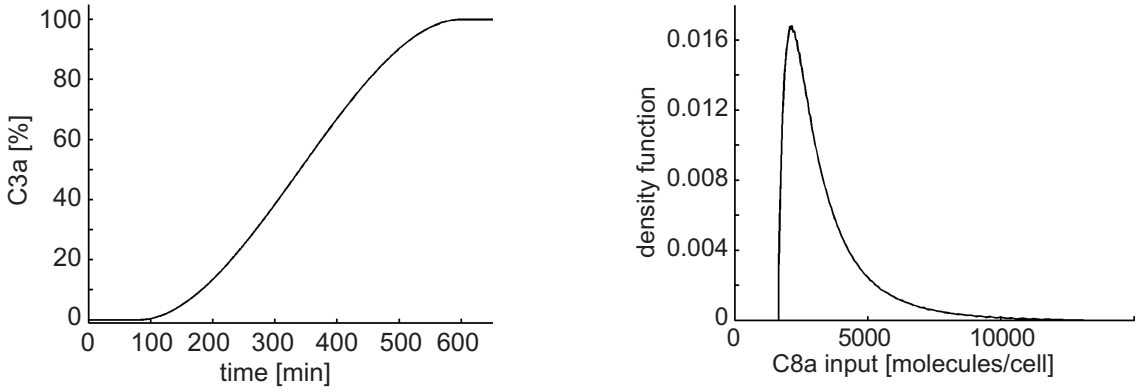

(a) Population behaviour

(b) Distributed input

Figure 6.5: 6.5(a) shows an idealized time course of caspase 3 activation as observed at the population level. 6.5(b) shows the density function of the input signal necessary to achieve the population behaviour depicted in 6.5(a), based on single cells behaving as described in Figure 4.3.

the maximal caspase 3 activation as a function of C8a input. Hereby we assume the maximal caspase activation to define the time point of cell death. This correlates the stochastic time point of cell death to a stochastic input signal for the single cells within a population. We assume a population behaviour as depicted in Figure 6.5(a), which can be interpreted as a cumulative probability distribution. We further assume that 100% of caspase activation corresponds to 100% cell death, i.e. caspase 3 becomes significantly activated in every cell within the population (necessary assumption to get a one to one relationship). From the original distribution of Figure 6.5(a), we obtain a distribution of cell death probability as a function of input activation. The corresponding probability density function shown in Figure 6.5(b) was derived by differentiation.

Thus an input distribution as depicted in Figure 6.5(b) into a fast switching single cell model as depicted in Figure 4.3 can yield a slow behaviour at the population level as depicted in Figure 6.5(a). Although this approach is very simplified, it already reconciles single cell and population data and shows a way of combining both in terms of understanding and modelling. Also, the required distributed input can be explained, for example, by different numbers of death receptors expressed in different cells. In fact, the distribution as shown in Figure 6.5(b) nicely matches observed receptor distributions in fluorescence-activated cell-sorting (FACS) experiments (Peter Scheurich, personal communication) and log-normal distributions for proteins more generally postulated by Hawkins et al. (2007).

In conclusion, in this section two different ways of reconciling single cell and population experiments are presented. Both approaches are based on the single cell model as detailed in Section 4.3 and both assume distributed parameters due to stochastic processes not further detailed themselves. While the first approach simulates the effects of random variations in the kinetic parameters to produce a different behaviour at the population level, the second approach counts back an input distribution needed in order to achieve a given population behaviour.

6.3 Summary and discussion

Biological processes are stochastic processes (Rao et al., 2002). We evaluated in this chapter how different stochastic effects can affect the performance of the extended model derived in Section 4.3. Thereby, these stochastic influences could explain observed differences in single cells and cell population experiments as outlined in Section 2.2.4.

The influences of the stochastic nature of the involved reactions was evaluated using stochastic simulations (Section 6.1). The main finding is that the model behaves almost deterministically for a relevant and large range of inputs because the inhibitors buffer the activated caspases and thereby filter out noise (Eissing et al., 2005a). While these results further legitimate an ODE modelling approach, they cannot explain the observed single cell and population differences. This can, however, easily be achieved by considering parameters that are stochastically distributed. Such distributed parameters can lead to a slow caspase activation at the population level, while these molecules are still rapidly activated in the single cells. Exemplary, we considered two set-ups. The first one assumes random variations in the kinetic parameters, while the second one assumes a distributed input whose distribution is calculated based on a given population behaviour (Eissing et al., 2004). Interestingly, the input distribution derived closely resembles receptor distributions observed in experiments. Further, the distribution closely resembles a log-normal distribution, which is more generally proposed as a suitable distribution to describe population heterogeneity (Hawkins et al., 2007). Combinations of both approaches are easily thinkable. In our approach, the distributed input is implemented as a distributed initial condition. Naturally, all protein concentrations and therefore initial conditions will vary among different cells within any given population. The number of caspase 8 inhibitors, for example, strongly influences the threshold, as also observed in siRNA experiments against CARPs (McDonald and El-Deiry, 2004). Likewise, kinetic parameters can be considered to slightly differ within a cell population. Thus, in nature it will likely be a combination of all involved parameters that accounts for the differences between the single cell and population level. The presented results could be extended to reflect this fact. However, the contribution of the different parameters to the variance should closely resemble the influences identified in Section 5.1.2. Further, more extensive simulations of the extended model with random parameters have been recently described by (Carotenuto et al., 2007b). The results provided, conceptually closely resemble the results described above.

Chapter 7

Conclusions

Section 7.1 summarizes the findings presented in this thesis and discusses selected aspects. Section 7.2 places the contributions into a more general context and outlines current and possible future roads to continue the work described.

7.1 Summary

This thesis aims to provide a better understanding of the signalling processes responsible for programmed cell death employing ideas from systems science as introduced in Chapter 1. Chapter 2 motivates the concept of viewing apoptosis as a robustly bistable system, which is relevant for the modelling and analysis presented in the following. Chapters 3 and 4 provide different mathematical models for apoptosis signalling, which are distinguished by their level of detail and mechanism they focus on or take into account. Bistability is evaluated as a key feature of the models presented. These analyses are extended and deepened in Chapters 5 and 6 with a focus on robustness of bistable behaviour towards parametric and stochastic influences.

Models of apoptosis pathways. Overall, five different models have been investigated in more detail. The three simple models used to evaluate design principles for generating bistability are named cooperative, inhibitor and zero-order model. The models more closely resembling apoptosis signalling are named basic and extended model. Important findings are summarized in the following.

Chapter 3 evaluates three different mechanisms to generate ultrasensitivity and bistability in proteolytic cascades such as encountered in apoptosis signalling or blood clotting: cooperativity, inhibitors, and enzyme saturation (zero-order). Whereas classically, the back-reaction has to be saturated to generate zero-order ultrasensitivity, the degradation can achieve this effect in irreversible proteolytic reactions. We further analyse the influence of zymogenicity in these simple models to reveal that it strongly impacts on the cooperative model while only mildly affecting the two other models (Eissing et al., 2007c).

Extending the inhibitor model, Chapter 4 describes a basic model, which reflects the widely accepted core reactions of the direct pathway of receptor induced apoptosis. Higher dimensional bifurcation analyses show that the model, while in principle allowing for bistability, does not allow

bistability anywhere close to parameter values reported in literature. This indicates the need to modify the model structure and reveals a lack of understanding of the system behaviour despite intensive research worldwide. Critically evaluating the basic model and current literature, a model extension is proposed to include additional inhibitors directly targeting initiator caspases. The hypothesis is supported by recent experimental results. The extended model is in agreement with key features observed in experiments and able to explain important phenomena from a systems perspective (Eissing et al., 2004).

Key features of the extended model. The extended model is in good agreement with key experimental observations including tolerance to sub-threshold stimuli and a fast activation of executioner caspases after a prolonged delay (Sections 4.3 and 4.4). Our analyses show that the caspase system includes interlinked feedback loops, which allow for the observed dual kinetics (Sections 4.3 and 4.4), although other explanations for the characteristic kinetics have been proposed, and are likely contributing, as discussed in Section 4.4. The mutual caspase activation constitutes a positive feedback loop responsible for the fast and decisive switching. The IAP binding can be interpreted as a double negative feedback loop and the long delay can be attributed to this reaction. Thereby, this feedback stabilizes the respective state of the cell – low caspase activity to allow for normal cellular function, and high caspase activity to allow a rapid, decisive and irreversible programmed cell death execution. In this context it is interesting to notice that interlinked slow and fast positive feedbacks have recently been reported as a widespread design to constitute 'dual-time' switches that drive reliable cell decisions (Brandman et al., 2005).

Sensitivity analyses of the extended model. Section 5.1 evaluates in detail the dependence of parameter changes on the performance of the extended model using different sensitivity analysis techniques. The results provide clear indications on how other signalling pathways can influence the behaviour of the core model (see Section 7.2). Also, the analyses support the idea of IAPs as key regulators of apoptosis. Further, an up-regulation of these molecules through increased expression can lead to temporally restricted caspase activation for strong apoptotic inputs, which could lead to pathological cellular conditions and contribute to tumour progression. An up-regulation through decreased degradation on the other hand preserves the switching characteristic (Eissing et al., 2006). These findings are especially interesting, as drugs targeting IAPs are under development (Schimmer et al., 2006).

Robustness of apoptosis models. As outlined in Section 2.2.3, robustness has been recognized as an important feature of biological systems in general, which is also essential for apoptosis signalling, and a robustness based model discrimination has been proposed. Many techniques for robustness evaluation are based on sensitivity analysis and often proceed through linearisation. These are of limited use to evaluate more global aspects (such as robustness) of complex nonlinear phenomena such as bistability. Instead, measures based on bifurcations have been proposed.
These ideas are extended in Section 5.2 employing a Monte Carlo based approach to define the volume allowing for bistable behaviour in higher dimensional spaces. The method also allows the extraction of further information, such as parameter relations, which can be identified by a principal component analysis. The approach is employed to evaluate and compare robustness

features of the models proposed. Section 5.3 provides clear evidences that the basic mechanisms for achieving bistability in apoptosis signalling as introduced in Chapter 3 are all able to produce a robust bistable performance (Eissing et al., 2007b), unlike reported otherwise (Bagci et al., 2006). Section 5.4 shows that the model extension proposed in Section 4.3 clearly increases the robustness compared to the basic model (Eissing et al., 2005a, 2007a). Especially, this allows for a faster mutual caspase activation further arguing for the proposed model extension.

Stochastic influences in apoptosis (models). As outlined in Section 2.2.4, biological processes are stochastic processes and stochastic effects have been observed for apoptosis. However, stochastic simulations show that the performance of the apoptosis models proposed is not significantly influenced by the stochastic nature of the reactions for a wide and significant range of inputs (Section 6.1). In this context, the inhibitors function as noise filters similar to chemical buffers (Eissing et al., 2005a). Section 6.2 illustrates how distributed parameters or inputs reproduce stochastic effects observed and reconcile experimental single cell and population data (Eissing et al., 2004). Thereby, the necessary distributions can be biologically well interpreted.

7.2 Perspective

Of course, the work described in this thesis cannot be considered complete in itself and certainly is not marking the end but hopefully contributing to the beginning of a deeper understanding of apoptosis employing mathematical modelling and systems theory. Following, the work developed in this thesis is further integrated into the wider context of systems biology and current and possible future roads are outlined.

Experimental verification. The work described is revealing interesting insights into apoptosis signalling. Necessarily for modelling and analysis, assumptions had to be made based on a critical evaluation of the current literature. Some important predictions and assumptions, though supported by some experiments, are awaiting a final experimental verification. Interesting new experimental techniques geared towards the modelling demands are being established. These include micro-injection of active caspases combined with measurements of active caspases at the single cell level corresponding to the model input and output. It can be hoped that these techniques will in the near future provide interesting new insight into the caspase system and provide data for model refinement, especially when combined with perturbations of apoptosis signalling like varied IAP levels. Although preliminary results indicate that both type I and II cells are indeed resistant towards small amounts of active caspase 8, while responding with a delayed and then decisive activation of caspase 3 (unpublished data, Institute of Cell Biology and Immunology, University of Stuttgart), conclusive data to prove bistability at the executioner caspase level remains elusive.

Possible model extensions for the direct pathway. As outlined above, the presented models are primarily qualitative but semi-quantitatively capture important characteristics. Parameters were estimated based on parameter studies. New experimental data will allow a more rigours identification of model parameters. Possibly, additional considerations have to be integrated structurally.

As described, the apoptosis models combine certain reactions such as the indirect positive feedback mediated by caspase 6 into an overall feedback. Further, IAPs are represented as one pool of inhibitors. Distinguishing between XIAP, which appears to mainly act as a direct inhibitor, and cIAPs, which appear to primarily act by facilitating degradation of activated caspase 3 and are postulated as to constitute a possible back-up mechanism (Eckelman et al., 2006), should clearly increase the robustness of the models presented. It has been indicated that CARP molecules are cleaved by activated caspase 8, similar to IAPs being cleaved by activated caspase 3 (McDonald and El-Deiry, 2004). Taking this into account could allow an even more decisive switching, or possibly a decisive switching with a less 'aggressive' positive feedback in the caspase centre. Also, the functions exerted by the cleavage products could be included into the model. However, especially for CARP these are largely unknown. Very recently, CARPs were shown to act as ubiquitin ligases for p53 and thus might also act on caspase 8 more in the way indicated for cIAPs rather than for XIAP acting on caspase 3 (Yang et al., 2007). Thereby, degradation saturation might contribute to the generation of ultrasensitivity as outlined in Section 3.2.2.
As described, the potential extensions should increase robustness, but will also make analysis more demanding. Experimental results should guide model extensions to include necessary elements needed to explain observed phenomena. Another promising way for extending the model is to embed it into other cellular signalling processes, which are known to interact with this pathway as exemplified in the following.

Embedding into cellular signalling. The extended model proposed in this thesis is restricted to one apoptosis pathway. Parallel pathways are known to exist and, further on, apoptosis signalling is embedded into other cellular signalling processes. One interesting example is TNF signalling as introduced in Section 2.1. TNF not only activates, cell type depended, the direct and the mitochondrial pathway of apoptosis, but in parallel induces NFκB and JNK signalling (compare Figure 2.2). Interestingly, NFκB up-regulates IAP and FLIP levels among many other, thus directly influencing apoptosis signalling. A mathematical model as outlined in Figure 7.1 including the two apoptotic routes and the NFκB pathway has been established in our group (Rumschinski, 2007; Schliemann, 2006; Schliemann et al., 2007). The model is build upon available knowledge gained through mathematical models of different modules including NFκB signalling (Barken et al., 2005; Hoffmann et al., 2002; Krishna et al., 2006; Lipniacki et al., 2004; Nelson et al., 2004, 2005; Sung and Simon, 2004; Werner et al., 2005), and the mitochondrial pathway of apoptosis (Bagci et al., 2006; Rehm et al., 2006). The JNK pathway, whose role is still controversial, as well as the TNFR2 are not considered so far (see Section 2.1).
The TNF signalling model is currently refined and analysed in the light of new biological data. Also, crosstalk phenomena with other signalling pathways such as epidermal growth factor (EGF) and insulin have recently been underlined analysing static models of dynamic time series data (Janes et al., 2005, 2006). Integrating these and possibly additional pathways into a dynamical model will clearly pose work and challenges for years to come.
Integrating different aspects of cellular signalling into mathematical models will allow the evaluation of dynamic cross-talk phenomena and point to roles for features that might not become evident in isolated sub-systems. For example, a physiological role for the dual kinetics of caspase activation described in this study, to include a delay before switching, should be the integration

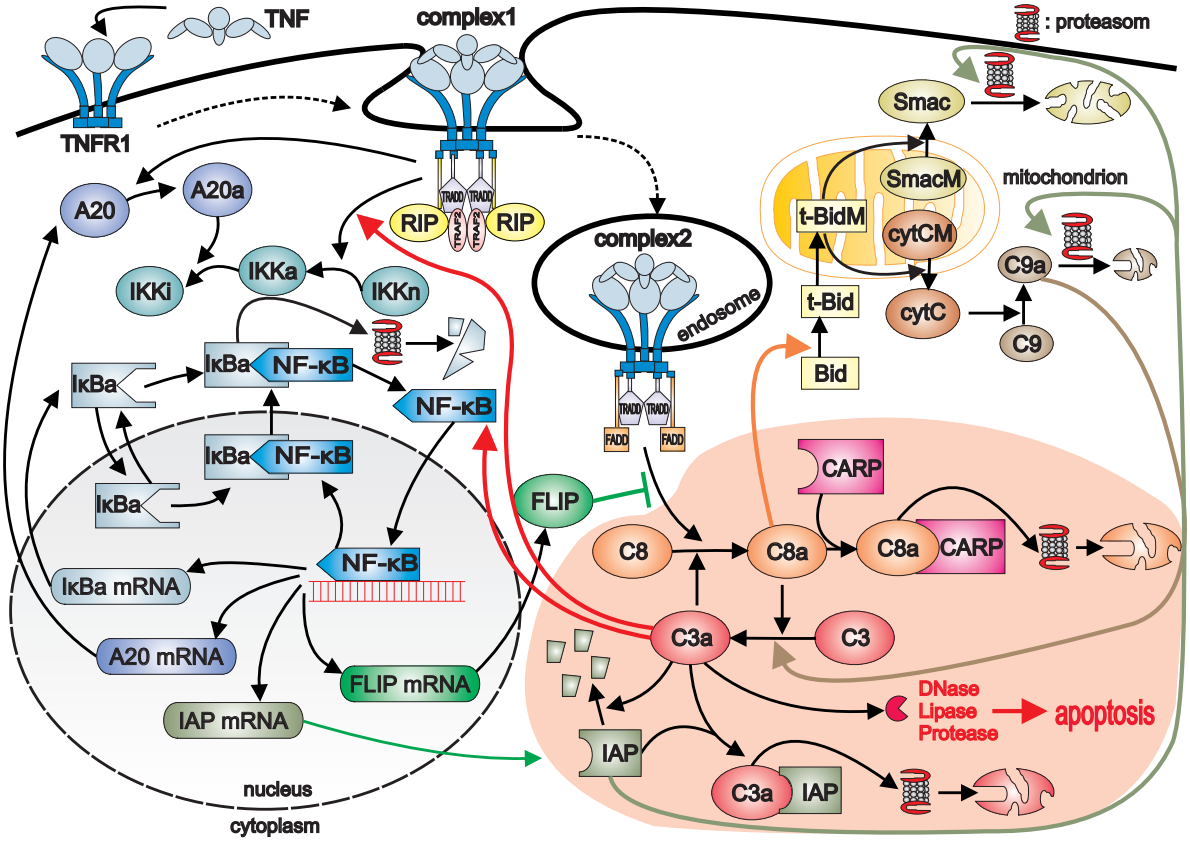

Figure 7.1: TNF signalling pathways. An overview on TNF signalling pathways as currently integrated into a mathematical model.

of different signals. Only if an apoptotic stimulus is really strong, apoptosis should be executed immediately. For weaker signals, the delay allows the cell time to react. If the cellular conditions are favourable and inhibitors can be up-regulated, e.g. by the NFκB pathway, these can influence the life and death decision. Potential influences are already outlined by analyses of the extended model targeted towards this interplay (Section 5.1; Eissing et al., 2006). However, the true dynamic interplay is best investigated in a larger model and likely often more hidden than in the current example (Sen, 2006).

Although larger models can reveal additional layers of communication and interest, it will still remain important to sometimes isolate smaller parts for a more detailed analysis. For example, it was recently shown that the positive feedback between caspases can be augmented by indirect feedback through IAPs in the mitochondrial pathway of apoptosis and thereby possibly contribute to bistability (Legewie et al., 2006). This would neither be easy to spot nor easy to analyse in a complex model containing ten additional pathways.

Sensitivity and stochasticity versus robustness – a physiological performance trade-off?

Apoptosis should be robust to prevent accidental cell death, as we argued in Section 2.2.3. On the one hand, our robustness analysis shows that the extended model is much more robust than the basic model and the region in parameters space allowing for bistability is comparatively large covering at least one decade for most parameters (Section 5.4). On the other hand, our sensitivity analyses indicate that quantitative aspects of the extended model are strongly dependent on the exact parameter values and changes by a factor of two often exert strong effects (Section 5.1).

Correspondingly, stochastic effects in apoptosis are observed experimentally, which according to our investigations presented in Chapter 6 are best explained by distributed parameters to which the model is sensitive. Recently, an important physiological role for such stochastic effects was highlighted (Hawkins et al., 2007; Hodgkin, 2007). The authors indicate that distributed delay times in apoptosis signalling might be an essential mechanism to regulate and fine-tune immune responses. Accordingly, it could be argued that at least some of the sensitivity observed in our model of apoptosis signalling is well reflecting the physiological requirements. The sensitivity analyses also indicate that pathological states can arise if bistability is lost. Therefore, opposing evolutionary constraints could enforce a robustness-performance-fragility trade-off in apoptosis signalling. On the one hand, qualitative aspects, such as bistability, should be as robust as possible to support proper decisions. On the other hand, this is limited because more quantitative aspects, such as delay times and bistable thresholds, should be sensitive to a certain extend. While intrinsic noise is filtered, extrinsic noise could comprise the signal itself and should therefore be efficiently passed. For example, NFκB can up-regulate IAPs (above and Section 5.1), shifting the mean concentration and the concentration distribution of IAPs in a population. The sensitivity towards these molecules then leads to variability in the population including distributed apoptotic thresholds and delay times for the immune system to act on. Thus variability is likely essential for functionality.
The above features are in accordance with the model proposed in this study. While we outlined above that certainly more robust models of apoptosis signalling can be thought of, quantitative experimental data will be needed to indicate how robust apoptosis is *in vivo*. It can be hypothesized that the robustness-performance trade-off proposed for biological systems as such, applies to models thereof – more robust models often consider additional, sometimes redundant, mechanisms, which make them more difficult to analyse and might not allow easy insight into other key features.

Systems science for biology. Reverse engineering of biological complexity is promising to elude the underlying functional principles of biological systems (Csete and Doyle, 2002). However, the theory and computational tools for dynamical systems are not easily able to deal with very large and nonlinear models as often encountered in biology (Kitano, 2002b). Also, the methods and tools available were often developed for technical systems and do not yet take into account the special features and demands of biological systems. Therefore, improvements in the mathematical tools for modelling and analysis are important in general.
Regarding the analysis presented in this thesis, several aspects can be extended. For example, the robustness results could be compared to other bistable signalling pathways. The principal component analysis could be further employed to restrict the parameter space. The quality of the ellipsoid fit could be further investigated by applying more advanced tools from multivariate statistics (Chapter 5). The evaluation of the stochastic influences could be extended to further identify key components, or processes, most strongly contributing the observed stochasticity (Chapter 6). However, one should bear in mind that the potential results will again show a reference parameter dependence and, as outlined above, the model is not yet quantitatively verified or identified.
Additional analyses techniques have been applied to the apoptosis models, as proposed in this thesis, and new tools have been developed and tested at the example. These and additional ideas will be shortly outlined in the following.

Various robustness measures are available as discussed in Section 5.3. Nevertheless, current robustness analyses techniques show certain shortcomings, and improved methods are desirable. Ideally, these methods would allow insight not restricted to certain parameter sets to allow more global considerations. However, local analyses are computationally more efficient. Promising approaches have been made, e.g. motivated by ideas routed in robust control (Kim et al., 2006; Ma and Iglesias, 2002). Furthermore, to date most robustness analyses focus on parametric uncertainties, while often the model structure itself is uncertain as well. Dynamic perturbations as can, for example, be included in a μ-analysis may reveal interesting and relevant new fragilities (Jacobsen and Cedersund, 2005).

A feedback representation and evaluation of biological models inspired by robust control ideas has further enabled robustness measures and can indicate components, which are less relevant for the generation of complex behaviour like bistability (Ma and Iglesias, 2002; Schmidt and Jacobsen, 2004). This knowledge can also be used for systematic model reduction – a challenge outlined by the complexity that is indicated above. Employing this technique can halve the size of the extended model, while preserving qualitative key features as outlined in Section 5.1.3 (Waldherr et al., 2007). Another approach was shortly discussed in Section 4.4 and comprises a projection to a slow manifold as detailed in Bullinger (2005). These results might be extended to allow the preservation of more quantitative features and/or larger reduction.

Chapter 6 introduced a stochastic framework to reconcile single cell and population differences. While a single cell has its unique steady states and can respond very quickly, the behaviour including steady states for different cells of the same type, as present in a population, differs and the response of the population as a whole can be graded rather than switch-like. Employing a new conceptional modelling framework that includes tube like activation and inhibition functions, a single cell model can describe a population and stable steady states can be translated into invariant sets employing a local notion of input to state stability (Chaves et al., 2006, 2008). This modelling framework also bridges a gap between Boolean and differential equation based modelling approaches and presents an interesting idea in the light of the data available. Despite the ever increasing amount of biological data, these are often not standardized, quantitative, or time resolved (enough) as to allow a rigorous identification with techniques available.

While systems science ideas are inspiring new ways of thinking in biology and offer interesting new opportunities for control engineers (Wellstead, 2007), vice versa the challenges encountered in biology can inspire new ideas in systems and control theory (Sontag, 2004). Billions of years of evolution have generated features in living organisms that cannot be met by technology today. Likely this holds true for the underlying mechanisms of signal processing and control, which will be best revealed in a reverse engineering manner.

Concluding remarks. Getting back to the first lines of this thesis where Schrödinger asked if super-physical laws will be needed to describe biology. A cell is a crowded environment where many thousand compounds and reactions happen simultaneously on a pico-litre scale. A human body consist of about 10^{14} such cells. The involved scales and the inherent complexity likely do not just follow one super-physical law – apart from evolution maybe. However, inherent properties, design principles and motifs of biological systems are emerging by analysing mathematical

models. This will not only help future modelling approaches but is strongly contributing to a true understanding of the biochemistry of life.

Bibliography

Acar, M., A. Becskei, and A. van Oudenaarden (2005). Enhancement of cellular memory by reducing stochastic transitions. *Nature* **435**(7039): 228–232.

Alberts, B., A. Johnson, J. Lewis, M. Raff, K. Roberts, and P. Walter (2002). *Molecular Biology of the Cell*. 4th edn. Garland Science, New York and London. ISBN: 0815340729.

Aldridge, B. B., G. Haller, P. K. Sorger, and D. A. Lauffenburger (2006). Direct Lyapunov exponent analysis enables parametric study of transient signalling governing cell behaviour. *IEE Syst. Biol.* **153**(6): 425–432.

Angeli, D. (2006). New analysis technique for multistability detection. *IEE Syst. Biol.* **153**(2): 61–69.

Angeli, D., J. E. Ferrell, Jr., and E. D. Sontag (2004). Detection of multistability, bifurcations, and hysteresis in a large class of biological positive-feedback systems. *Proc. Natl. Acad. Sci. U. S. A.* **101**(7): 1822–1827.

Aplan, P. D. (2006). Causes of oncogenic chromosomal translocation. *Trends Genet.* **22**(1): 46–55.

Ashkenazi, A. (2002). Targeting death and decoy receptors of the tumour-necrosis factor superfamily. *Nat. Rev. Cancer* **2**(6): 420–430.

Bagci, E. Z., Y. Vodovotz, T. R. Billiar, G. B. Ermentrout, and I. Bahar (2006). Bistability in apoptosis: Roles of Bax, Bcl-2 and mitochondrial permeability transition pores. *Biophys. J.* **90**: 1546–1559.

Bard, Y. (1973). *Nonlinear Parameter Estimation*. Academic Press, New York, NY. ISBN: 0120782502.

Barkai, N. and S. Leibler (1997). Robustness in simple biochemical networks. *Nature* **387**(6636): 913–917.

Barken, D., C. J. Wang, J. Kearns, R. Cheong, A. Hoffmann, and A. Levchenko (2005). Comment on "Oscillations in NF-kappaB signaling control the dynamics of gene expression". *Science* **308**(5718): 52a.

Beltrami, E. and J. Jesty (1995). Mathematical analysis of activation thresholds in enzyme-catalyzed positive feedbacks: application to the feedbacks of blood coagulation. *Proc. Natl. Acad. Sci. U. S. A.* **92**(19): 8744–8748.

Bentele, M., I. Lavrik, M. Ulrich, S. Stosser, D. W. Heermann, H. Kalthoff, P. H. Krammer, and R. Eils (2004). Mathematical modeling reveals threshold mechanism in CD95-induced apoptosis. *J. Cell Biol.* **166**(6): 839–851.

Berg, J. M., J. L. Tymoczko, and L. Stryer (2007). *Biochemistry*. 6th edn. W. H. Freeman and Co., New York. ISBN: 0716787245.

Bertalanffy, L., von (1969). *General System Theory, Foundations, Development, Applications*. George Braziller, New York. ISBN: 0807604534.

Bhalla, U. S. and R. Iyengar (1999). Emergent properties of networks of biological signaling pathways. *Science* **283**(5400): 381–387.

Bhalla, U. S. and R. Iyengar (2001). Robustness of the bistable behavior of a biological signaling feedback loop. *Chaos* **11**(1): 221–226.

Bhalla, U. S., P. T. Ram, and R. Iyengar (2002). MAP kinase phosphatase as a locus of flexibility in a mitogen-activated protein kinase signaling network. *Science* **297**(5583): 1018–1023.

Blüthgen, N. and H. Herzel (2001). MAP-Kinase-Cascade: Switch, Amplier or Feedback Controller? In: R. Gauges, C. van Gend, and U. Kummer (eds.), *Proceedings of the 2nd Workshop on Computation of Biochemical Pathways and Genetic Networks*, Logos-Verlag, Berlin, pp. 55–62.

Blüthgen, N. and H. Herzel (2003). How robust are switches in intracellular signaling cascades? *J. Theor. Biol.* **225**(3): 293–300.

Blüthgen, N., F. J. Bruggeman, S. Legewie, H. Herzel, H. V. Westerhoff, and B. N. Kholodenko (2006). Effects of sequestration on signal transduction cascades. *FEBS J.* **273**(5): 895–906.

Brandman, O., J. E. Ferrell, R. Li, and T. Meyer (2005). Interlinked fast and slow positive feedback loops drive reliable cell decisions. *Science* **310**(5747): 496–498.

Breckenridge, D. G., M. Nguyen, S. Kuppig, M. Reth, and G. C. Shore (2002). The procaspase-8 isoform, procaspase-8L, recruited to the BAP31 complex at the endoplasmic reticulum. *Proc. Natl. Acad. Sci. U. S. A.* **99**(7): 4331–4336.

Bullinger, E. (2005). System analysis of a programmed cell death model. In: *Proceedings of the 44th IEEE Conference on Decison and Control (CDC)*, Seville, Spain, pp. 7994–7999.

Bureeva, S., J. Andia-Pravdivy, and A. Kaplun (2005). Drug design using the example of the complement system inhibitors' development. *Drug Discov. Today* **10**(22): 1535–1542.

Carlson, J. M. and J. Doyle (2000). Highly optimized tolerance: robustness and design in complex systems. *Phys. Rev. Lett.* **84**(11): 2529–2532.

Carlson, J. M. and J. Doyle (2002). Complexity and robustness. *Proc. Natl. Acad. Sci. U. S. A.* **99 Suppl. 1**: 2538–2545.

Carotenuto, L., V. Pace, D. Bellizzi, and G. De Benedictis (2007a). Dynamical analysis of the programmed cell death pathway. In: *Proceedings of the European Control Conference (ECC)*, Kos, Greece, pp. 3747–3754.

Carotenuto, L., V. Pace, D. Bellizzi, and G. De Benedictis (2007b). Equilibrium, stability and dynamical response in a model of the extrinsic apoptosis pathway. *J. Biol. Syst.* **15**(3): 261–285.

Carroll, M. C. (2004). The complement system in regulation of adaptive immunity. *Nat. Immunol.* **5**(10): 981–986.

Chaves, M., R. Albert, and E. D. Sontag (2005). Robustness and fragility of Boolean models for genetic regulatory networks. *J. Theor. Biol.* **235**(3): 431–449.

Chaves, M., T. Eissing, and F. Allgöwer (2006). Identifying mechanisms for bistability in an apoptosis network. In: *Journée thematique "Réseaux d'Interactions: Analyse, Modélisation et Simulation" (RIAMS)*, Integrative Post-Genomics, Lyon, France.

Chaves, M., T. Eissing, and F. Allgöwer (2008). Bistable biological systems: a characterization through local compact input-to-state stability. *IEEE Transactions on Automatic Control* **53**(1): 87–100.

Chen, B. S., Y. C. Wang, W. S. Wu, and W. H. Li (2005). A new measure of the robustness of biochemical networks. *Bioinformatics* **21**(11): 2698–2705.

Chen, C., J. Cui, H. Lu, R. Wang, S. Zhang, and P. Shen (2007a). Modeling of the role of a Bax-activation switch in the mitochondrial apoptosis decision. *Biophys. J.* **92**(12): 4304–4315.

Chen, C., J. Cui, W. Zhang, and P. Shen (2007b). Robustness analysis identifies the plausible model of the Bcl-2 apoptotic switch. *FEBS Lett.* **581**(26): 5143–5150.

Chen, G. and D. V. Goeddel (2002). TNF-R1 signaling: a beautiful pathway. *Science* **296**(5573): 1634–1635.

Cherry, J. L. and F. R. Adler (2000). How to make a biological switch. *J. Theor. Biol.* **203**(2): 117–133.

Choi, H.-S., S. Han, H. Yokota, and K.-H. Cho (2007). Coupled positive feedbacks provoke slow induction plus fast switching in apoptosis. *FEBS Lett.* **581**(14): 2684–2690.

Chong, L. and L. B. Ray (2002). Whole-istic Biology. *Science* **295**(5560): 1661.

Cimatoribus, C., T. Eissing, N. Elvassore, F. Allgöwer, and E. Bullinger (2005). Model discrimination tools in apoptosis. In: *Proceedings of the 1st International Conference Foundations of Systems Biology in Engineering (FOSBE)*, Santa Barbara, CA, USA, pp. 197–200.

Cinquin, O. and J. Demongeot (2002). Positive and negative feedback: striking a balance between necessary antagonists. *J. Theor. Biol.* **216**(2): 229–241.

Conzelmann, H. (2003). Modeling and analysis of the EGF signaling pathway and caspase activation. Diplomarbeit, Institute for System Dynamics and Control Engineering, University of Stuttgart.

Cornish-Bowden, A. (2006). Putting the systems back into systems biology. *Perspect. Biol. Med.* **49**(4): 475–489.

Cowling, V. and J. Downward (2002). Caspase-6 is the direct activator of caspase-8 in the cytochrome c-induced apoptosis pathway: absolute requirement for removal of caspase-6 prodomain. *Cell Death Differ.* **9**(10): 1046–1056.

Craciun, G., Y. Tang, and M. Feinberg (2006). Understanding bistability in complex enzyme-driven reaction networks. *Proc. Natl. Acad. Sci. U. S. A.* **103**(23): 8697–8702.

Csete, M. E. and J. C. Doyle (2002). Reverse engineering of biological complexity. *Science* **295**(5560): 1664–1669.

Dahlbäck, B. (2000). Blood coagulation. *Lancet* **355**(9215): 1627–1632.

Danial, N. N. and S. J. Korsmeyer (2004). Cell death: critical control points. *Cell* **116**(2): 205–219.

Dash, C., A. Kulkarni, B. Dunn, and M. Rao (2003). Aspartic peptidase inhibitors: implications in drug development. *Crit. Rev. Biochem. Mol. Biol.* **38**(2): 89–119.

De Jong, H. (2002). Modeling and simulation of genetic regulatory systems: a literature review. *J. Comput. Biol.* **9**(1): 67–103.

Debatin, K.-M. and P. H. Krammer (2004). Death receptors in chemotherapy and cancer. *Oncogene* **23**(16): 2950–2966.

Deveraux, Q. L., R. Takahashi, G. S. Salvesen, and J. C. Reed (1997). X-linked IAP is a direct inhibitor of cell-death proteases. *Nature* **388**(6639): 300–304.

Deveraux, Q. L., E. Leo, H. R. Stennicke, K. Welsh, G. S. Salvesen, and J. C. Reed (1999). Cleavage of human inhibitor of apoptosis protein XIAP results in fragments with distinct specificities for caspases. *EMBO J.* **18**(19): 5242–5251.

Devi, G. R. (2004). XIAP as target for therapeutic apoptosis in prostate cancer. *Drug News Perspect.* **17**(2): 127–134.

Ditzel, M. and P. Meier (2002). IAP degradation: decisive blow or altruistic sacrifice? *Trends Cell Biol.* **12**(10): 449–452.

Donepudi, M., A. Mac Sweeney, C. Briand, and M. G. Grutter (2003). Insights into the regulatory mechanism for caspase-8 activation. *Mol. Cell* **11**(2): 543–549.

Eckelman, B. P., G. S. Salvesen, and F. L. Scott (2006). Human inhibitor of apoptosis proteins: why XIAP is the black sheep of the family. *EMBO Rep.* **7**(10): 988–994.

Eissing, T. (2002). Biological advancement and systems analysis of a mathematical TNF signaling network model. Diplomarbeit, Institute of Cell Biology and Immunology, University of Stuttgart.

Eissing, T., H. Conzelmann, E. D. Gilles, F. Allgöwer, E. Bullinger, and P. Scheurich (2004). Bistability analyses of a caspase activation model for receptor-induced apoptosis. *J. Biol. Chem.* **279**(35): 36892–36897.

Eissing, T., F. Allgöwer, and E. Bullinger (2005a). Robustness properties of apoptosis models with respect to parameter variations and stochastic influences. *IEE Syst. Biol.* **152**(4): 221–228.

Eissing, T., P. Scheurich, and F. Allgöwer (2005b). To Be or Not to Be - Mathematical Systems Theory to Analyze Biological Signal Processing. *Themenheft Forschung, Universität Stuttgart* **1**: 32–40.

Eissing, T., S. Waldherr, C. Gondro, E. Bullinger, O. Sawodny, F. Allgöwer, P. Scheurich, and T. Sauter (2006). Sensitivity analysis of programmed cell death and implications for crosstalk phenomena during Tumor Necrosis Factor stimulation. In: *Proceedings of the IEEE International Conference on Control Applications (CCA)*, Munich, Germany, pp. 1746–1752.

Eissing, T., S. Waldherr, and F. Allgöwer (2007a). *Biology and Control Theory: Current Challenges*, chap. Modelling and Analysis of Cell Death Signalling, pp. 161–180. Lecture Notes in Control and Information Sciences, 357 edn. Springer-Verlag Berlin Heidelberg.

Eissing, T., S. Waldherr, F. Allgöwer, P. Scheurich, and E. Bullinger (2007b). Response to Bistability in Apoptosis: Roles of Bax, Bcl-2, and Mitochondrial Permeability Transition Pores. *Biophys. J.* **92**(9): 3332–3334.

Eissing, T., S. Waldherr, F. Allgöwer, P. Scheurich, and E. Bullinger (2007c). Steady state and (bi-) stability evaluation of simple protease signalling networks. *BioSystems* **90**(3): 591–601.

Ekert, P. G., J. Silke, and D. L. Vaux (1999). Caspase inhibitors. *Cell Death Differ.* **6**(11): 1081–1086.

El-Samad, H., H. Kurata, J. C. Doyle, C. A. Gross, and M. Khammash (2005). Surviving heat shock: control strategies for robustness and performance. *Proc. Natl. Acad. Sci. U. S. A.* **102**(8): 2736–2741.

Elowitz, M. B., A. J. Levine, E. D. Siggia, and P. S. Swain (2002). Stochastic gene expression in a single cell. *Science* **297**(5584): 1183–1186.

Ermentrout, B. (2002). *Simulating, Analyzing, and Animating Dynamical Systems. A Guide to XPPAUT for Researchers and Students*. SIAM, Philadelphia, PA. ISBN-13: 978-0898715064.

Fall, C. P., E. S. Marland, J. M. Wagner, and J. J. Tyson (2002). *Computational Cell Biology*, vol. 20 of *Interdisciplinary Applied Mathematics*. Springer-Verlag, New York, NY.

Ferrell, J. E., Jr. (1996). Tripping the switch fantastic: how a protein kinase cascade can convert graded inputs into switch-like outputs. *Trends Biochem. Sci.* **21**(12): 460–466.

Ferrell, J. E., Jr. (1997). How responses get more switch-like as you move down a protein kinase cascade. *Trends Biochem. Sci.* **22**(8): 288–289.

Ferrell, J. E., Jr. (2002). Self-perpetuating states in signal transduction: positive feedback, double-negative feedback and bistability. *Curr. Opin. Cell Biol.* **14**(2): 140–148.

Ferrell, J. E., Jr. and E. M. Machleder (1998). The biochemical basis of an all-or-none cell fate switch in Xenopus oocytes. *Science* **280**(5365): 895–898.

Ferrell, J. E., Jr. and W. Xiong (2001). Bistability in cell signaling: How to make continuous processes discontinuous, and reversible processes irreversible. *Chaos* **11**(1): 227–236.

Fischer, U., R. U. Jänicke, and K. Schulze-Osthoff (2003). Many cuts to ruin: a comprehensive update of caspase substrates. *Cell Death Differ.* **10**(1): 76–100.

Fladmark, K. E., O. T. Brustugun, R. Hovland, R. Boe, B. T. Gjertsen, B. Zhivotovsky, and S. O. Doskeland (1999). Ultrarapid caspase-3 dependent apoptosis induction by serine/threonine phosphatase inhibitors. *Cell Death Differ.* **6**(11): 1099–1108.

Fotin-Mleczek, M., F. Henkler, D. Samel, M. Reichwein, A. Hausser, I. Parmryd, P. Scheurich, J. A. Schmid, and H. Wajant (2002). Apoptotic crosstalk of TNF receptors: TNF-R2-induces depletion of TRAF2 and IAP proteins and accelerates TNF-R1-dependent activation of caspase-8. *J. Cell Sci.* **115**(13): 2757–2770.

Fussenegger, M., J. E. Bailey, and J. Varner (2000). A mathematical model of caspase function in apoptosis. *Nat. Biotechnol.* **18**(7): 768–774.

Gadkar, K. G., R. Gunawan, and F. J. Doyle, 3rd (2005a). Iterative approach to model identification of biological networks. *BMC Bioinformatics* **6**: 155.

Gadkar, K. G., J. Varner, and F. J. Doyle, 3rd (2005b). Model identification of signal transduction networks from data using a state regulator problem. *IEE Syst. Biol.* **2**(1): 17–30.

Garcia-Calvo, M., E. P. Peterson, D. M. Rasper, J. P. Vaillancourt, R. Zamboni, D. W. Nicholson, and N. A. Thornberry (1999). Purification and catalytic properties of human caspase family members. *Cell Death Differ.* **6**(4): 362–369.

Gibson, M. A. and J. Bruck (2000). Efficient exact stochastic simulation of chemical systems with many species and many channels. *J. Phys. Chem.* **104**(9): 1876–1889.

Gillespie, D. T. (1975). Exact Method for Numerically Simulating Stochastic Coalescence Process in a Cloud. *J. Atmos. Sci.* **32**(10): 1977–1989.

Gillespie, D. T. (1976). General Method for Numerically Simulating Stochastic Time Evolution of Coupled Chemical-Reactions. *J. Comput. Phys.* **22**(4): 403–434.

Goldbeter, A. and D. E. Koshland (1981). An amplified sensitivity arising from covalent modification in biological systems. *Proc. Natl. Acad. Sci. U. S. A.* **78**(11): 6840–6844.

Goldbeter, A. and D. E. Koshland (1984). Ultrasensitivity in biochemical systems controlled by covalent modification. Interplay between zero-order and multistep effects. *J. Biol. Chem.* **259**(23): 14441–14447.

Goldstein, J. C., N. J. Waterhouse, P. Juin, G. I. Evan, and D. R. Green (2000). The coordinate release of cytochrome c during apoptosis is rapid, complete and kinetically invariant. *Nat. Cell Biol.* **2**(3): 156–162.

Grabowskal, U., T. J. Chambers, and M. Shiroo (2005). Recent developments in cathepsin K inhibitor design. *Curr. Opin. Drug. Discov. Devel.* **8**(5): 619–630.

Grell, M., G. Zimmermann, D. Hulser, K. Pfizenmaier, and P. Scheurich (1994). TNF receptors TR60 and TR80 can mediate apoptosis via induction of distinct signal pathways. *J. Immunol.* **153**(5): 1963–1972.

Grell, M., E. Douni, H. Wajant, M. Lohden, M. Clauss, B. Maxeiner, S. Georgopoulos, W. Lesslauer, G. Kollias, K. Pfizenmaier, and P. Scheurich (1995). The transmembrane form of tumor necrosis factor is the prime activating ligand of the 80 kDa tumor necrosis factor receptor. *Cell* **83**(5): 793–802.

Grell, M., H. Wajant, G. Zimmermann, and P. Scheurich (1998). The type 1 receptor (CD120a) is the high-affinity receptor for soluble tumor necrosis factor. *Proc. Natl. Acad. Sci. U. S. A.* **95**(2): 570–575.

Grell, M., G. Zimmermann, E. Gottfried, C. M. Chen, U. Grunwald, D. C. Huang, Y. H. Wu Lee, H. Durkop, H. Engelmann, P. Scheurich, H. Wajant, and A. Strasser (1999). Induction of cell death by tumour necrosis factor (TNF) receptor 2, CD40 and CD30: a role for TNF-R1 activation by endogenous membrane- anchored TNF. *EMBO J.* **18**(11): 3034–3043.

Guo, C. and H. Levine (1999). A thermodynamic model for receptor clustering. *Biophys. J.* **77**(5): 2358–2365.

Hanahan, D. and R. A. Weinberg (2000). The hallmarks of cancer. *Cell* **100**(1): 57–70.

Harlin, H., S. B. Reffey, C. S. Duckett, T. Lindsten, and C. B. Thompson (2001). Characterization of XIAP-deficient mice. *Mol. Cell. Biol.* **21**(10): 3604–3608.

Hartwell, L. (1997). Theoretical biology. A robust view of biochemical pathways. *Nature* **387**(6636): 855–857.

Hartwell, L. H., J. J. Hopfield, S. Leibler, and A. W. Murray (1999). From molecular to modular cell biology. *Nature* **402**(6761 Suppl): C47–52.

Hawkins, E. D., M. L. Turner, M. R. Dowling, C. van Gend, and P. D. Hodgkin (2007). A model of immune regulation as a consequence of randomized lymphocyte division and death times. *Proc. Natl. Acad. Sci. U. S. A.* **104**(12): 5032–5037.

Heemels, M. T., R. Dhand, and L. Allen (2000). Apoptosis. *Nature* **407**(6805): 769.

Heinrich, R. and T. A. Rapoport (1974). A linear steady-state treatment of enzymatic chains. General properties, control and effector strength. *Eur. J. Biochem.* **42**(1): 89–95.

Heinrich, R., B. G. Neel, and T. A. Rapoport (2002). Mathematical models of protein kinase signal transduction. *Mol. Cell* **9**(5): 957–970.

Hengartner, M. O. (2000). The biochemistry of apoptosis. *Nature* **407**(6805): 770–776.

Hentze, H., I. Schmitz, M. Latta, A. Krueger, P. H. Krammer, and A. Wendel (2002). Glutathione Dependence of Caspase-8 Activation at the Death-inducing Signaling Complex. *J. Biol. Chem.* **277**(7): 5588–5595.

Hodgkin, A. L. and A. F. Huxley (1952). A quantitative description of membrane current and its application to conduction and excitation in nerve. *J. Physiol.* **117**(4): 500–544.

Hodgkin, P. D. (2007). A probabilistic view of immunology: Drawing parallels with physics. *Immunol. Cell Biol.* In press, doi: 10.1038/sj.icb.7100061.

Hoffmann, A., A. Levchenko, M. L. Scott, and D. Baltimore (2002). The IkappaB-NF-kappaB signaling module: temporal control and selective gene activation. *Science* **298**(5596): 1241–1245.

Hornberg, J. J., B. Binder, F. J. Bruggeman, B. Schoeberl, R. Heinrich, and H. V. Westerhoff (2005a). Control of MAPK signalling: from complexity to what really matters. *Oncogene* **24**(36): 5533–5542.

Hornberg, J. J., F. J. Bruggeman, B. Binder, C. R. Geest, A. J. M. B. de Vaate, J. Lankelma, R. Heinrich, and H. V. Westerhoff (2005b). Principles behind the multifarious control of signal transduction. ERK phosphorylation and kinase/phosphatase control. *FEBS J.* **272**(1): 244–258.

Hsu, H., J. Xiong, and D. V. Goeddel (1995). The TNF receptor 1-associated protein TRADD signals cell death and NF- kappa B activation. *Cell* **81**(4): 495–504.

Huang, C. Y. and J. E. Ferrell, Jr. (1996). Ultrasensitivity in the mitogen-activated protein kinase cascade. *Proc. Natl. Acad. Sci. U. S. A.* **93**(19): 10078–10083.

Huber, H. J., M. Rehm, M. Plchut, H. Düssmann, and J. H. M. Prehn (2007). APOPTO-CELL–a simulation tool and interactive database for analyzing cellular susceptibility to apoptosis. *Bioinformatics* **23**(5): 648–650.

Ingalls, B. P. (2004). Autonomously oscillating biochemical systems: parametric sensitivity of extrema and period. *IEE Syst. Biol.* **1**(1): 62–70.

Ingolia, N. T. and A. W. Murray (2002). Signal transduction. History matters. *Science* **297**(5583): 948–949.

Jacobsen, E. and G. Cedersund (2005). On Parametric Sensitivity and Structural Robustness of Cellular Functions – the Oscillatory Metabolism of Activated Neutrophils. In: *Proceedings of*

the 44th IEEE Conference on Decision and Control (CDC) and European Control Conference (ECC), Seville, Spain, pp. 3681– 3686.

Janes, K. A., J. G. Albeck, S. Gaudet, P. K. Sorger, D. A. Lauffenburger, and M. B. Yaffe (2005). A systems model of signaling identifies a molecular basis set for cytokine-induced apoptosis. *Science* **310**(5754): 1646–1653.

Janes, K. A., S. Gaudet, J. G. Albeck, U. B. Nielsen, D. A. Lauffenburger, and P. K. Sorger (2006). The response of human epithelial cells to TNF involves an inducible autocrine cascade. *Cell* **124**(6): 1225–1239.

Janeway, C. A., P. Travers, M. Walport, and S. M. (2004). *Immunobiology: the immune system in helth and disease*. 6th edn. Garland Science, New York and London. ISBN: 0815341016.

Jesty, J., E. Beltrami, and G. Willems (1993). Mathematical analysis of a proteolytic positive-feedback loop: dependence of lag time and enzyme yields on the initial conditions and kinetic parameters. *Biochemistry* **32**(24): 6266–6274.

Jesty, J., J. Rodriguez, and E. Beltrami (2005). Demonstration of a threshold response in a proteolytic feedback system: control of the autoactivation of factor XII. *Pathophysiol. Haemost. Thromb.* **34**(2-3): 71–79.

Jiang, X. and X. Wang (2004). Cytochrome C-mediated apoptosis. *Annu. Rev. Biochem.* **73**: 87–106.

Johnson, R. A. and D. W. Wichern (1992). *Applied Multivariate Statistical Analysis*. Prentice-Hall, Englewood Cliffs, NJ.

Kacser, H. and J. A. Burns (1973). The control of flux. *Symp. Soc. Exp. Biol.* **27**: 65–104.

Kaiser, H. (1960). The Application of Electronic Computers to Factor Analysis. *Educ. Psychol. Meas.* **20**(1): 141–151.

Keener, J. and J. Sneyd (1998). *Mathematical Physiology*. Springer-Verlag New York, Inc. ISBN: 0387983813.

Khalil, H. K. (2002). *Nonlinear Systems*. 3rd edn. Prentice Hall, Upper Saddle River, NJ. ISBN: 0130673897.

Kim, J., I. Postlethwaite, L. Ma, and P. A. Iglesias (2006). Robustness analysis of biochemical network models. *IEE Syst. Biol.* **153**(3): 96–104.

Kitano, H. (2002a). Computational systems biology. *Nature* **420**(6912): 206–210.

Kitano, H. (2002b). Systems biology: a brief overview. *Science* **295**(5560): 1662–1664.

Klipp, E., R. Herwig, A. Kowald, C. Wierling, and H. Lehrach (2005). *Systems Biology in Practice. Concepts, Implementation and Application*. Wiley-VCH, Weinheim. ISBN-13: 978-3527310784.

Kollmann, M., L. Løvdok, K. Bartholomé, J. Timmer, and V. Sourjik (2005). Design principles of a bacterial signalling network. *Nature* **438**(7067): 504–507.

Koshland, D. E. (1998). The era of pathway quantification. *Science* **280**(5365): 852–853.

Koshland, D. E., A. Goldbeter, and J. B. Stock (1982). Amplification and adaptation in regulatory and sensory systems. *Science* **217**(4556): 220–225.

Krippner-Heidenreich, A., F. Tubing, S. Bryde, S. Willi, G. Zimmermann, and P. Scheurich (2002). Control of receptor-induced signaling complex formation by the kinetics of ligand/receptor interaction. *J. Biol. Chem.* **277**(46): 44155–44163.

Krishna, S., M. H. Jensen, and K. Sneppen (2006). Minimal model of spiky oscillations in NF-kappaB signaling. *Proc. Natl. Acad. Sci. U. S. A.* **103**(29): 10840–10845.

Kurata, H., H. El-Samad, R. Iwasaki, H. Ohtake, J. C. Doyle, I. Grigorova, C. A. Gross, and M. Khammash (2006). Module-based analysis of robustness tradeoffs in the heat shock response system. *PLoS Comput. Biol.* **2**(7): e59.

Kuznetsov, Y. A. (1995). *Elements of Applied Bifurcation Theory*. Springer-Verlag.

Lafortune, E. (1996). Mathematical Models and Monte Carlo Algorithms for Physically Based Rendering. PhD thesis, Katholieke Universiteit Leuven.

Lai, R. and T. L. Jackson (2004). A mathematical model of receptor-mediated apoptosis: Dying to know why FASL is a trimer. *Math. Biosci. Eng.* **1**(2): 325–338.

Lamkanfi, M., N. Festjens, W. Declercq, T. V. Berghe, and P. Vandenabeele (2007). Caspases in cell survival, proliferation and differentiation. *Cell Death Differ.* **14**(1): 44–55.

Lauffenburger, D. A. (2000). Cell signaling pathways as control modules: complexity for simplicity? *Proc. Natl. Acad. Sci. U. S. A.* **97**(10): 5031–5033.

Lavrik, I., A. Krueger, I. Schmitz, S. Baumann, H. Weyd, P. H. Krammer, and S. Kirchhoff (2003). The active caspase-8 heterotetramer is formed at the CD95 DISC. *Cell Death Differ.* **10**(1): 144–145.

Lavrik, I. N., A. Golks, D. Riess, M. Bentele, R. Eils, and P. H. Krammer (2007). Analysis of CD95 threshold signaling: Triggering of CD95 (Fas/APO-1) at low concentrations primarily results in survival signaling. *J. Biol. Chem.* **282**(18): 13664–13671.

Lazebnik, Y. (2002). Can a biologist fix a radio?–Or, what I learned while studying apoptosis. *Cancer Cell* **2**(3): 179–182.

Legewie, S., N. Blüthgen, and H. Herzel (2005). Quantitative analysis of ultrasensitive responses. *FEBS J.* **272**(16): 4071–4079.

Legewie, S., N. Blüthgen, and H. Herzel (2006). Mathematical Modeling Identifies Inhibitors of Apoptosis as Mediators of Positive Feedback and Bistability. *PLoS Comput. Biol.* **2**(9): e120.

Legewie, S., B. Schoeberl, N. Blüthgen, and H. Herzel (2007). Competing docking interactions can bring about bistability in the MAPK cascade. *Biophys. J.* **93**(7): 2279–2288.

Li, M., T. Song, Z.-F. Yin, and Y.-Q. Na (2007). XIAP as a prognostic marker of early recurrence of nonmuscular invasive bladder cancer. *Chin. Med. J. (Engl.)* **120**(6): 469–473.

Lipniacki, T., P. Paszek, A. R. Brasier, B. Luxon, and M. Kimmel (2004). Mathematical model of NF-kappaB regulatory module. *J. Theor. Biol.* **228**(2): 195–215.

Lisman, J. E. (1985). A mechanism for memory storage insensitive to molecular turnover: a bistable autophosphorylating kinase. *Proc. Natl. Acad. Sci. U. S. A.* **82**(9): 3055–3057.

Luo, K. Q., V. C. Yu, Y. Pu, and D. C. Chang (2003). Measuring dynamics of caspase-8 activation in a single living HeLa cell during TNFalpha-induced apoptosis. *Biochem. Biophys. Res. Commun.* **304**(2): 217–222.

Ma, L. and P. A. Iglesias (2002). Quantifying robustness of biochemical network models. *BMC Bioinformatics* **3**: 38.

Mangan, S. and U. Alon (2003). Structure and function of the feed-forward loop network motif. *Proc. Natl. Acad. Sci. U. S. A.* **100**(21): 11980–11985.

Manoharan, A., T. Kiefer, S. Leist, K. Schrader, C. Urban, D. Walter, U. Maurer, and C. Borner (2006). Identification of a 'genuine' mammalian homolog of nematodal CED-4: is the hunt over or do we need better guns? *Cell Death Differ.* **13**(8): 1310–1317.

Markevich, N. I., J. B. Hoek, and B. N. Kholodenko (2004). Signaling switches and bistability arising from multisite phosphorylation in protein kinase cascades. *J. Cell Biol.* **164**(3): 353–359.

Mason, O. and M. Verwoerd (2007). Graph theory and networks in Biology. *IET Syst. Biol.* **1**(2): 89–119.

McDonald, E. R., 3rd and W. S. El-Deiry (2004). Suppression of caspase-8- and -10-associated RING proteins results in sensitization to death ligands and inhibition of tumor cell growth. *Proc. Natl. Acad. Sci. U. S. A.* **101**(16): 6170–6175.

Mesarović, M. D. (ed.) (1968). *Systems Theory and Biology: Proceedings of the 3rd Systems Symposium, Cleveland, Ohio, Oct. 1966.* Springer-Verlag, New York.

Micheau, O. and J. Tschopp (2003). Induction of TNF receptor I-mediated apoptosis via two sequential signaling complexes. *Cell* **114**(2): 181–190.

Milo, R., S. Shen-Orr, S. Itzkovitz, N. Kashtan, D. Chklovskii, and U. Alon (2002). Network motifs: simple building blocks of complex networks. *Science* **298**(5594): 824–827.

Morohashi, M., A. E. Winn, M. T. Borisuk, H. Bolouri, J. Doyle, and H. Kitano (2002). Robustness as a measure of plausibility in models of biochemical networks. *J. Theor. Biol.* **216**(1): 19–30.

Nachmias, B., Y. Ashhab, and D. Ben-Yehuda (2004). The inhibitor of apoptosis protein family (IAPs): an emerging therapeutic target in cancer. *Semin. Cancer Biol.* **14**(4): 231–243.

Nakagawa, Y., M. Hasegawa, M. Kurata, K. Yamamoto, S. Abe, M. Inoue, T. Takemura, K. Hirokawa, K. Suzuki, and M. Kitagawa (2005). Expression of IAP-family proteins in adult acute mixed lineage leukemia (AMLL). *Am. J. Hematol.* **78**(3): 173–180.

Nakagawa, Y., S. Abe, M. Kurata, M. Hasegawa, K. Yamamoto, M. Inoue, T. Takemura, K. Suzuki, and M. Kitagawa (2006). IAP family protein expression correlates with poor outcome of multiple myeloma patients in association with chemotherapy-induced overexpression of multidrug resistance genes. *Am. J. Hematol.* **81**(11): 824–831.

Nelson, D. E., A. E. Ihekwaba, et al. (2004). Oscillations in NF-kappaB signaling control the dynamics of gene expression. *Science* **306**(5696): 704–708.

Nelson, D. E., J. R. Johnson, G. Nelson, V. See, C. A. Horton, D. G. Spiller, D. B. Kell, and M. R. White (2005). Response to Comments on "Oscillations in NF-kappaB signaling control the dynamics of gene expression". *Science* **308**(5718): 52b.

Newton, K. and A. Strasser (2003). Caspases signal not only apoptosis but also antigen-induced activation in cells of the immune system. *Genes Dev.* **17**(7): 819–825.

Nordling, T. E. M., N. Hiroi, A. Funahashi, and H. Kitano (2007). Deduction of intracellular sub-systems from a topological description of the network. *Mol. Biosyst.* **3**(8): 523–529.

Novick, A. and M. Weiner (1957). Enzyme Induction as an All-or-None Phenomenon. *Proc. Natl. Acad. Sci. U. S. A.* **43**(7): 553–566.

Oltvai, Z. N. and A. L. Barabasi (2002). Systems biology. Life's complexity pyramid. *Science* **298**(5594): 763–764.

Oppenheim, A. B., O. Kobiler, J. Stavans, D. L. Court, and S. Adhya (2005). Switches in bacteriophage lambda development. *Annu. Rev. Genet.* **39**: 409–429.

Ortega, F., L. Acerenza, H. V. Westerhoff, F. Mas, and M. Cascante (2002). Product dependence and bifunctionality compromise the ultrasensitivity of signal transduction cascades. *Proc. Natl. Acad. Sci. U. S. A.* **99**(3): 1170–1175.

Ortega, F., J. L. Garcés, F. Mas, B. N. Kholodenko, and M. Cascante (2006). Bistability from double phosphorylation in signal transduction. Kinetic and structural requirements. *FEBS J.* **273**(17): 3915–3926.

Oudejans, J. J., A. Harijadi, S. A. G. M. Cillessen, P. Busson, I. B. Tan, D. F. Dukers, W. Vos, B. Hariwiyanto, J. Middeldorp, and C. J. L. M. Meijer (2005). Absence of caspase 3 activation in neoplastic cells of nasopharyngeal carcinoma biopsies predicts rapid fatal outcome. *Mod. Pathol.* **18**(7): 877–885.

Overall, C. M. and C. López-Otín (2002). Strategies for MMP inhibition in cancer: innovations for the post-trial era. *Nat. Rev. Cancer* **2**(9): 657–672.

Ozbudak, E. M., M. Thattai, H. N. Lim, B. I. Shraiman, and A. V. Oudenaarden (2004). Multistability in the lactose utilization network of Escherichia coli. *Nature* **427**(6976): 737–740.

Perkins, N. D. (2007). Integrating cell-signalling pathways with NF-kappaB and IKK function. *Nat. Rev. Mol. Cell Biol.* **8**(1): 49–62.

Piccardi, C. and S. Rinaldi (2002). Remarks on excitability, stability and sign of equilibria in cooperative systems. *Syst. Cont. Lett.* **46**: 153–163.

Pomerening, J., E. Sontag, and J.E. Ferrell, Jr. (2003). Building a cell cycle oscillator: hysteresis and bistability in the activation of Cdc2. *Nat. Cell Biol.* **5**: 346–351.

Qin, Z. H., Y. Wang, K. K. Kikly, E. Sapp, K. B. Kegel, N. Aronin, and M. DiFiglia (2001). Pro-caspase-8 is predominantly localized in mitochondria and released into cytoplasm upon apoptotic stimulation. *J. Biol. Chem.* **276**(11): 8079–8086.

Qu, Z., W. R. MacLellan, and J. N. Weiss (2003). Dynamics of the cell cycle: checkpoints, sizers, and timers. *Biophys. J.* **85**(6): 3600–3611.

Ramp, U., T. Krieg, E. Caliskan, C. Mahotka, T. Ebert, R. Willers, H. E. Gabbert, and C. D. Gerharz (2004). XIAP expression is an independent prognostic marker in clear-cell renal carcinomas. *Hum. Pathol.* **35**(8): 1022–1028.

Rao, C. V., D. M. Wolf, and A. P. Arkin (2002). Control, exploitation and tolerance of intracellular noise. *Nature* **420**(6912): 231–237.

Rehm, M., H. Dussmann, R. U. Janicke, J. M. Tavare, D. Kogel, and J. H. Prehn (2002). Single-cell fluorescence resonance energy transfer analysis demonstrates that caspase activation during apoptosis is a rapid process. *J. Biol. Chem.* **277**(27): 24506–24514.

Rehm, M., H. J. Huber, H. Dussmann, and J. H. M. Prehn (2006). Systems analysis of effector caspase activation and its control by X-linked inhibitor of apoptosis protein. *EMBO J.* **25**(18): 4338–4349.

Rosen, R. (1968). A Means toward a New Holism - Book review: Systems Theory and Biology. *Science* **161**(3836): 34–35.

Rumschinski, P. (2007). Modellierung und Analyse des mitochondrialen Signaltransduktionsweges der Apoptose. Diplomarbeit, Institute for Systems Theory and Automatic Control, University of Stuttgart.

Saez-Rodriguez, J., A. Kremling, H. Conzelmann, K. Bettenbrock, and E. D. Gilles (2004). Modular Analysis of Signal Transduction Networks. *IEEE Cont. Syst. Mag.* **24**(4): 35–52.

Saez-Rodriguez, J., A. Kremling, and E. D. Gilles (2005). Dissecting the puzzle of life: modularization of signal transduction networks. *Comput. Chem. Eng.* **29**(3): 619–629.

Salvesen, G. S. and C. S. Duckett (2002). IAP proteins: blocking the road to death's door. *Nat. Rev. Mol. Cell Biol.* **3**(6): 401–410.

Samejima, K. and W. C. Earnshaw (2005). Trashing the genome: the role of nucleases during apoptosis. *Nat. Rev. Mol. Cell Biol.* **6**(9): 677–688.

Samraj, A. K., E. Keil, N. Ueffing, K. Schulze-Osthoff, and I. Schmitz (2006). Loss of caspase-9 provides genetic evidence for the type I/II concept of CD95-mediated apoptosis. *J. Biol. Chem.* **281**(40): 29652–29659.

Savageau, M. A. (1971). Parameter sensitivity as a criterion for evaluating and comparing the performance of biochemical systems. *Nature* **229**(5286): 542–544.

Savill, J. and V. Fadok (2000). Corpse clearance defines the meaning of cell death. *Nature* **407**(6805): 784–788.

Scaffidi, C., S. Fulda, A. Srinivasan, C. Friesen, F. Li, K. J. Tomaselli, K. M. Debatin, P. H. Krammer, and M. E. Peter (1998). Two CD95 (APO-1/Fas) signaling pathways. *EMBO J.* **17**(6): 1675–1687.

Scaffidi, C., I. Schmitz, J. Zha, S. J. Korsmeyer, P. H. Krammer, and M. E. Peter (1999). Differential modulation of apoptosis sensitivity in CD95 type I and type II cells. *J. Biol. Chem.* **274**(32): 22532–22538.

Schimmer, A. D. and S. Dalili (2005). Targeting the IAP Family of Caspase Inhibitors as an Emerging Therapeutic Strategy. *Hematology Am. Soc. Hematol. Educ. Program* pp. 215–219.

Schimmer, A. D., S. Dalili, R. A. Batey, and S. J. Riedl (2006). Targeting XIAP for the treatment of malignancy. *Cell Death Differ* **13**(2): 179–188.

Schliemann, M. (2006). Mathematische Modellierung des TNF-induzierten apoptotischen und antiapoptotischen Signaltransduktionsweges in Säugerzellen. Diplomarbeit, Institute of Cell Biology and Immunology, University of Stuttgart.

Schliemann, M., T. Eissing, P. Scheurich, and E. Bullinger (2007). Mathematical modelling of TNF-α induced apoptotic and anti-apoptotic signalling pathways in mammalian cells based on dynamic and quantitative experiments. In: *Proceedings of the 2nd International Conference Foundations of Systems Biology in Engineering (FOSBE)*, Stuttgart, Germany, pp. 213–218.

Schmidt, H. and E. Jacobsen (2004). Identifying feedback mechanisms behind complex cell behavior. *IEEE Cont. Syst. Mag.* **24**(4): 91–102.

Schmidt, H. and M. Jirstrand (2005). Systems Biology Toolbox for MATLAB: a computational platform for research in Systems Biology. *Bioinformatics* **22**(4): 514–515.

Schneider-Brachert, W., V. Tchikov, et al. (2004). Compartmentalization of TNF receptor 1 signaling: internalized TNF receptosomes as death signaling vesicles. *Immunity* **21**(3): 415–428.

Schoeberl, B. (2002). Mathematical Modeling of Signal Transduction Pathways in Mammalian cells at the Example of the EGF induced MAP kinase cascade and TNF receptor crosstalk. PhD thesis, Max-Planck-Institut für Dynamik komplexer technischer Systeme, Magdeburg.

Schoeberl, B., E. D. Gilles, and P. Scheurich (2001). A mathematical vision of TNF receptor interaction. In: T. Yi, M. Hucka, M. Morohashi, and H. Kitano (eds.), *Proceedings of the 2nd International Conference on Systems Biology, Pasadena, CA*, Omnipress, Madison, WI, pp. 158–167.

Schrödinger, E. (1944). *What is life? The Physical Aspect of the Living Cell*. Cambridge University Press, Cambridge, UK.

Sen, R. (2006). Control of B lymphocyte apoptosis by the transcription factor NF-kappaB. *Immunity* **25**(6): 871–883.

Shmulevich, I., S. A. Kauffman, and M. Aldana (2005). Eukaryotic cells are dynamically ordered or critical but not chaotic. *Proc. Natl. Acad. Sci. U. S. A.* **102**(38): 13439–13444.

Slee, E. A., M. T. Harte, R. M. Kluck, B. B. Wolf, C. A. Casiano, D. D. Newmeyer, H. G. Wang, J. C. Reed, D. W. Nicholson, E. S. Alnemri, D. R. Green, and S. J. Martin (1999). Ordering the cytochrome c-initiated caspase cascade: hierarchical activation of caspases-2, -3, -6, -7, -8, and -10 in a caspase-9-dependent manner. *J. Cell Biol.* **144**(2): 281–292.

Sloane, B. F., S. Yan, I. Podgorski, B. E. Linebaugh, M. L. Cher, J. Mai, D. Cavallo-Medved, M. Sameni, J. Dosescu, and K. Moin (2005). Cathepsin B and tumor proteolysis: contribution of the tumor microenvironment. *Semin. Cancer Biol.* **15**(2): 149–157.

Sohn, D., K. Schulze-Osthoff, and R. U. Jänicke (2005). Caspase-8 can be activated by interchain proteolysis without receptor-triggered dimerization during drug-induced apoptosis. *J. Biol. Chem.* **280**(7): 5267–5273.

Sontag, E. (2004). Some new directions in control theory inspired by systems biology. *IEE Syst. Biol.* **1**: 9–18.

Stegh, A. H., B. C. Barnhart, J. Volkland, A. Algeciras-Schimnich, N. Ke, J. C. Reed, and M. E. Peter (2002). Inactivation of caspase-8 on mitochondria of Bcl-xL-expressing MCF7-Fas cells: role for the bifunctional apoptosis regulator protein. *J. Biol. Chem.* **277**(6): 4351–4360.

Stelling, J., S. Klamt, K. Bettenbrock, S. Schuster, and E. D. Gilles (2002). Metabolic network structure determines key aspects of functionality and regulation. *Nature* **420**(6912): 190–193.

Stelling, J., E. D. Gilles, and F. J. Doyle, 3rd (2004a). Robustness properties of circadian clock architectures. *Proc. Natl. Acad. Sci. U. S. A.* **101**(36): 13210–13215.

Stelling, J., U. Sauer, Z. Szallasi, F. J. Doyle, 3rd, and J. Doyle (2004b). Robustness of cellular functions. *Cell* **118**(6): 675–685.

Stennicke, H. R. and G. S. Salvesen (1999). Catalytic properties of the caspases. *Cell Death Differ.* **6**(11): 1054–1059.

Stennicke, H. R., J. M. Jurgensmeier, et al. (1998). Pro-caspase-3 is a major physiologic target of caspase-8. *J. Biol. Chem.* **273**(42): 27084–27090.

Strogatz, S. H. (2001). *Nonlinear dynamics and chaos: With applications to physics, biology, chemistry, and engineering*. Perseus Books, Cambridge, MA. ISBN: 0738204536.

Stucki, J. W. and H. U. Simon (2005). Mathematical modeling of the regulation of caspase-3 activation and degradation. *J. Theor. Biol.* **234**(1): 123–131.

Sun, X. M., S. B. Bratton, M. Butterworth, M. MacFarlane, and G. M. Cohen (2002). Bcl-2 and Bcl-xL inhibit CD95-mediated apoptosis by preventing mitochondrial release of Smac/DIABLO and subsequent inactivation of X-linked inhibitor-of-apoptosis protein. *J. Biol. Chem.* **277**(13): 11345–11351.

Sung, M.-H. and R. Simon (2004). In silico simulation of inhibitor drug effects on nuclear factor-kappaB pathway dynamics. *Mol. Pharmacol.* **66**(1): 70–75.

Svingen, P. A., D. Loegering, et al. (2004). Components of the cell death machine and drug sensitivity of the National Cancer Institute Cell Line Panel. *Clin. Cancer Res.* **10**(20): 6807–6820.

Takeuchi, H., J. Kim, A. Fujimoto, N. Umetani, T. Mori, A. Bilchik, R. Turner, A. Tran, C. Kuo, and D. S. B. Hoon (2005). X-Linked inhibitor of apoptosis protein expression level in colorectal cancer is regulated by hepatocyte growth factor/C-met pathway via Akt signaling. *Clin. Cancer Res.* **11**(21): 7621–7628.

Thornberry, N. A. and Y. Lazebnik (1998). Caspases: enemies within. *Science* **281**(5381): 1312–1316.

Thron, C. D. (1994). Theoretical dynamics of the cyclin B-MPF system: a possible role for p13suc1. *BioSystems* **32**(2): 97–109.

Thron, C. D. (1997). Bistable biochemical switching and the control of the events of the cell cycle. *Oncogene* **15**(3): 317–325.

Thurmond, R. L., S. Sun, L. Karlsson, and J. P. Edwards (2005). Cathepsin S inhibitors as novel immunomodulators. *Curr. Opin. Investig. Drugs* **6**(5): 473–482.

Tyas, L., V. A. Brophy, A. Pope, A. J. Rivett, and J. M. Tavare (2000). Rapid caspase-3 activation during apoptosis revealed using fluorescence-resonance energy transfer. *EMBO Rep.* **1**(3): 266–270.

Tyson, J. J. (2007). Bringing cartoons to life. *Nature* **445**(7130): 823.

Tyson, J. J. and H. G. Othmer (1978). *Progress in Theoretical Biology*, vol. 5, chap. The dynamics of feedback control circuits in biochemical pathways, pp. 1–62. Academic Press, New York.

Tyson, J. J., K. Chen, and B. Novak (2001). Network dynamics and cell physiology. *Nat. Rev. Mol. Cell Biol.* **2**(12): 908–916.

Tyson, J. J., K. C. Chen, and B. Novak (2003). Sniffers, buzzers, toggles and blinkers: dynamics of regulatory and signaling pathways in the cell. *Curr. Opin. Cell Biol.* **15**(2): 221–231.

Van de Craen, M., W. Declercq, I. Van den Brande, W. Fiers, and P. Vandenabeele (1999). The proteolytic procaspase activation network: an in vitro analysis. *Cell Death Differ.* **6**(11): 1117–1124.

Vanag, V. K., D. G. Míguez, and I. R. Epstein (2006). Designing an enzymatic oscillator: Bistability and feedback controlled oscillations with glucose oxidase in a continuous flow stirred tank reactor. *J. Chem. Phys.* **125**(19): 194515.

Ventura, B. D., C. Lemerle, K. Michalodimitrakis, and L. Serrano (2006). From in vivo to in silico biology and back. *Nature* **443**(7111): 527–533.

Vilar, J. M. G., C. C. Guet, and S. Leibler (2003). Modeling network dynamics: the lac operon, a case study. *J. Cell Biol.* **161**(3): 471–476.

Wajant, H. (2002). The Fas signaling pathway: more than a paradigm. *Science* **296**(5573): 1635–1636.

Wajant, H., M. Grell, and P. Scheurich (1999). TNF receptor associated factors in cytokine signaling. *Cytokine Growth Factor Rev.* **10**(1): 15–26.

Wajant, H., K. Pfizenmaier, and P. Scheurich (2003a). Non-apoptotic Fas signaling. *Cytokine Growth Factor Rev.* **14**(1): 53–66.

Wajant, H., K. Pfizenmaier, and P. Scheurich (2003b). Tumor necrosis factor signaling. *Cell Death Differ.* **10**(1): 45–65.

Waldherr, S., T. Eissing, M. Chaves, and F. Allgöwer (2007). Bistability preserving model reduction in apoptosis. In: *Proceedings of the 10th IFAC Computer Applications in Biotechnology (CAB)*, Cancún, Mexico, Preprint Vol. 2, pp. 327–332.

Watson, J. D. and F. H. Crick (1953). Molecular structure of Nucleic Acids. *Nature* **171**(4356): 737–738.

Weingärtner, M., D. Siegmund, U. Schlecht, M. Fotin-Mleczek, P. Scheurich, and H. Wajant (2002). Endogenous membrane tumor necrosis factor (TNF) is a potent amplifier of TNF receptor 1-mediated apoptosis. *J. Biol. Chem.* **277**(38): 34853–34859.

Weiss, J. N. (1997). The Hill equation revisited: uses and misuses. *FASEB J.* **11**(11): 835–841.

Wellstead, P. (2007). Control opportunities in systems biology. In: *Proceedings of the 10th IFAC Computer Applications in Biotechnology (CAB)*, Cancún, Mexico, Preprint Vol. 2, pp. 1–17.

Werner, S. L., D. Barken, and A. Hoffmann (2005). Stimulus specificity of gene expression programs determined by temporal control of IKK activity. *Science* **309**(5742): 1857–1861.

Wiener, N. (1948). Cybernetics or Control and Communication in the Animal and the Machine. *MIT Press, Cambridge, MA* .

Wingreen, N. and D. Botstein (2006). Back to the future: education for systems-level biologists. *Nat. Rev. Mol. Cell Biol.* **7**(11): 829–832.

Wolf, D. M. and A. P. Arkin (2003). Motifs, modules and games in bacteria. *Curr. Opin. Microbiol.* **6**(2): 125–134.

Wolf, J., S. Becker-Weimann, and R. Heinrich (2005). Analysing the robustness of cellular rhythms. *IEE Syst. Biol.* **2**: 35–41.

Wolkenhauer, O. and M. Mesarović (2005). Feedback dynamics and cell function: Why systems biology is called Systems Biology. *Mol. BioSyst.* **1**(1): 14–16.

Xiong, W. and J. E. Ferrell, Jr. (2003). A positive-feedback-based bistable 'memory module' that governs a cell fate decision. *Nature* **426**(6965): 460–465.

Yamamoto, K., S. Abe, Y. Nakagawa, K. Suzuki, M. Hasegawa, M. Inoue, M. Kurata, K. Hirokawa, and M. Kitagawa (2004). Expression of IAP family proteins in myelodysplastic syndromes transforming to overt leukemia. *Leuk. Res.* **28**(11): 1203–1211.

Yamashima, T. (2004). Ca2+-dependent proteases in ischemic neuronal death: a conserved 'calpain-cathepsin cascade' from nematodes to primates. *Cell Calcium* **36**(3-4): 285–293.

Yan, Y., C. Mahotka, S. Heikaus, T. Shibata, N. Wethkamp, J. Liebmann, C. V. Suschek, Y. Guo, H. E. Gabbert, C. D. Gerharz, and U. Ramp (2004). Disturbed balance of expression between XIAP and Smac/DIABLO during tumour progression in renal cell carcinomas. *Br. J. Cancer* **91**(7): 1349–1357.

Yang, W., L. M. Rozan, E. R. McDonald, A. Navaraj, J. J. Liu, E. M. Matthew, W. Wang, D. T. Dicker, and W. S. El-Deiry (2007). CARPs are ubiquitin ligases that promote MDM2-independent p53 and phospho-p53ser20 degradation. *J. Biol. Chem.* **282**(5): 3273–3281.

Yeger-Lotem, E., S. Sattath, N. Kashtan, S. Itzkovitz, R. Milo, R. Y. Pinter, U. Alon, and H. Margalit (2004). Network motifs in integrated cellular networks of transcription-regulation and protein-protein interaction. *Proc. Natl. Acad. Sci. U. S. A.* **101**(16): 5934–5939.

Yi, T.-M., Y. Huang, M. I. Simon, and J. Doyle (2000). Robust perfect adaptation in bacterial chemotaxis through integral feedback control. *Proc. Natl. Acad. Sci. U. S. A.* **97**(9): 4649–4653.

Yoo, S. J., J. R. Huh, I. Muro, H. Yu, L. Wang, S. L. Wang, R. M. Feldman, R. J. Clem, H. A. Muller, and B. A. Hay (2002). Hid, Rpr and Grim negatively regulate DIAP1 levels through distinct mechanisms. *Nat. Cell Biol.* **4**(6): 416–424.

Zarnitsina, V. I., F. I. Ataullakhanov, A. I. Lobanov, and O. L. Morozova (2001). Dynamics of spatially nonuniform patterning in the model of blood coagulation. *Chaos* **11**(1): 57–70.

Zhang, H., Q. Xu, S. Krajewski, M. Krajewska, Z. Xie, S. Fuess, S. Kitada, K. Pawlowski, A. Godzik, and J. C. Reed (2000). BAR: An apoptosis regulator at the intersection of caspases and Bcl-2 family proteins. *Proc. Natl. Acad. Sci. U. S. A.* **97**(6): 2597–2602.